

FACILITY FORM 602

N67-25871

(ACCESSION NUMBER)

249

(PAGES)

CR-83881

(NASA CR OR TMX OR AD NUMBER)

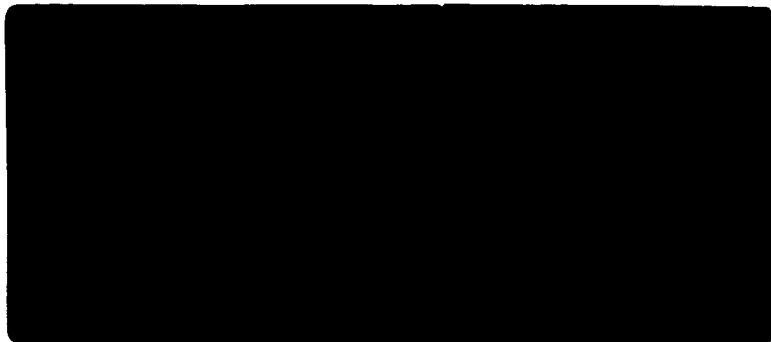
(THRU)

1

(CODE)

09

(CATEGORY)



*Analog Technology Corporation*



This work was performed for the Jet Propulsion Laboratory,  
California Institute of Technology, sponsored by the  
National Aeronautics and Space Administration under  
Contract NAS7-100.

Final Report  
Photomultiplier Tube  
Amplifier-Discriminator

JPL CONTRACT NO. 951585

Prepared for the  
Jet Propulsion Laboratory  
California Institute of Technology  
4800 Oak Grove Drive  
Pasadena, California

13 January 1967

By Staff  
Analog Technology Corporation  
3410 E. Foothill Boulevard  
Pasadena, California

Approved by:



J. Howard Marshall PhD  
Vice-President  
Advanced Planning

## Table of Contents

	<u>Page Number</u>
1.0 INTRODUCTION	1.0-1
2.0 AMPLIFIER DESIGN ANALYSIS	1.0-1
2.1 Pulse Shaping and Approximate Impulse Response Function	2.1-1
2.2 Stability Against Oscillation	2.2-1
2.3 Gain Drifts	2.3-1
2.3.1 DC Level Stability	2.3-1
2.3.2 Pulse-Gain Stability	2.3-3
2.3.3 Linearity	2.3-5
3.0 DISCRIMINATOR DESIGN ANALYSIS	3.0-1
3.1 Threshold Stability	3.0-1
3.2 Pulse Width and Recovery Time	3.2-1
4.0 TESTING	4.0-1
4.1 Test Procedures	4.0-1
4.2 Test Results	4.2-1
Appendix A - Linear Circuit Design Principles	
Appendix B - Pulse Shaping in Pulse-Height Analyzer Systems	
Appendix C - Magnetic Element Design and Fabrication Instruction	

## Final Report

### Photomultiplier Tube Amplifier-Discriminator

#### 1.0 INTRODUCTION

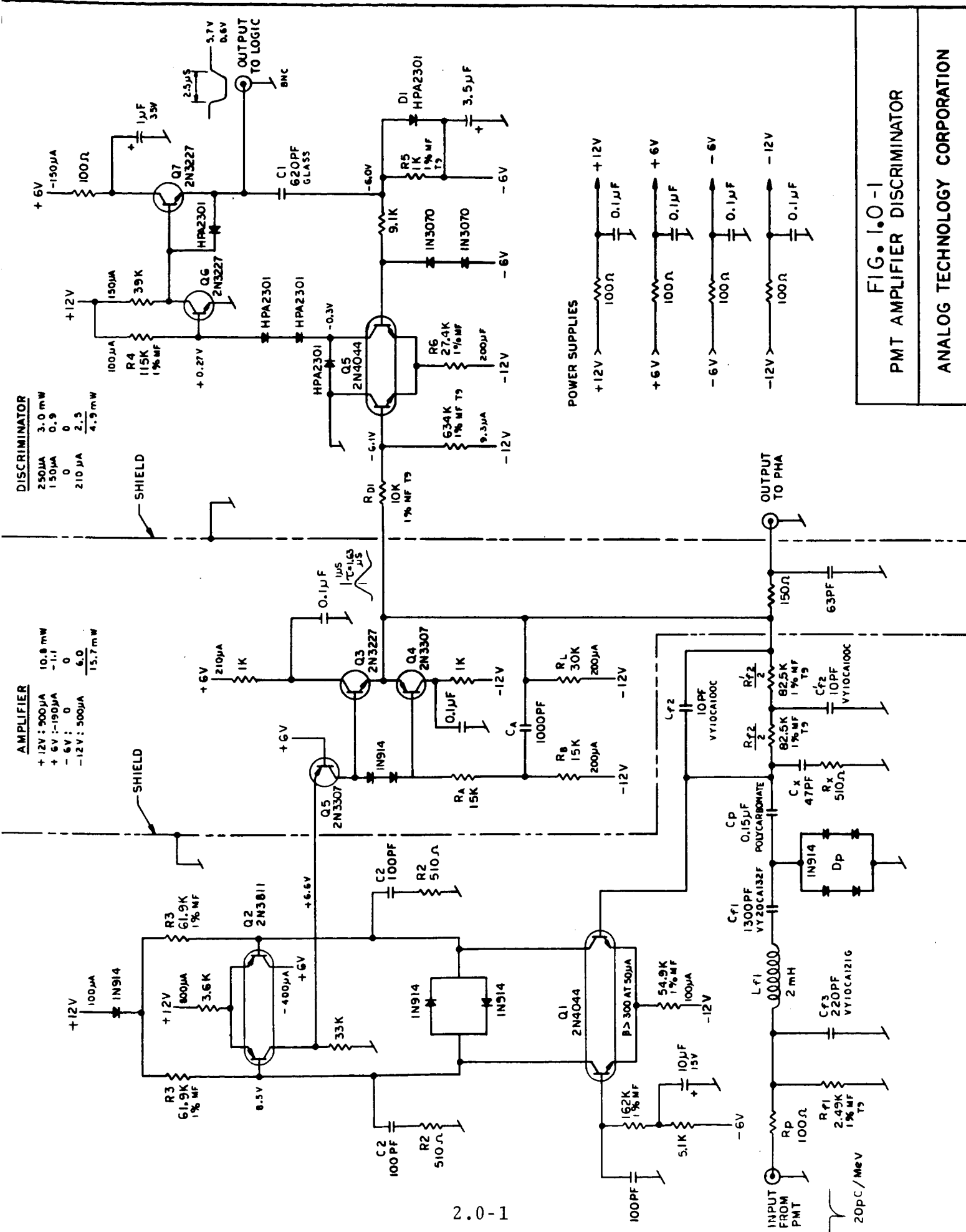
In accordance with the requirements of Contract No. 951585, the amplifier-discriminator system shown in Figure 1.0-1 was designed, constructed and tested. This report describes the results of that development program.

The amplifier receives signals from photomultiplier tubes looking at NaI crystals and converts them into pulses suitable for pulse-height analysis. Appropriate gain and pulse shaping are provided by the amplifier for the observation of gamma rays with energies in the 100 KeV to 10 MeV range.

A discriminator connected to the amplifier output provides a pulse when the amplifier output signal exceeds 1% of full scale (10 V). In this way an accurate determination of counting rates above this threshold can be made independently of analyzer dead time. Also coincidence gating and other such logic functions can be performed using this pulse.

#### 2.0 AMPLIFIER DESIGN ANALYSIS

The amplifier described herein employs the operational-amplifier configuration with pulse shaping performed by the feedback elements. A heavy reliance on negative feedback produces a response nearly independent of temperature, amplitude or counting rate. The results of a detailed analysis of the expected performance of the amplifier is given in this section. Actual measured values consistent with the theoretical behavior are presented in Section 4.



<b>DISCRIMINATOR</b>	
250 $\mu$ A	3.0 mW
150 $\mu$ A	0.9
0	0
210 $\mu$ A	2.5
	<hr/> 4.9 mW

<b>AMPLIFIER</b>	
12V : 900 $\mu$ A	10.8 mW
6V : -190 $\mu$ A	-1.1
6V : 0	0
12V : 500 $\mu$ A	<u>6.0</u>
	15.7 mW

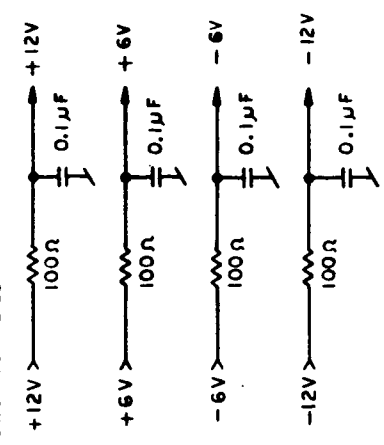
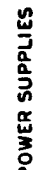


FIG. 1.0-1  
PMT AMPLIFIER DISCRIMINATOR

ANALOG TECHNOLOGY CORPORATION

Transistors Q1 and Q2 form a double-differential amplifier, while transistors Q3 and Q4 provide a bootstrapped, complementary emitter-follower output stage. The grounded-base stage Q5 reduces the Miller capacity of the second stage, resulting in increased amplifier bandwidth and reduced problems with rate limiting. The transistor operating biases are determined by external feedback via  $R_{f2}$ , which is also involved in the pulse-shaping and pulse-gain determination. The double-differential configuration was chosen to achieve a high degree of dc output-voltage stability. Because the operating currents of Q2a and Q2b are approximately equal, their base voltages are also nearly identical, resulting in very closely matched collector currents and voltages for Q1a and Q2a. Because Q1a and Q2a are a tightly matched pair and have the same dc resistance connected to their bases, their base currents and voltages are also nearly equal, providing a large degree of temperature compensation of output voltage drifts. In this way, subsequent circuits can be direct-coupled to the amplifier output without markedly upsetting their bias stability. Thus, the advantages of a direct-coupled system in reducing baseline shifts caused by pulse-tail pile-up can be realized in practice.

The pulse shape and gain are determined by the feedback elements ( $R_{f1}$ ,  $L_{f1}$ ,  $R_{f2}$  and  $C_{f2}$ ). The placement of the pulse-shaping networks in the feedback loop allows the amplifier dynamic range to be larger than that which would result if pulse shaping were performed after the amplifier output. As a result power is not wasted in unnecessary standing voltages or currents, and the entire amplifier standby power becomes only 15.7 mW.

In order to provide a gain characteristic which is only weakly dependent on temperature, output amplitude or counting rate, all active elements should be enclosed within the negative feedback loop and their operating biases should be kept nearly independent of output amplitude. Therefore, the output emitter follower, which provides a low output impedance for driving subsequent circuits, is enclosed in the feedback loop. In addition its source resistor RA is bootstrapped via CA so that the component of current in Q2a used for driving resistive loads is not output-amplitude dependent. In order to reduce the variations in the component of this current for capacitive loads, transistors with low values of  $C_{ob}$  and high values of  $f_T$  are used for Q3 and Q4. Otherwise the capacity at the collector of Q2a could cause rate-limiting effects, which produce either non-linearities or the need for a larger standing current in Q2 and the concurrent power increase.

The complementary configuration provides a low output impedance for both the positive and negative portions of the output pulse. If the PNP transistor were not present, then capacitive loads could be driven negatively only by the standing current in Q3. This current would result in standby power, mostly eliminated by the complementary emitter follower. The 1-Kilo-ohm resistors in the collectors of Q3 and Q4 both aid in decoupling pulse currents from the power supply and also protect the output stage in the event of a short circuit. Because the amplifier is direct-coupled and its output rests at -6 V, (chosen for convenience in the discriminator design), output shorts to ground could draw damaging currents in the output stage. However, the 1-K resistor limits this fault current to 12 mA by forcing Q4 to saturate. As a result power dissipation remains well within tolerable limits, and no damage is done to the transistor. The complementary configuration is

also self-protecting against excessive emitter-base voltages, because the emitter-base junction of one transistor acts as a diode clamp for the other. Similarly, the resistor-diode-capacitor configuration at the input ( $R_p$ ,  $D_p$ ,  $C_p$ ) protects the input transistor from damage in the event that a high voltage pulse from the photomultiplier supply is applied to the input. Such pulses can arise if the phototube anode is placed at a positive high-voltage potential and capacitively coupled to the amplifier.

## 2.1 Pulse Shaping and Approximate Impulse Response Function

The correct choice of amplifier pulse shape is essentially a compromise between pulse pile-up effects and independence of the NaI scintillation-decay time constant. A detailed analysis of the effects of pulse shaping on nuclear detection systems is given in Appendix B.

From this analysis, it becomes apparent that the optimum system, from the standpoints of low pulse pile-up and low noise, employs amplifiers with no ac couplings producing secondary time constants. In the presence of secondary time constants, at least two differentiating networks must be present to prevent the coupling capacitors from accumulating a large average charge producing baseline shifts. Because the Fabri-Tek pulse-height analyzer contains several such secondary time constants, double differentiation is chosen for this amplifier. No secondary time constants are present in the amplifier so that use with a direct-coupled analyzer is possible. Direct coupling to the discriminator is provided, and protective components prevent damage in the event that the output is short circuited.

The leading edge of the pulse is shaped by integrating networks so that the peak amplitude does not depend strongly on the amplifier cut-off frequency. Also, smoothly rising pulses require less standing current, and thus less power, to prevent



rate limiting and the associated non-linearities. The resulting pulse possesses a nearly symmetrical positive portion with a peak at 1.4  $\mu$ s and a width above the base line of 3.2  $\mu$ s. A negative portion following the positive portion has an equal area, so that the total charge transmitted by the pulse is zero.

A block diagram of the amplifier and the pulse-shaping networks is shown in Figure 2.1-1. A capacitor (Cf3) in parallel with Rf1 has been neglected in this figure. This capacitor reduces the initial slope of the output pulse and increases the peak amplitude by 8%. Its principal functions are the reduction of rate limiting and the prevention of the coupling of fast signals to the amplifier through the stray capacity across LF1.

If the voltage gain ( $M_V$ ) of the amplifier is infinitely large, then the input voltage ( $V_1$ ) of the amplifier is approximately zero, and the output voltage is related to the input current by

$$\frac{V_{out}}{i_s} \approx \frac{R_{f2} \left[ 1 + p\frac{\tau}{4} \right] 2\tau}{\left[ 1 + p\tau \right]^2 \left[ 1 + p\frac{\tau}{2} \right]^2} \quad (2.1-1)$$

where  $p$  = Laplace transform variable

$\tau$  = shaping time constant

$$C_{f3}R_{f1} \ll \tau$$

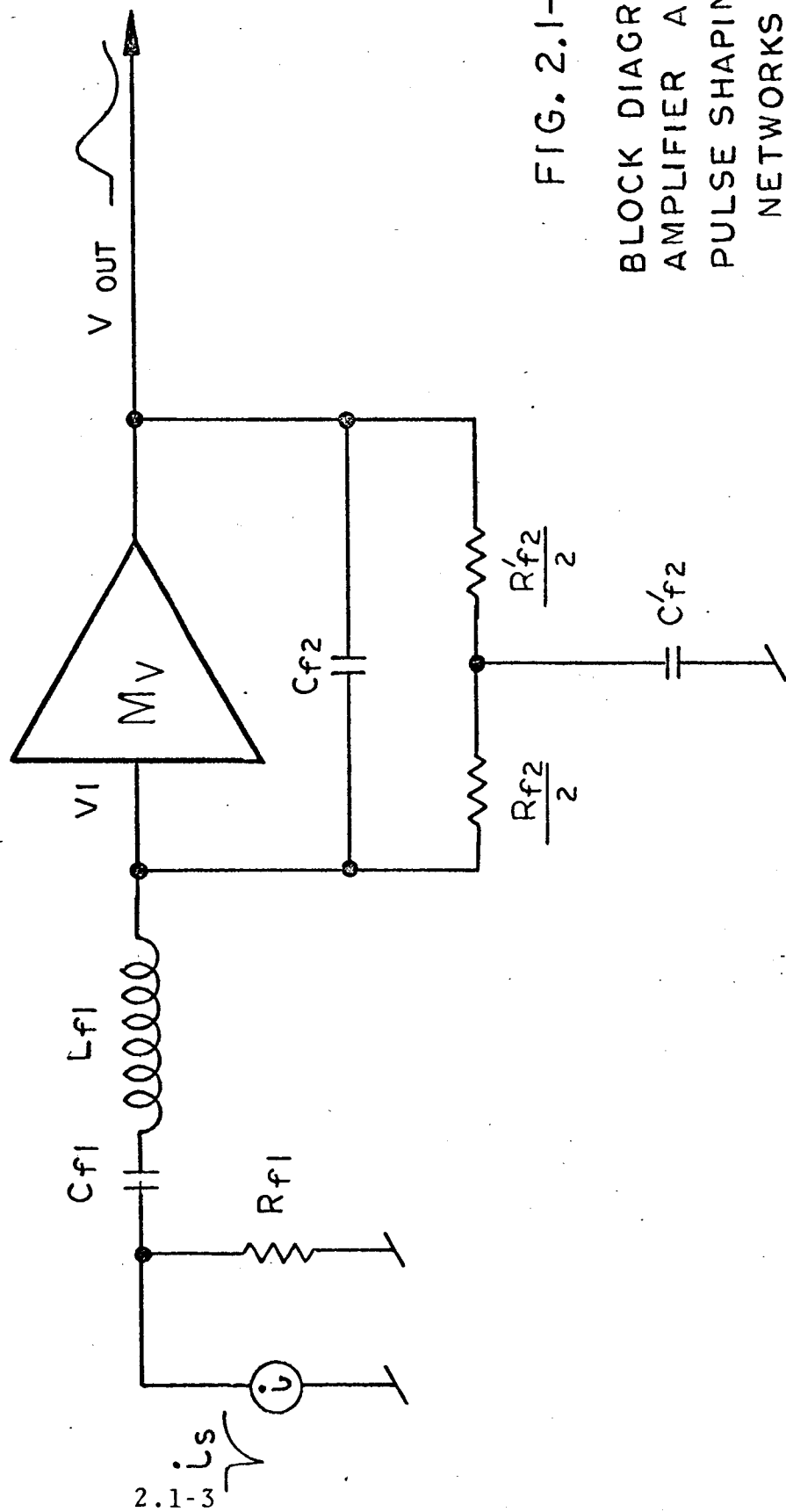


FIG. 2.1-1  
BLOCK DIAGRAM  
AMPLIFIER AND  
PULSE SHAPING  
NETWORKS

Critical damping has been assumed in the above formula. This condition requires that

$$L_{f1} = \frac{C_{f1} R_{f1}^2}{4} \quad (2.1-2a)$$

$$C_{f2}' = C_{f2} \quad (2.1-2b)$$

$$R_{f2}' = R_{f2} \quad (2.1-2c)$$

Also, to obtain nearly symmetrical waveforms we have chosen

$$\tau = \sqrt{L_{f1} C_{f1}'} = \frac{R_{f1} C_{f1}}{2} \quad (2.1-3)$$

and

$$\tau = R_{f2} C_{f2} \quad (2.1-4)$$

If the duration of the input current pulse is short compared to the shaping time constant, it can be approximated by

$$i_s \cong Q \delta(t) \quad (2.1-5)$$

resulting in an output pulse given by

$$V_{out} \cong \frac{8Q}{C_{f2}} \left\{ \left[ 2 - \frac{3}{4} \left( \frac{t}{\tau} \right) \right] e^{-t/\tau} - \left[ 2 + \frac{t}{\tau} \right] e^{-2t/\tau} \right\} \quad (2.1-6)$$

This waveform has a peak at  $t = 0.61 \tau$  with a peak value of  $\frac{0.528Q}{C_{f2}}$ . For the values used in this amplifier,

$$V_{\text{peak}} = 0.053 \text{ V/pC} \quad (2.1-7a)$$

$$T_{\text{peak}} = 1.0 \text{ } \mu\text{s} \quad (2.1-7b)$$

The presence of  $C_{f3}$  modifies these values to

$$V_{\text{peak}} = 0.057 \text{ V/pC} \quad (2.1-8a)$$

$$T_{\text{peak}} = 1.4 \text{ } \mu\text{s} \quad (2.1-8b)$$

This pulse shaping is similar to the double-differentiated, single-integrated shaping described in Appendix B. An increase in gain of 14% and a slightly more symmetrical pulse result from the bridged -T feedback network compared to simple RC feedback. Because of the similarity of these two shaping networks, the pulse pile-up theory developed in Appendix B will be applied to this amplifier. Evaluating equation 2.2.2-26 of Appendix B for this pulse shape and assuming that the pulse-height analyzer busy time is long compared to  $\tau$ , one obtains for the average peak shift  $\Delta V$

$$\frac{\Delta V}{\bar{V}} \approx 3.5 (R\tau)^2 \quad (2.1-9)$$

where

$R$  = average counting rate

$\bar{V}$  = average input pulse height

For  $R = 10^4$  and  $\tau = 1.6 \mu s$ , then

$$\frac{\Delta V}{\bar{V}} = 0.09\% \quad (2.1-10)$$

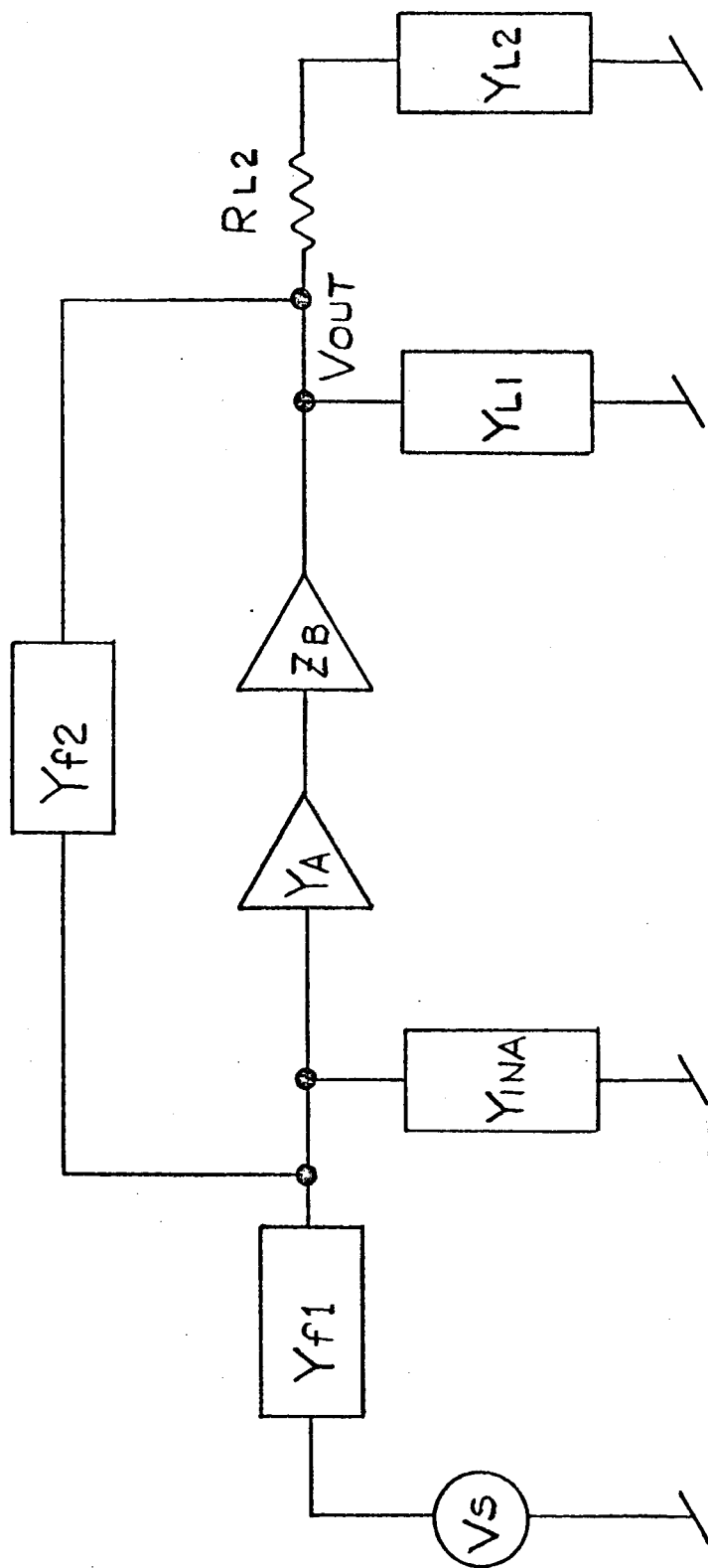
Secondary ac-couplings in the pulse-height analyzer may increase the peak shift and may cause additional peak smearing at high rates, particularly if the rates themselves are variable. The use of a doubly-differentiated waveform reduces this effect as much as possible without complicated circuitry.

## 2.2 Stability Against Oscillation

In order to produce an amplifier with a high inherent gain stability, a large amount of negative feedback for frequencies centered about the corner frequency given by the reciprocal of the shaping time constant is required. As a result, the frequency of gain cross-over approaches 10 MHz, requiring careful analysis if the amplifier is not to oscillate. The basic theory of feedback amplifiers, together with the poles and zeros resulting from several active networks, is given in Appendix A. In this section this theory will be applied to the amplifier.

An equivalent circuit of the amplifier is given in Figure 2.2-1, using a voltage source for the input. This voltage source is the Thevenin equivalent of the current source representing the phototube anode, and its magnitude is given by

$$V_s = R_{f1} i_s \quad (2.2-1)$$



2.2-2

$Y_A$  = TRANSFER ADMITTANCE OF THE DOUBLE-DIFFERENTIAL AMPLIFIER (Q1, Q2)

$Z_B$  = TRANSFER IMPEDANCE OF THE EMITTER FOLLOWER (Q3, Q4)

$Y_{INA}$  = INPUT ADMITTANCE OF THE DOUBLE-DIFFERENTIAL AMPLIFIER

$Y_{L1}$  = DIRECT LOAD ADMITTANCE ON THE EMITTER FOLLOWER

$Y_{L2}$  = AMPLIFIER OUTPUT LOAD ADMITTANCE

$R_{L2} = 150\Omega$

## AMPLIFIER EQUIVALENT CIRCUIT

FIGURE 2.2-1

For the purpose of this analysis the amplifier will be divided into two halves at the grounded-base stage (Q5). The double-differential amplifier will be represented by its transfer admittance  $Y_A$ , given by the ratio of the signal current at the collector of Q5 to the signal voltage at the base of Q1b. The emitter follower transforms this current signal into an output voltage at the emitters of Q3 and Q4, and the ratio of this voltage to the output current from the double-differential amplifier will be called  $Z_B$ .

The basic theory of feedback amplifier design is presented in Section 2 of Appendix A. The analysis given in Section 2.3 (Appendix A) shows that the behavior of the feedback factor in the neighborhood of gain cross-over determines the stability of the amplifier. [The frequency of gain cross-over is that frequency for which the magnitude of the complex feedback factor is one. It is often convenient to refer to a gain cross-over time ( $t_c$ ), defined as the reciprocal of the angular gain cross-over frequency ( $\omega_c$ ).] For this amplifier the feedback factor is given by

$$F = \frac{-Y_A Z_B Y_{f2}}{Y_{f1} + Y_{f2} + Y_{INA}} \quad (2.2-2)$$

where the gains and admittances are defined by Figure 2.2-1.

The amplifier will be stable if the slope of the logarithm of the feedback factor plotted as a function of the logarithm of the angular frequency does not become less than -2 for frequencies near the gain cross-over frequency. This criterion implies that the number of poles must not exceed the number of zeros by more than two in this frequency region.

As further calculation will show, the major region of concern lies for times from 1 ns to 100 ns and that the gain cross-over time is of the order of 10 ns. Thus, poles and zeros smaller than about 0.5 ns will be neglected in the analysis, while poles and zeros larger than 200 ns will be considered completely dominant compared to one. Thus,

$$Y_{f1} \cong \frac{C_{f1}}{p\tau^2} \quad (2.2-3)$$

$$Y_{f2} \cong \frac{p\tau}{R_{f2}} \quad (2.2-4)$$

$$\tau = \sqrt{L_{f1} C_{f1}} = \frac{R_{f1} C_{f1}}{2} = R_{f2} C_{f2} = 1.6 \mu s \quad (2.2-5)$$

$$M_o = 2R_{f2}/R_{f1} = 132 \quad (2.2-6)$$

and the feedback factor becomes approximately

$$F \cong \frac{-Y_A Z_B}{1 + \frac{Y_{INA}}{pC_{f2}} + \frac{M_o}{(p\tau)^2}} \quad (2.2-7)$$

(Notice that we have written the feedback factor as a function of the Laplace operator,  $p$ , instead of as a function of frequency,  $\omega$ . These two quantities are simply related by

$$p = j\omega \quad (2.2-8)$$



Because the time constants involved in this analysis are easily represented by RC products, we prefer the time (or Laplace) domain rather than the frequency representation. In evaluating approximations, the quantity  $p$  will be considered to have units of reciprocal time.)

For times for which

$$t \ll \frac{\tau}{\sqrt{M_0}} = 140 \text{ ns} \quad (2.2-9)$$

The feedback factor simplifies to

$$F \approx \frac{-Y_A Z_B}{1 + \frac{Y_{INA}}{pC_{f2}}} \quad (2.2-10)$$

We will first calculate the transfer impedance of the emitter follower using Section 4.2 of Appendix A. The output load admittance is almost purely capacitive, caused by the interconnecting cable, because the input resistance of the pulse-height analyzer is 100 K. Thus, we will approximate

$$Y_{L2} \approx pC_{L2} \quad (2.2-11)$$

where  $C_{L2}$  will be allowed to vary between 63 and 263 pF.

The biasing of the output emitter follower is such that Q3 conducts with Q4 barely cut-off, except during the negative-going portions of the output pulse. For the remainder of this analysis, we will neglect the resistive component of  $Y_{e4}$  and include the emitter-transistion capacity of Q4 in  $Y_{e3}$ . This

approximation is equivalent to setting the transconductance ( $g_{e4}$ ) of  $Q_4$  equal to zero, as results when its collector current vanishes.

Because the emitter follower is bootstrapped, the variable transformation described in Section 4.2.1 of Appendix A will be performed. Thus

$$\beta_3' = \beta_3 \frac{R_A}{\beta_3 r_{e3} + R_A} \quad (2.2-12)$$

$$Y_L'' = Y_L' + \frac{1}{R_B} \quad (2.2-13)$$

The total load admittance,  $Y_L'$ , is given by

$$Y_L' = Y_{L1} + Y_{f2} + p(C_{ob} - C_c) + \frac{pC_{L2}}{1 + pR_{L2}C_{L2}} \quad (2.2-14)$$

where

$$Y_{L1} = \frac{1}{R_L} + \frac{1}{R_{D1}} + pC_{e4}$$

$C_{e4}$  = emitter-collector capacitance of  $Q_4$

$R_L$  = emitter-follower load resistance

$R_{D1}$  = discriminator input resistance

If one defines

$$G_{L1} = \frac{1}{R_{f2}} + \frac{1}{R_B} + \frac{1}{R_L} + \frac{1}{R_{D1}} \quad (2.2-15)$$

$$C_{L1} = C_{ob} - C_c + C_{f2} + C_{e4} \quad (2.2-16)$$

$$G_{L2} = \frac{1}{R_{L2}}, \quad (2.2-17)$$

then

$$Y_L'' = \frac{G_{L1}G_{L2} + p(C_{L1}G_{L2} + C_{L2}G_{L1} + C_{L2}G_{L2}) + p^2C_{L1}G_{L2}}{G_{L2} + pC_{L2}} \quad (2.2-18)$$

and the analysis given in Section 4.2.3 of Appendix A applies directly. The transfer impedance, given by equation 4.2.3-2 (Appendix A), becomes

$$Z_B = \frac{\beta_3' R_{L1}(1 + p\tau_{\alpha3})(1 + p\tau_{L2})}{1 + pA + p^2B + p^3C} \quad (2.2-19)$$

where

$$R_{L1} = \frac{1}{G_{L1}}$$

$$\tau_{\alpha3} = C_{e3} r_{e3}$$

$$\tau_{L2} = R_{L2} C_{L2}$$

$$C_1 = C_{ob3} + C_{ob4} + C_{ob5}$$

$$A = \beta_3' [C_1 R_{L1} + (C_{e3} + C_1) r_{e3}]$$

$$+ (C_{L1} + C_{L2}) R_{L1} + C_{L2} R_{L2}$$

$$B = \beta_3' R_{L1} C_1 (\tau_{\alpha 3} + \tau_{L2}) + \beta_3' r_{e3} (C_{e3} + C_1)$$

$$(\tau_{L1} + \tau_{L2} + C_{L2} R_{L1}) + R_{L1} C_{L1} \tau_{L2}$$

$$C = r_{e3} \tau_{L2} C_1 (C_{e3} + C_1)$$

Many of the quantities in the above formulas are fixed and easily determined. The values of these fixed quantities are given in Table 2.2-1. For the calculation of  $C_{e3}$ , the alpha cut-off frequency of the 2N3227, including the emitter-transition capacitance of Q4, was assumed to be about 500 MHz at a collector current of 1 mA or higher and to be 200 MHz at 200  $\mu$ A. Including 1 pF for the emitter transition capacitance of Q4, we obtain a value for  $C_{e3}$  of 6 pF for a collector current of 200  $\mu$ A, and above 1 mA, the alpha time constant,  $\tau_{\alpha 3}$ , was fixed at 0.3 ns.

The remaining quantities depend on load, transistor type and operating bias, or temperature. For example, if the output signal exceeds 6 V, Q5a at the discriminator input saturates and  $R_{L1}$  becomes 4.9 K. Otherwise,  $R_{L1}$  approaches its maximum value of 9.4 K. Similarly, we will consider a range of  $r_{e3}$  extending from 125  $\Omega$  to near zero. The current gain,  $\beta_3$ , has a minimum value at room temperature of 100, which could

Table 2.2-1

Fixed Quantities in the Emitter-Follower Calculation

Quantity	Value
$R_{f2}$	165 K
$R_A$	15 K
$R_B$	15 K
$R_L$	30 K
$R_{L2}$	150 $\Omega$
$C_{L1}$	12 pF
$C_{ob3}$	3 pF
$C_{ob4}$	1.5 pF
$C_{ob5}$	1.2 pF
$C_1$	5.7 pF

decrease by a factor of two at low temperatures. This parameter will be considered over a range extending from 50 to 200. The modified current gain,  $\beta_3'$ , then ranges from a minimum value of 35.2, produced when  $\beta_3$  is 50 and  $r_{e3}$  is 125  $\Omega$ , to a maximum value of 200 at high collector currents and high temperatures.

For all cases both  $R_{L2}$  and  $r_{e3}$  are small compared to  $R_{L1}$ , and  $\beta_3'$  is large compared to one. Furthermore,  $C_{L1}$  can be neglected compared to  $\beta_3' C_1$ , while  $\tau_{\alpha 3}$  is small compared to  $C_1 R_{L1}$ . With these approximations,

$$A \approx \beta_3' R_{L1} \left[ C_1 + \frac{C_{L1} + C_{L2}}{\beta_3'} \right] \quad (2.2-20)$$

Because the minimum value of A exceeds 2  $\mu s$ , which is long compared to the time of gain cross-over, we will neglect one compared to pA and write for the transfer impedance

$$Z_B \approx \frac{(1 + p\tau_{\alpha 3})(1 + p\tau_{L2})}{pC_{IN3}(1 + p\tau_A)(1 + p\tau_B)} \quad (2.2-21)$$

where

$$C_{IN3} = C_1 + \frac{C_{L1} + C_{L2}}{\beta_3'}$$

$$\tau_A + \tau_B = \frac{C_1\tau_{L2} + (C_{L1} + C_{L2})(\tau_{\alpha 3} + C_1 r_{e3})}{C_{IN3}}$$

$$\tau_A \tau_B = \frac{\tau_{L2} C_1 (\tau_{\alpha 3} + C_{L1} r_{e3})}{C_{IN3}}$$

$$\tau_{L2} \gg \tau_{\alpha 3} \quad 2.2-10$$

For currents in excess of about 3 mA,  $r_{e3}$  becomes sufficiently small so that

$$\beta_3' \approx \beta_3 \quad (2.2-22)$$

and

$$\tau_A + \tau_B \approx \frac{C_{L2}(R_{L2}C_1 + \tau_{\alpha 3}) + C_{L1}\tau_{\alpha 3}}{C_{IN3}} \quad (2.2-23)$$

$$\tau_A \tau_B \approx \frac{\tau_{L2} C_1 \tau_{\alpha 3}}{C_{IN3}} \quad (2.2-24)$$

where

$$\tau_{\alpha 3} = 0.3 \text{ ns}$$

Several values of the above quantities are given in Table 2.2-2 for different values of  $\beta_3$  and  $C_{L2}$ . Because  $\tau_A$  and  $\tau_{L2}$  are closely equal, and because  $\tau_{\alpha 3}$  and  $\tau_B$  are small and also nearly equal, the transfer impedance of the emitter follower at high currents is almost purely capacitive and is given by

$$Y_B \approx \frac{1}{pC_{IN3}} \quad (2.2-25)$$

For the collector current at its minimum value of 200  $\mu$ A,  $r_{e3}$  becomes 125  $\Omega$ , and  $\beta_3'$  ranges from 35.2 for  $\beta_3 = 50$  to 75

Table 2.2-2

Emitter-Follower Values at High Collector Currents

Quantity	$\beta_3 = 50$		$\beta_3 = 200$	
	$C_{L2} = 63 \text{ pF}$	$C_{L2} = 263 \text{ pF}$	$C_{L2} = 63 \text{ pF}$	$C_{L2} = 263 \text{ pF}$
$C_{IN3}$	7.2 pF	11.2 pF	6.1 pF	7.1 pF
$\tau_{\alpha 3}$	0.3 ns	0.3 ns	0.3 ns	0.3 ns
$\tau_{L2}$	9.45 ns	39.4 ns	9.45 ns	39.4 ns
$\tau_A$	10.4 ns	27.2 ns	12.3 ns	43.1 ns
$\tau_B$	0.22 ns	0.22 ns	0.22 ns	0.22 ns

$$Y_B = \frac{(1 + p\tau_{\alpha 3})(1 + p\tau_{L2})}{pC_{IN3}(1 + p\tau_A)(1 + p\tau_B)}$$



for  $\beta_3 = 200$ . For values of capacitance in picofarads and for time constants measured in nanoseconds, then

$$\tau_A + \tau_B = \frac{2.32 C_{L2} + 17.6}{C_{IN3}} \quad (2.2-26)$$

$$\tau_A \tau_B = \frac{1.92 C_{L2}}{C_{IN3}} \quad (2.2-27)$$

where

$$\tau_{\alpha 3} = 0.75 \text{ ns}$$

Several values of the above quantities are given in Table 2.2-3. In this case  $\tau_{\alpha 3}$  and  $\tau_B$  nearly cancel, but  $\tau_{L2}$  and  $\tau_A$  are considerably further separated. Therefore, at low currents we will approximate  $Y_B$  by

$$Y_B \cong \frac{(1 + p\tau_{L2})}{pC_{IN3}(1 + p\tau_A)} \quad (2.2-28)$$

We now turn to the calculation of the response function of the double-differential amplifier (Q1, Q2, Q5). The basic theory of such an amplifier is given in Section 5 of Appendix A. From equation 5.2.1-6 (Appendix A), the voltage gain becomes

$$M_{VA} \cong \frac{-g_{e1}g_{e2}}{2 \left\{ Y_3'Y_2'' + \frac{g_{e2}Y_{c2}}{2} \right\}} \quad (2.2-29)$$

Table 2.2-3

Emitter-Follower Values at Low Collector Currents

Quantity	$\beta_3 = 50$		$\beta_3 = 200$	
	$C_{L2} = 63 \text{ pF}$	$C_{L2} = 263 \text{ pF}$	$C_{L2} = 63 \text{ pF}$	$C_{L2} = 263 \text{ pF}$
$C_{IN3}$	7.8 pF	13.2 pF	6.7 pF	9.2 pF
$\tau_{\alpha 3}$	0.75 ns	0.75 ns	0.75 ns	0.75 ns
$\tau_{L2}$	9.45 ns	39.4 ns	9.45 ns	39.4 ns
$\tau_A$	20.2 ns	46.7 ns	23.3 ns	67.5 ns
$\tau_B$	0.77 ns	0.82 ns	0.77 ns	0.82 ns

$$Y_B = \frac{(1 + p\tau_{\alpha 3})(1 + p\tau_{L2})}{pC_{IN3}(1 + p\tau_A)(1 + p\tau_B)}$$

where the subscripts refer to the transistor numbers given in Figure 1.0-1 and are different from those used in Appendix A. Thus,

$$g_{e1} = \text{transconductance of } Q_1 \quad (2.2-30a)$$

$$g_{e2} = \text{transconductance of } Q_2 \quad (2.2-30b)$$

$$Y_{c1} = \text{collector-base admittance of } Q_1 \quad (2.2-30c)$$

$$Y_{c2} = \text{collector-base admittance of } Q_2 \quad (2.2-30d)$$

$$Y_{e1} = \text{base-emitter admittance of } Q_1 \quad (2.2-30e)$$

$$Y_{e2} = \text{base-emitter admittance of } Q_2 \quad (2.2-30f)$$

$$Y_2 = \text{external load admittance on the base of } Q_2 \text{ and the collector of } Q_1 \quad (2.2-30g)$$

$$Y_3 = \text{external load admittance on the collector of } Q_2 \quad (2.2-30h)$$

The primed quantities are defined by

$$Y_2' = Y_2 + Y_{c1} + Y_{c2} \quad (2.2-31a)$$

$$Y_2'' = Y_2 + Y_{c1} + Y_{c2} + Y_{e2} \quad (2.2-31b)$$

$$Y_3' = Y_3 + Y_{c2} \quad (2.2-31c)$$

Because the impedance at the emitter of the grounded-base stage  $Q_5$  is negligibly small, and because the current gain of  $Q_5$  is close to unity for all frequencies of interest, the transfer admittance becomes

$$Y_A = \lim_{Y_3 \rightarrow \infty} Y_3 M_{VA} = \frac{-g_{e1} g_{e2}}{2Y_2''} \quad (2.2-32)$$

For the remainder of this analysis, the resistive portion of  $Y_c$  will be neglected compared to the capacitive portion because we are interested in times short compared to  $r_c C_c$  ( $\sim 10 \mu s$ ). Thus,

$$Y_{c1} \approx pC_{c1} \quad (2.2-33)$$

$$Y_{c2} \approx pC_{c2} \quad (2.2-34)$$

and  $Y_2''$  becomes

$$Y_2'' = \frac{1 + p[C_2 R_3' + C_{e2}' R_3' + C_2 R_2] + p^2 C_2 R_2 C_{e2}' R_3'}{R_3' [1 + pC_2 R_2]} \quad (2.2-35)$$

where

$$R_3' = \frac{R_3 \beta_2 r_{e2}}{R_3 + \beta_2 r_{e2}}$$

$$C_{e2}' = C_{e2} + C_{c1} + C_{c2}$$

$$C_{e2} = \frac{\tau_{a2}}{r_{e2}}$$

The transfer admittance then becomes

$$Y_A = \frac{-1}{R_A} \left\{ \frac{1 + pC_2 R_2}{(1 + p\tau_c)(1 + p\tau_D)} \right\} \quad (2.2-36)$$

where  $\tau_C$  and  $\tau_D$  are the roots of the quadratic in the numerator of equation for  $Y_2''$  (2.2-35) and  $R_A = \frac{2r_{e1}r_{e2}}{R_3}$ .

Typical values of the parameters for the double-differential amplifier are given in Table 2.2-4. The values for the emitter resistances are those at room temperature. Because the emitter resistance is proportional to the absolute temperature, variations in  $r_e$  of  $\pm 17\%$  will exist over a  $100^\circ\text{C}$  temperature range. This variation has been neglected as being small compared to the current-gain changes.

When  $\beta_2$  has its lowest value of 100, then the quantities in equation 2.2-36 become

$$R_A = 11 \, \Omega \quad (2.2-37)$$

$$\tau_C = 807 \, \text{ns}$$

$$\tau_D = 12.8 \, \text{ns}$$

For  $\beta_2$  at its highest value of 400, then

$$R_A = 3.5 \, \Omega \quad (2.2-38)$$

$$\tau_C = 2.46 \, \mu\text{s}$$

$$\tau_D = 13.2 \, \text{ns}$$

For the calculation of the stability against oscillation, we will consider  $\tau_C$  to be large compared to gain cross-over,

Table 2.2-4

Parameters of the Double-Differential Amplifier

Quantity	Value
$g_{e1}$	2000 $\mu\text{mho}$
$r_{e1}$	500 $\Omega$
$g_{e2}$	16,000 $\mu\text{mho}$
$r_{e2}$	62.5 $\Omega$
$R_2$	510 $\Omega$
$\beta_2$	100 to 400
$R_3$	61.9 K
$C_2$	100 pF
$\tau_{\alpha 2}$	2.0 ns
$C_{e2}$	32 pF
$C_{c1}$	0.8 pF
$C_{c2}$	3.0 pF
$C_{e2}'$	35.8 pF
$R_2 C_2$	51 ns

so that

$$Y_A \approx \frac{-(1 + pC_2R_2)}{pR_A\tau_C(1 + p\tau_D)} \quad (2.2-39)$$

In this case  $Y_A$  is nearly independent of  $\beta_2$  and becomes approximately

$$Y_A \approx \frac{-(1 + p51ns)}{(p8.74\Omega-\mu s)(1 + p13ns)} \quad (2.2-40)$$

The remaining problem is the calculation of the input impedance of the double-differential amplifier. From equation 5.2.1-11 of Appendix A, the input admittance becomes

$$Y_{INA} = Y_{c1} + \frac{Y_{e1}}{2} + Y_{M1} + Y_x \quad (2.2-41)$$

where

$$Y_{e1} = \frac{g_{e1}}{\beta_1} + pC_{e1}$$

$$Y_{M1} = Y_{c1} M_{V1} \approx pC_{c1} M_{V1}$$

$$Y_x = \frac{pC_x}{1 + pR_xC_x}$$

The first stage voltage gain,  $M_{V1}$ , is given by

$$M_{V1} = \frac{g_{e1}}{2Y_2''} = -Y_A r_{e2} \quad (2.2-42)$$

If the alpha cut-off frequency of Q1 is assumed to be 50 MHz at a collector current of 50  $\mu$ A, then

$$C_{e1} = 6.4 \text{ pF} \quad (2.2-43)$$

and for  $\beta_1 = 100$ ,

$$\frac{C_{e1}\beta_1}{g_{e1}} \approx 320 \text{ ns} \quad (2.2-44)$$

Therefore,  $g_{e1}/\beta_1$  will be neglected in the remainder of this analysis, giving for the feedback factor

$$F \approx \frac{-C_{f2} Y_A Z_B}{C_{f2} + \frac{C_{e1}}{2} + C_{c1} + \frac{C_x}{1 + p\tau_x} + C_{c1}M_{V1}} \quad (2.2-45)$$

where

$$\tau_x = C_x R_x = 24 \text{ ns}$$

Expanding equation 2.2-42, one obtains

$$M_{V1} = \frac{r_{e2}}{R_A} \left\{ \frac{1 + pC_2R_2}{(1 + p\tau_c)(1 + p\tau_D)} \right\} \quad (2.2-46)$$



For times short compared to  $\tau_c$  ( $\sim 1 \mu s$ ), equation 2.2-40 can be used for  $Y_A$ , yielding

$$M_{V1} \approx \frac{(1 + p51ns)}{(p140ns)(1 + p13ns)} \quad (2.2-47)$$

Because of the small value of  $C_{c1}$  (0.8 pF) compared to  $C_x$  (47 pF) and  $C_{f2}$  (10 pF),  $M_{V1} C_{c1}$  is negligible compared to the other capacitive components for all times shorter than about 0.5  $\mu s$ . Even for long times, the maximum value of  $M_{V1} C_{c1}$  is about 14 pF, which is not particularly significant compared to  $C_x + C_{f2} + \frac{C_{e1}}{2} + C_{c1}$  at 61 pF. As a result the term in  $M_{V1} C_{c1}$  will be neglected in the remainder of this analysis.

Then

$$F \approx \frac{-a Y_A Z_B (1 + p\tau_x)}{1 + pc\tau_x} \quad (2.2-48)$$

where

$$a = \frac{C_{f2}}{C_{f2} + C_{c1} + \frac{C_{e1}}{2} + C_x} = 0.164$$

$$c = \frac{C_{f2} + C_{c1} + \frac{C_{e1}}{2}}{C_{f2} + C_{c1} + \frac{C_{e1}}{2} + C_x} = 0.23$$

Substituting the gains given by equations 2.2-28 and 2.2-39, one obtains for the feedback factor

$$F \approx \frac{a(1 + p\tau_{L2})(1 + p\tau_x)(1 + pC_2R_2)}{p^2R_A\tau_C C_{IN3}(1 + p\tau_A)(1 + p\tau_D)(1 + pC\tau_x)} \quad (2.2-49)$$

The quantities in equation 2.2-49 are given in Table 2.2-5 for the collector current of Q3 equal to 200  $\mu$ A and in Table 2.2-6 for a value in excess of 3 mA. Also  $C_{L2}$  is allowed to take on its minimum value of 63 pF and a loaded value of 263 pF.

The time of gain cross-over for a 200  $\mu$ A current is given by

$$t_c = \frac{R_A \tau_C C_{IN3} \tau_A \tau_D}{a \tau_{L2} \tau_x C_2 R_2} \quad (2.2-50)$$

Similarly for the higher current, the gain cross-over time becomes

$$t_c = \sqrt{\frac{R_A \tau_C C_{IN3} \tau_A \tau_D}{a \tau_{L2} C_2 R_2}} \quad (2.2-51)$$

In both cases the time of gain cross-over is well removed from additional poles which might cause oscillation. Because the quantities in equation 2.2-49 are mostly fixed by external components and only depend weakly ( $\sim \pm 25\%$ ) on transistor parameters, we conclude that this amplifier is not likely to oscillate during reasonable excursions of temperature or transistor parameters.

Table 2.2-5

Feedback Factor Parameters near Gain Cross-Over for Low Values  
of the Collector Current of Q3

Quantity	$\beta_3 = 50$		$\beta_3 = 200$	
	$C_{L2} = 63 \text{ pF}$	$C_{L2} = 263 \text{ pF}$	$C_{L2} = 63 \text{ pF}$	$C_{L2} = 263 \text{ pF}$
a	0.164	0.164	0.164	0.164
$\tau_{L2}$	9.45 ns	39.4 ns	9.45 ns	39.4 ns
$\tau_x$	24 ns	24 ns	24 ns	24 ns
$C_2 R_2$	51 ns	51 ns	51 ns	51 ns
$R_A \tau_C$	$8.74 \Omega\text{-}\mu\text{s}$	$8.74 \Omega\text{-}\mu\text{s}$	$8.74 \Omega\text{-}\mu\text{s}$	$8.74 \Omega\text{-}\mu\text{s}$
$C_{IN3}$	7.8 pF	13.2 pF	6.7 pF	9.2 pF
$\tau_A$	20.2 ns	46.7 ns	23.3 ns	67.5 ns
$\tau_D$	13 ns	13 ns	13 ns	13 ns
$C \tau_x$	5.5 ns	5.5 ns	5.5 ns	5.5 ns
$t_C$	9.5 ns	8.9 ns	7.9 ns	5.7 ns

$$F \approx \frac{a(1 + p\tau_{L2})(1 + p\tau_x)(1 + pC_2R_2)}{p^2R_A\tau_C C_{IN3}(1 + p\tau_A)(1 + p\tau_D)(1 + pC\tau_x)}$$

Table 2.2-6

Feedback Factor Parameters near Gain Cross-Over for High  
Values of the Collector Current of Q3

Quantity	$\beta_3 = 50$		$\beta_3 = 200$	
	$C_{L2} = 63 \text{ pF}$	$C_{L2} = 263 \text{ pF}$	$C_{L2} = 63 \text{ pF}$	$C_{L2} = 263 \text{ pF}$
a	0.164	0.164	0.164	0.164
$\tau_{L2}$	9.45 ns	39.4 ns	9.45 ns	39.4 ns
$\tau_x$	24 ns	24 ns	24 ns	24 ns
$C_2 R_2$	51 ns	51 ns	51 ns	51 ns
$R_A \tau_c$	8.74 $\Omega$ - $\mu$ s	8.74 $\Omega$ - $\mu$ s	8.74 $\Omega$ - $\mu$ s	8.74 $\Omega$ - $\mu$ s
$C_{IN3}$	7.2 pF	11.2 pF	6.1 pF	7.1 pF
$\tau_A$	10.4 ns	27.2 ns	12.3 ns	43.1 ns
$\tau_D$	13 ns	13 ns	13 ns	13 ns
$c \tau_x$	5.5 ns	5.5 ns	5.5 ns	5.5 ns
$t_c$	5.0 ns	4.9 ns	4.6 ns	3.8 ns

$$F \approx \frac{a(1 + p\tau_{L2})(1 + p\tau_x)(1 + pC_2R_2)}{p^2R_A\tau_cC_{IN3}(1 + p\tau_A)(1 + p\tau_D)(1 + pc\tau_x)}$$

## 2.3 Gain Drifts

Gain drifts can arise from three principal sources. First, in direct-coupled systems variations of the amplifier output dc level contribute to offset changes. Second, drifts in the amplifier pulse gain cause variations in the slope of the transfer characteristic. Third, non-linearities at high levels caused by changing feedback factor or rate limiting produce unstable deviations from an ideal and predictable response.

### 2.3.1 DC Level Stability

The configuration of the feedback networks was chosen so that the voltage gain of this amplifier would be unity for slowly varying signals. In this way the thermally induced variations of the tracking of the emitter-base voltages of Q1a and Q1b are not amplified. In addition a very large feedback factor is present for dc signals, resulting in a highly predictable operating point. The 2N4044 is specified to have a maximum mismatch of the emitter-base voltage tracking of  $3 \mu\text{V}/^\circ\text{C}$ , producing a  $300 \mu\text{V}$  output voltage variation for a  $100^\circ\text{C}$  temperature swing. The double-differential amplifier configuration ensures a close match of the operating conditions of Q1a and Q1b, so that the good tracking inherent in these transistors can be achieved in practice.

A more serious contributor to output voltage drifts arises from the base currents in the input stage. These currents flow in the feedback resistor ( $R_{f2}$ ) and in the resistor from the base of Q1a to the -6-V supply. If the two resistors were identical and if the two base currents were equal, then the amplifier output voltage would be independent of the absolute value of the current gain of the input stage. The 2N4044 is guaranteed by the manufacturer to possess a beta match of 10% and should be selected for a minimum gain of 300 at a collector current

of 50  $\mu$ A. Then, a 50% change in the matching would result in a maximum output voltage shift of 1.24 mV. Such a change is a conservative estimate of the effect of a 100°C temperature change on this transistor. It should be pointed out that the 2N4044 contains two transistors deposited on the same substrate and enclosed in the same can. Because both transistors are manufactured at the same time in identical diffusion environments and because they continue to be exposed to the same environment and operating conditions throughout their life, long term stability of this close matching can be expected.

Because this amplifier has been designed with similar techniques as those used in the construction of highly stable power supplies, the output dc level drifts should be conservatively less than 1.6 mV. Typically drifts of the order of 0.5 mV can be expected over a 100°C temperature span, because the matching of the transistors usually well exceeds the manufacturer's worst-case specification.

### 2.3.2 Pulse-Gain Stability

The principal contributors to thermally induced gain drifts are the components in the feedback networks and the amplifier feedback factor.

The resistors and capacitors used in the feedback networks are the most stable that are commercially available without special order. (An improvement in stability by over a factor of two is possible if specially selected parts are purchased.) Metal film resistors with a temperature coefficient less than  $\pm 25$  ppM/ $^{\circ}$ C (T9) are employed in gain-determining networks. The capacitors use a compensated ceramic dielectric to provide a temperature coefficient which is also less than  $\pm 25$  ppM/ $^{\circ}$ C.

The inductor (Lf1) had to be specially constructed in order to achieve high stability in a small size. The specifications for this choke are given in Appendix C. For such an inductor, the inductance depends purely on the number of turns and on the permeability of the iron core. Because the number of turns is fixed, the principal contributor to thermal drifts is the permeability of the core. This core is constructed out of stabilized permalloy powdered iron, which has a temperature coefficient of permeability of less than  $\pm 25$  ppM/ $^{\circ}$ C.

It is also necessary to keep the series resistance of the choke small compared to 2.49 K because of the large temperature coefficient of resistance of copper wire. Typically this resistance is less than 2 ohms. Similarly, the self-resonant frequency must be large compared to the 100 KHz corresponding to the pulse-shaping time constant. The resonance of this inductor at 2.4 MHz is sufficiently high for this application.

The total gain variations from the feedback components thus becomes less than  $\pm 50$  ppM/ $^{\circ}$ C. Typically some compensation occurs, resulting in temperature coefficients in the neighborhood of 25 ppM/ $^{\circ}$ C or a gain drift of 0.25% for a  $100^{\circ}$ C temperature variation.

The remaining source of gain drifts arises from the finite value of the amplifier feedback factor. Using the analysis of the previous section and keeping only poles and zeros which are significant compared to the shaping time constant, one obtains for the feedback factor

$$F \approx \frac{(1 + p\tau)^3}{p^2 C_{f1} R_{f2} C_{IN3} R_A (1 + p\tau_c)} \quad (2.3.2-1)$$

The gain correction produced by the finite feedback factor is given approximately by

$$\frac{\Delta G}{G} \approx - \frac{1}{|F(j/\tau)|} \quad (2.3.2-2)$$

where  $G$  = gain for infinite feedback factor

$\Delta G$  = gain change caused by a finite feedback factor

$|F(j/\tau)|$  = magnitude of the feedback factor at an angular frequency equal to the reciprocal of the shaping time constant.

(In the above approximation, we have assumed that this pulse amplifier is similar to a tuned amplifier with a center frequency corresponding to the shaping time constant. This approximation has been justified in the past for similar pulse shaping configurations after tedious numerical calculations. The accuracy of the approximation is of the order of 30%.)



Substituting equation 2.3.2-1 into equation 2.3.2-2, one obtains

$$\frac{\Delta G}{G} = \frac{-2^{3/2} \tau^2}{C_{f1} R_{f2} C_{IN3} R_A \sqrt{1 + \left(\frac{\tau_C}{\tau}\right)^2}} \quad (2.3.2-3)$$

Several values for the gain shift are given in Table 2.3.2-1. The "low beta" cases assume that both the gain of Q2 and of Q3 are minimal together. Similarly the "high beta" cases are for both gains at their maximum values. The difference of these two cases then represents the difference between low and high temperatures.

From this table several dependencies become apparent. The maximum gain drift with temperature becomes 0.31% in the case of 263 pF and low collector current. The effect of changing the load capacity from 63 pF to 263 pF is an 0.2% gain decrease at low temperatures and an 0.05% decrease at high temperatures. These drifts, combined with those resulting from variations of the feedback components, indicate that the worst-case gain shift over a 100°C temperature range should be less than 0.8%. Because of partial drift compensation, total gain drifts over this range should typically be about 0.5%.

### 2.3.3 Linearity

As the magnitude of the output pulse increases, the operating currents within the amplifier change, resulting in varying feedback factor and concurrent changes in the differential gain. As a result the gain for large amplitude pulses may be different than that for small amplitude pulses, producing a non-linearity in the transfer characteristic.

Table 2.3.2-1

Gain Changes ( $\Delta G/G$ ) Caused by a Finite  
Feedback Factor

Low Beta $\beta_2 = 100$ $\beta_3 = 50$		High Beta $\beta_2 = 400$ $\beta_3 = 200$	
$I_3 = 200 \mu A$	$I_3 > 3 \text{ mA}$	$I_3 = 200 \mu A$	$I_3 > 3 \text{ mA}$
-0.284%	-0.262%	-0.127%	-0.115%
-0.480%	-0.408%	-0.174%	-0.134%

$C_{L2} = 63 \text{ pF}$

$C_{L2} = 263 \text{ pF}$

$$\frac{\Delta G}{G} = \frac{-1}{|F(j/\tau)|}$$

One contributor to such non-linearities is the dependence of the collector current of Q3 on output amplitude. If the output pulse rises at a rate of 10 V in 0.8  $\mu$ s (maximum slope for an output pulse of maximum amplitude), the current supplied by Q3 into a capacitive load of 263 pF becomes

$$i_3 = \frac{263 \text{ pF} \times 10 \text{ V}}{0.8 \text{ } \mu\text{s}} = 3.3 \text{ mA} \quad (2.3.3-1)$$

From Table 2.3.2-1 the gain correction  $\frac{\Delta G}{G}$  at low temperatures changes from -0.48% for small currents to -0.408% for currents of the above order of magnitude. As a result an 0.072% differential non-linearity will result from this effect. For higher temperatures or lower capacitances this effect is reduced.

Another contributor to such non-linearities arises from the current required to swing the base of Q3 for large output amplitudes. The resistive component of this current is reduced by bootstrapping  $R_A$ . However, the current required to charge the capacitance at this base ( $C_{IN3}$ ) must be supplied from the second stage. The maximum value of this current becomes

$$i_{2c} = 13.2 \text{ pF} \frac{10 \text{ V}}{0.8 \text{ } \mu\text{s}} = 165 \text{ } \mu\text{A} \quad (2.3.3-2)$$

If one includes about 135  $\mu$ A for the base drive of Q3, 300  $\mu$ A of current swing must be available from Q2. Because 400  $\mu$ A is conducting through Q2b in the quiescent state, the 300  $\mu$ A can be safely supplied by the second stage.

This current unbalance results in a change in the feedback factor, which is inversely proportional to the sum of

the emitter resistances of Q2a and Q2b. This sum goes from a value of 125  $\Omega$  at balance to a value of 290  $\Omega$  at maximum unbalance. The worst-case non-linearity caused by this decrease in feedback factor becomes 0.66% when the load capacity is 263 pF and the current gains are low. Typically differential non-linearities of the order of 0.3% to 0.4% should be expected for less extreme values of beta and load capacity.

### 3.0 DISCRIMINATOR DESIGN ANALYSIS

The postamplifier is direct-coupled to a discriminator, which is a biased one-shot with a stable threshold. With no input signal, the amplifier rests at -6 V, and the base of Q5a is biased 0.1 V more negatively than the base of Q5b. Q6 is then cut off, and Q7 holds the output near +6 V. When the positive output from the amplifier is large enough to overcome the 0.1-V bias, Q5a starts to conduct, eventually causing Q6 to conduct also. Positive feedback then produces regeneration through C1 such that Q6 saturates, placing the output near ground. After the charge on C1 decays, the circuit returns to its quiescent state with C1 being rapidly recovered by the diode D1. The proper pulse width can be obtained by using a suitable value for C1.

With the exception of the timing capacitor (C1), this circuit is also completely dc coupled to avoid baseline shifts and unnecessary dead times at high counting rates. The power required by this circuit is 4.9 mW.

#### 3.1 Threshold Stability

The stability of the discriminator threshold depends on the gain and voltage matching of Q5a and Q5b. Readily available matched, differential-amplifier transistor pairs provide a total drift of about 0.5 mV for temperatures between -50°C and +50°C. Variations of the resistors in the bias network for the base of Q5b add to the threshold drifts. If matched metal-film resistors are used, drifts from this cause will be about 0.2% over a 100°C temperature span.

A further error results from the fact that the voltage at the base of Q6 must swing by about 0.4 V, while the collector must swing about 0.5 V, in order for the output voltage to start moving negatively. These voltage swings require that

about 5 pC be delivered to the 3 pF collector-base capacitance and to the 3 pF emitter-transition capacitance of Q6. The effect of this charge on the threshold can be calculated as follows:

The current flowing into the capacitance at the base of Q6 can be written as

$$i_c = I_o - i_{c2} \qquad i_{c2} < I_o \qquad (3.1-1)$$

$$i_c = 0 \qquad i_{c2} > I_o$$

where

$i_{c2}$  = current flowing into the collector of Q5b

$I_o$  = bias current in R4

For input voltages (V) near the threshold voltage ( $V_T$ ) on the base of Q5b, the collector current becomes

$$i_{c2} \cong I_o - \frac{(V - V_T)}{2r_e} \qquad (3.1-2)$$

where  $r_e$  is the emitter resistance of Q5, given by  $\frac{kT}{qI_o}$ , and it has been assumed that the amplifier is biased such that the collector current for  $V = V_T$  is equal to the current in R4. Thus, the current into the capacitance becomes

$$i_c = \frac{(V - V_T)}{2r_e} \qquad V > V_T \qquad (3.1-3)$$

$$i_c = 0 \qquad V < V_T$$

When the input pulse is barely large enough to trigger the discriminator, the peak input voltage ( $V_p$ ) should nearly equal the threshold voltage, if the discriminator is to have a stable and passively determined threshold. Therefore, one is led to use a simplified form for  $V(t)$  produced by expanding it in a power series to second order about the peak. From equation 3.2-39 of Appendix B,  $V(t)$  is given approximately by

$$V(t) = \frac{V_p t'(2-t') e^{-t'}}{0.231 \times 2} - 6 \quad (3.1-4)$$

where

$$t' = t/\tau$$

$$V_p = \text{peak value of the input signal pulse above } -6 \text{ V}$$

and the single-integrated, double-differentiated waveform has been used as an approximation to equation 2.1-6. (Note that both the amplifier and the discriminator are referenced to the -6-V supply.)

The power series expansion yields

$$V(t) \approx V_p \left\{ 1 - 1.7 (t_p' - t')^2 \right\} - 6 \quad (3.1-5)$$

where

$$t_p' \tau = \text{time at which } V(t) \text{ passes through its first maximum}$$

$$t_p' = 0.586$$

and the capacitor-charging current becomes

$$i_c(t) \approx \frac{\Delta V}{2r_e} \left\{ 1 - x^2 \right\} \quad |x| < 1 \quad (3.1-6)$$

$$i_c(t) = 0 \quad |x| > 1$$

where

$\Delta V$  = amount by which the peak input voltage exceeds the threshold voltage =  $V_p - V_T - 6$

$$x^2 = \frac{1.7 V_p (t - t_p)^2}{\Delta V \tau^2}$$

The charge supplied to the capacitor  $Q_c$  then becomes

$$Q_c = \int_{x=-1}^{x=+1} i_c(t) dt = \frac{2(\Delta V)^{3/2} \tau}{3r_e \sqrt{1.7V_p}} \quad (3.1-7)$$

For  $V_p$  nearly equal to the difference of  $V_T$  from -6 V, the relative threshold shift  $\frac{\Delta V}{V_T}$  is given by

$$\frac{\Delta V}{V_T - 6} \approx 1.56 \left( \frac{r_e Q_c}{\tau V_T - 6} \right)^{2/3} \quad (3.1-8)$$



For our proposed design

$$V_{T-6} = 0.1 \text{ V} \quad (3.1-9a)$$

and

$$\frac{\Delta V}{V_{T-6}} = 5\% \quad (3.1-9b)$$

Over a 100°C temperature range changes in  $r_e$  and changes in  $Q_c$  resulting from thermal variations in the emitter-base voltage of Q6 will cause a 32% variation in the above correction, resulting in a threshold drift of 1.6%. This drift is partially compensated by two effects. First, the diodes in the collector circuit of Q5b keep the voltage swing at the base of Q6 relatively constant as a function of temperature. Second, the fraction of the standing current in R6 which is flowing in R4 at triggering varies with temperature because of a small dependence on the forward voltage drops of Q5 and Q6. This latter effect compensates for the charge variations caused by the changing of the collector voltage swing of Q6 required for triggering. The total drift from these effects is of the order of 0.8 mV over a 100°C temperature range.

The total rms thermal drift of the discriminator threshold level, including variations in the postamplifier dc output voltage, is then estimated to be 1.6 mV or 1.6% for temperatures between -50°C and +50°C. The maximum, worst-case drift becomes 3.2 mV or 3.2%. The drifts are given in Table 3.1-1.

Table 3.1-1

Calculated Drifts in Discriminator Threshold

Cause	Magnitude
Emitter-base voltage and current gain of Q5	0.5 mV
Resistor drifts	0.2 mV
Charge on the base of Q6, diodes in the collector of Q5b, and emitter-base diode drifts of Q5 and Q6	0.8 mV
Base current of Q1	1.2 mV
Emitter-base voltage of Q1	0.3 mV
Total rms drift	1.6 mV
Fraction of 100 mV threshold	1.6%
Maximum drift	3.2 mV
Maximum fraction of 100 mV threshold	3.2%

### 3.2 Pulse Width and Recovery Time

The discriminator output pulse width is determined by the output voltage, the bias level, and the decay time of C1. When the discriminator is triggered, the voltage on the base of Q5b with respect to the base of Q5a is given by

$$V_2 = -V_O e^{-t/\tau_f} + V_T \quad (3.2-1)$$

where

$V_2$  = voltage on the base of Q5b

$V_O$  = amplitude of the output voltage swing

$t$  = time from triggering

$\tau_f = R_5 C_1$

If the input pulse has returned to zero by the time that the voltage across C1 has decayed sufficiently for the circuit to return to its quiescent state, then the pulse width ( $T_w$ ) is given by

$$T_w = \tau_f \ln \frac{V_O}{V_T} \quad (3.2-2)$$

For the discriminator proposed here,  $\tau_f$  is 600 ns and  $T_w$  becomes 2.4  $\mu$ s.

When the discriminator returns to its quiescent state, the capacitor C1 discharges through D1, leaving the base voltage of Q5b initially near -5.8 V. (A hot-carrier diode is used for D1 because of its low forward-voltage drop and fast recovery time.) This shifted threshold voltage then decays toward the nominal -6.0-V level with a 600-ns time constant. After 1.4  $\mu$ s, this error in the threshold will have decayed to about 20 mV. The discriminator will then be ready to trigger on another input pulse exceeding the threshold by a factor of 1.2.

## 4.0 TESTING

Extensive tests were performed on the amplifier-discriminator system to verify proper operation of the circuits. The procedure used in performing these tests is described in Section 4.1, while the actual test results are presented in Section 4.2.

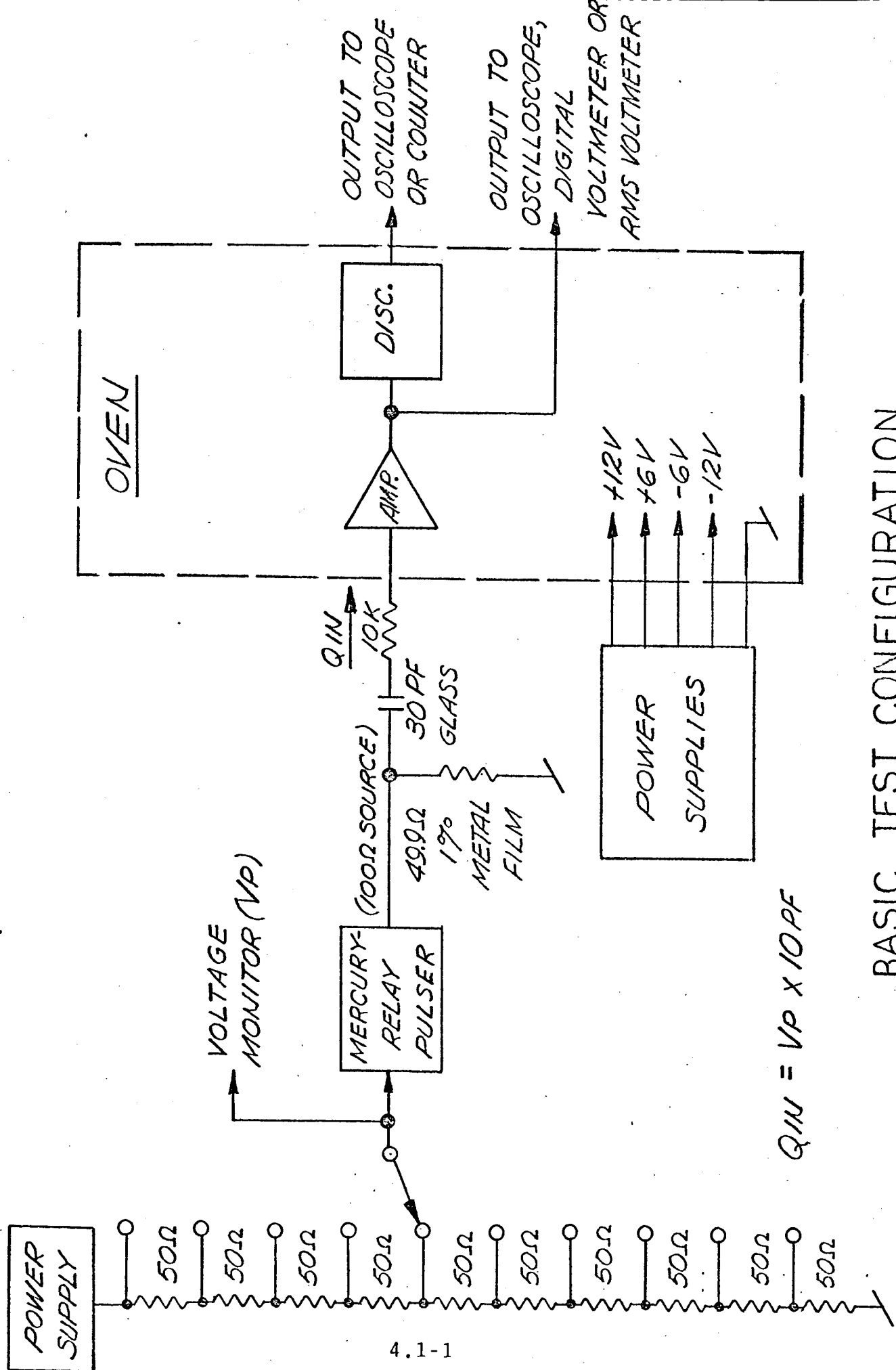
### 4.1 Test Procedures

The basic test configuration is illustrated by Figure 4.1-1. Precise voltage pulses are generated by a mercury-relay pulser, such as the RIDL Model 47-7. This pulser was used with an external power supply and a precision resistive divider, so that a reference voltage more accurately known than that internal to the pulser could be generated.

The voltage pulses were converted to current pulses by a resistor-capacitor combination at the amplifier input. Because the amplifier input appeared as a virtual ground, the input current through the 30 pF capacitor had an exponentially decaying waveform with a 300 ns time constant, and the total charge was determined by the pulser reference voltage and by the coupling capacitor to the amplifier. This current pulse simulated the NaI - photomultiplier system output signal.

For temperature tests, the amplifier-discriminator system was placed in a temperature-controlled oven. The pulser, its coupling network, the power supplies and the performance monitoring equipment were outside the oven to avoid unnecessary measurement errors.

For the amplifier gain tests the output pulse was observed on a Tektronix 545B oscilloscope with a Type W plug-in unit.



BASIC TEST CONFIGURATION  
FIGURE 4.1-1

This plug-in unit allows accurate pulse amplitude measurements, which are independent of oscilloscope gain. A stable, adjustable dc voltage is generated in the plug-in unit and subtracted from the input signal. By adjusting this voltage such that the pulse peak just reaches the baseline on the oscilloscope viewing screen, the pulse amplitude becomes equal to the easily measured dc voltage. The amplifier output pulses can also be measured using a stable, precision pulse-height analyzer if such an instrument is available.

The amplifier output dc level could be monitored by connecting a digital voltmeter to the output. For this measurement no input signals should be applied to the amplifier, and the value of the -6-V supply should be monitored because it is used as the reference for the amplifier. Similarly, the amplifier noise level can be determined by connecting a wideband rms voltmeter to the amplifier output. A suitable instrument is the Hewlett-Packard Model 3400 A.

The discriminator threshold was monitored by connecting the discriminator output pulse to a scaler connected as a frequency meter. The mercury-relay pulser was synchronized to the ac power line so that it ran at a stable rate of 120 pulses per second. The pulser power supply was then adjusted so that the frequency meter indicated  $60 \pm 5$  Hz over several one-second averaging intervals. The value of the pulser power supply was then taken as being proportional to the discriminator threshold. This technique allows the center of the signal-plus-noise Gaussian amplitude distribution to be placed accurately at the discriminator threshold.

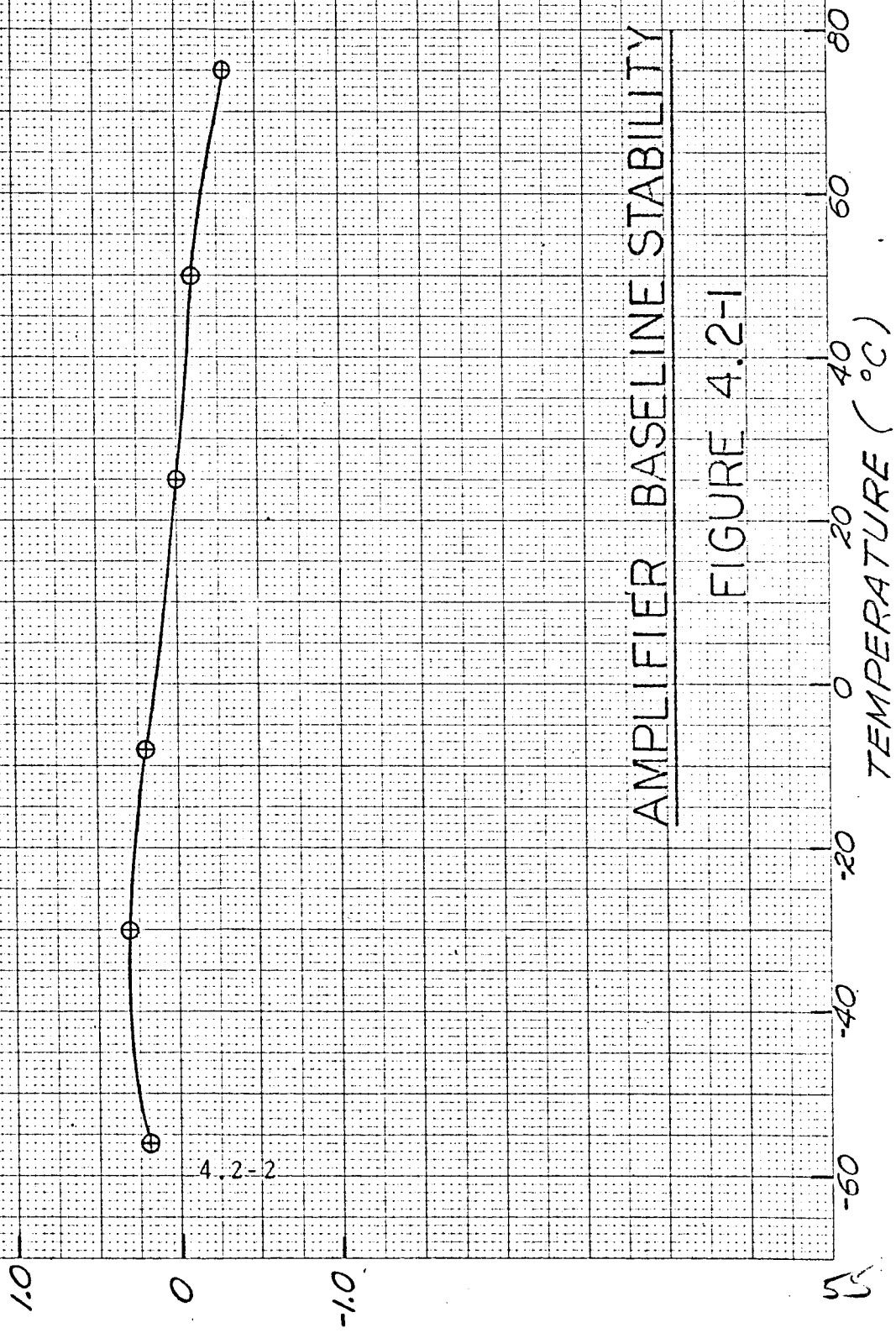
## 4.2 Test Results

The results of several tests performed at room temperature ( $\sim 20^{\circ}\text{C}$ ) are given in Table 4.2-1. From these data it is apparent that the gain and discriminator threshold desired have been achieved. Also, the dc output level equals the -6-V reference within 4 mV, and the rms amplifier noise of 300  $\mu\text{V}$  is small compared to the analyzer channel width of 39 mV.

The effects of temperature variations are illustrated in Figures 4.2-1, 4.2-2 and 4.2-3. For temperatures between  $-50^{\circ}\text{C}$  and  $+50^{\circ}\text{C}$ , the amplifier baseline drifts by 0.5 mV and the gain changes by 0.4%. Over the same temperature range, the discriminator threshold drifts by 0.75%, including amplifier drifts, and by 0.32%, excluding amplifier drifts.

Because of the extensive theoretical analysis which preceded the construction of actual hardware, the behavior of the circuits during test could be generally predicted in advance. The agreement of the test data with the theoretical predictions within the accuracies of measurement and calculation generates confidence that the worst-case estimates for gain drift, linearity, etc. are correct and actually do correspond to the operation of actual hardware.

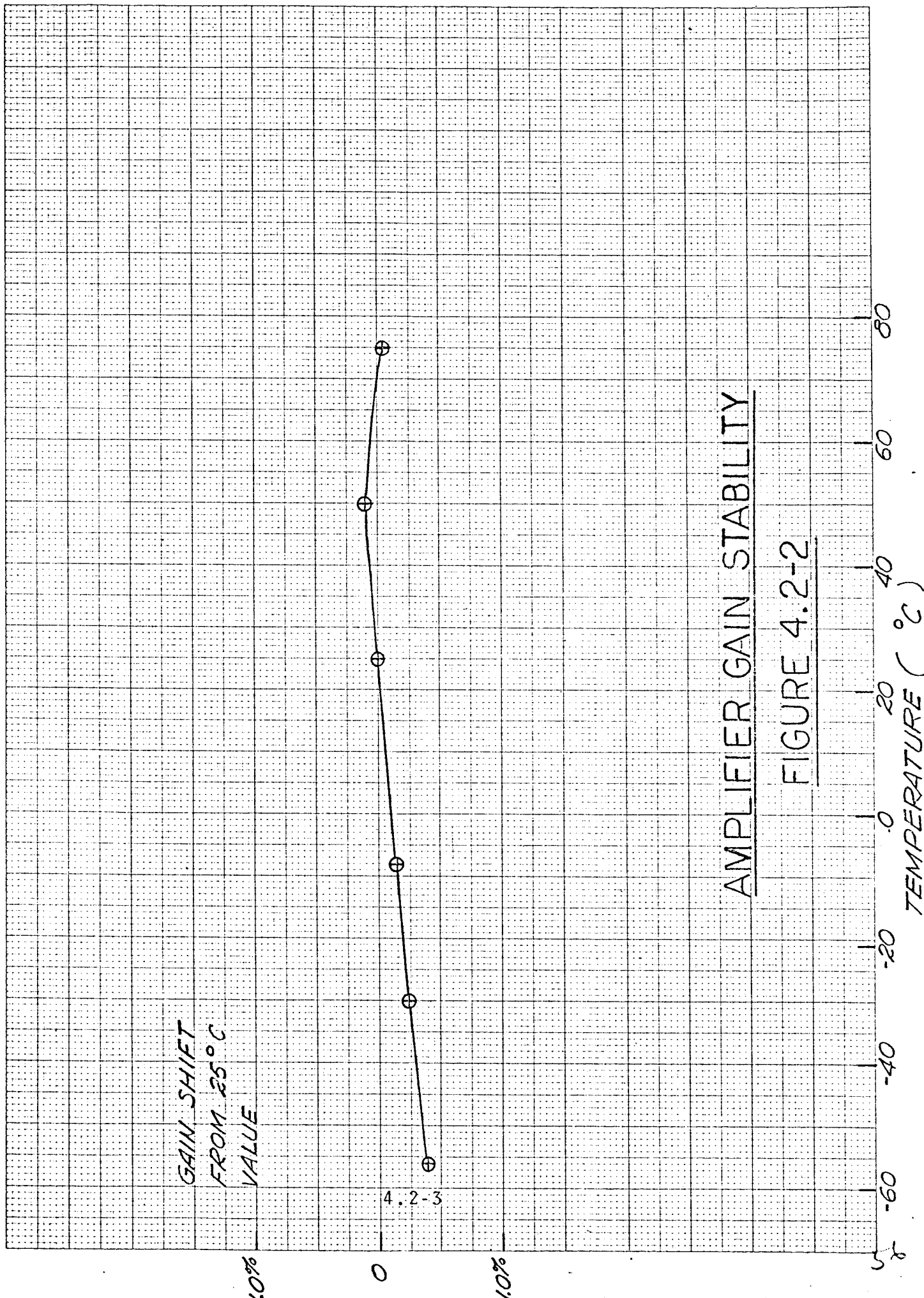
SHIFT IN DC  
OUTPUT LEVEL  
FROM 25°C VALUE  
(mV)



AMPLIFIER BASELINE STABILITY

FIGURE 4.2-1





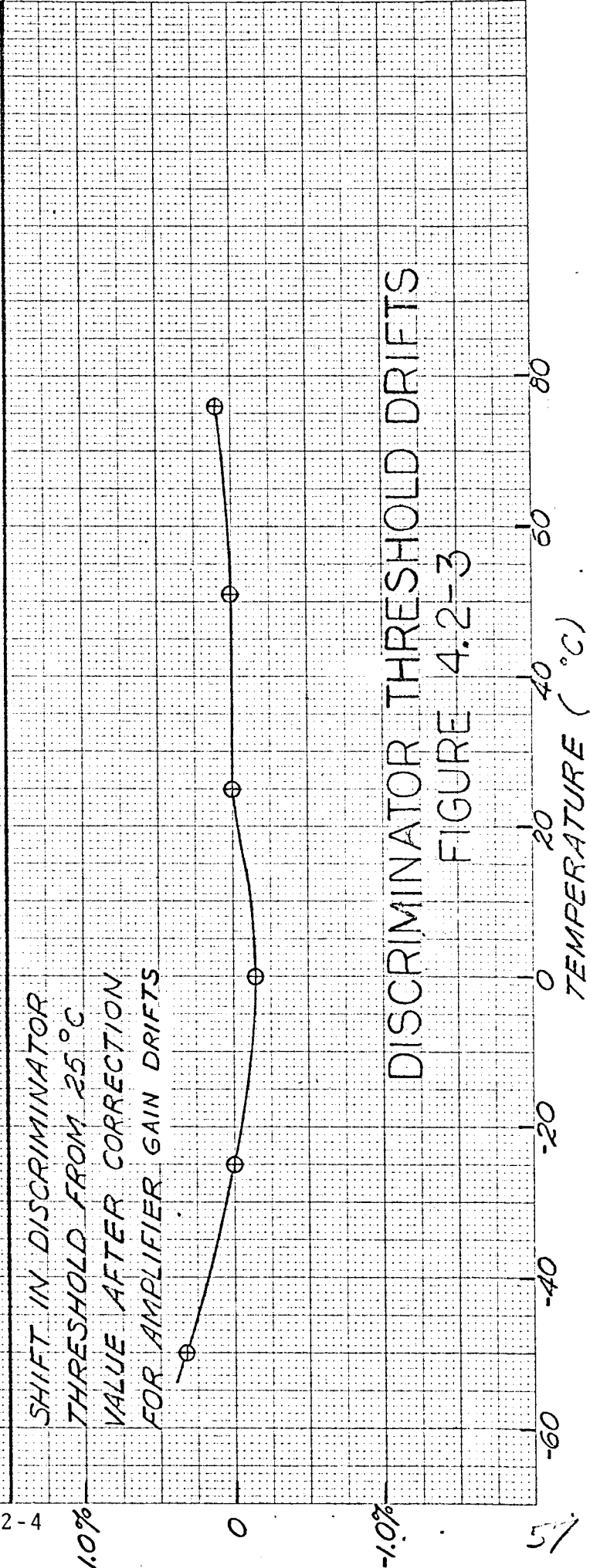
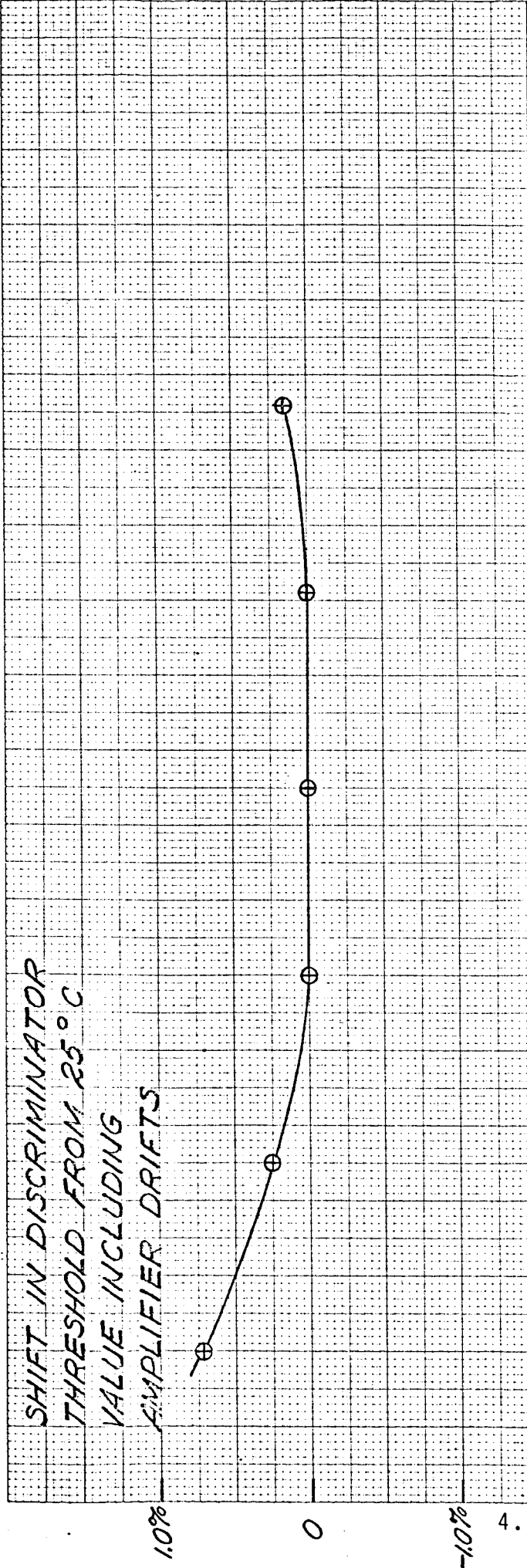
GAIN SHIFT  
FROM 25°C  
VALUE

4.2-3

AMPLIFIER GAIN STABILITY

FIGURE 4.2-2

TEMPERATURE ( °C )



DISCRIMINATOR THRESHOLD DRIFTS  
FIGURE 4.2-3

Table 4.2-1

Results of Room Temperature Tests

Parameter	Value
Conversion gain	0.0515 V/pC
Conversion capacitance	19.4 pF
Deviation of output dc level from the value of the -6-V supply	-3.7 mV
Discriminator threshold referred to the amplifier input	1.98 pC
Discriminator threshold referred to the amplifier output	102 mV
RMS amplifier output noise	300 $\mu$ V

Appendix A

Linear Circuit  
Design Principles

Linear Circuit  
Design Principles

By

J. H. Marshall

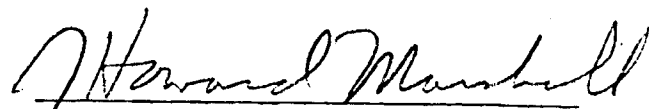
ATC Internal Report Number 1

March 15, 1966

Revised September 22, 1966

Analog Technology Corporation  
3410 E. Foothill Boulevard  
Pasadena, California 91107

Approved by:



J. Howard Marshall  
Vice President  
Advanced Planning

# Linear Circuit Design Principles

## Contents

	<u>Page No.</u>
1.0 INTRODUCTION	1.0-1
2.0 BASIC FEEDBACK THEORY	1.0-1
2.1 The Difference Between an Amplifier and an Oscillator	2.1-1
2.2 Conditions for Oscillation	2.2-1
2.3 Special Cases	2.3-1
2.3.1 Single Pole	2.3-1
2.3.2 Two Poles	2.3-3
2.3.3 Two Poles and One Zero	2.3-4
3.0 TRANSISTOR EQUIVALENT CIRCUITS	3.0-1
3.1 Grounded Base	3.0-1
3.2 Grounded Emitter	3.2-1
3.3 Grounded Collector	3.3-1
4.0 SINGLE TRANSISTOR AMPLIFIERS	3.3-1
4.1 The Grounded Emitter Amplifier	3.3-1
4.1.1 Input Admittance and Voltage Gain Representation	4.1-7
4.2 The Emitter Follower	4.2-1
4.2.1 Bootstrapped Source Resistance	4.2-4
4.2.2 Parallel RC Load and Source Impedances	4.2-5
4.2.3 Series RC Load Impedance	4.2-8
4.2.4 Input Admittance and Voltage Gain Representation	4.2-11
4.3 The Grounded Base Amplifier	4.3-1
5.0 THE DOUBLE DIFFERENTIAL AMPLIFIER	5.0-1
5.1 General Solution	5.0-1
5.2 Symmetrical, Single-Ended Double Differential Amplifier	5.2-1
5.2.1 Input Admittance and Voltage Gain Representation	5.2-11

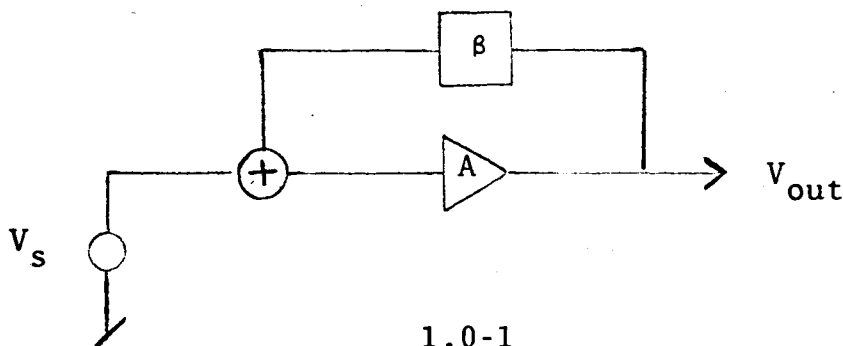
## 1.0 INTRODUCTION

If a high degree of gain stability is required in a linear amplifier, feedback is generally employed. The analysis of such a feedback amplifier can become complicated if a thorough understanding of gain drifts, transient response and oscillations is needed. Although many texts thoroughly develop feedback theory, a concise exposition of its application to practical design does not seem to be available. Therefore, these notes have been compiled to provide a general summary of the principals of linear circuit design and a ready reference of solved problems.

Basic knowledge of linear differential equations and transform methods of solution are assumed, together with the usual techniques of circuit analysis. The reader not familiar with these items is referred to such texts as Thomason, Linear Feedback Analysis. The purpose of these notes is to generate simplified expressions useful in performing practical design, rather than providing a rigorous mathematical treatise on a subject already overworked. The details of the analysis are included to aid in finding errors and also to make possible generalization to cases where stated approximations are no longer valid.

## 2.0 BASIC FEEDBACK THEORY

The usual feedback system is illustrated in the sketch below.



For such a system, the output is related to the input by:

$$\frac{V_{out}}{V_s} = A_{CL} = \frac{1}{\beta} \left[ \frac{F}{1-F} \right] \quad (2.0-1)$$

where  $F$  = feedback factor =  $A\beta$

Generally the feedback attenuation network ( $\beta$ ) depends only on passive elements with all active parameters lumped into the amplifier ( $A$ ). By differentiating the closed-loop gain ( $A_{CL}$ ) with respect to  $A$ , one can find the dependence of this gain on active elements, that is:

$$\left( \frac{dA_{CL}}{A_{CL}} \right) \approx \left( \frac{dA}{A} \right) \left( \frac{-1}{F} \right) \quad (2.0-2)$$

for  $F \gg 1$

From this, one sees that changes in open loop gain ( $dA/A$ ) are attenuated by the feedback factor. Because the open loop gain typically drifts from age, temperature, or other causes by 100%, the accuracy of the closed loop gain of an amplifier is of the order of the reciprocal of the feedback factor. This result is one of the primary motivations for the use of negative feedback.

Not all feedback is negative. Positive feedback is useful for regenerative circuits such as discriminators or flip-flops. Also, using positive feedback are oscillators (sine-wave or otherwise) and various waveform generators. Most such circuits are characterized by the fact that any input signal from noise or otherwise produces a divergent response limited by amplifier non-linearities.



## 2.1 The Difference Between an Amplifier and an Oscillator

A vexing problem in feedback circuit design is the production of an oscillator when an amplifier is desired or vice-versa. The difference between these two types of circuits depends on the closed-loop transfer function. Using Laplace transforms with "p" as the transform variable, the time dependence of the output voltage to an input stimulus can be expressed as

$$V_{\text{out}}(p) = A_{\text{CL}}(p) V_s(p) \quad (2.1-1)$$

$$\text{where } V(p) = \int_0^{\infty} V(t) e^{-pt} dt$$

For circuits containing only resistors, capacitors and inductors or active elements which can be equivalently expressed in terms of the above, the closed loop transfer function becomes the ratio of two polynomials of finite order with real coefficients, that is:

$$A_{\text{CL}}(p) = \frac{\sum_{i=0}^N a_i p^i}{\sum_{j=0}^M b_j p^j} = \frac{N(p)}{D(p)} \quad (2.1-2)$$

Such a polynomial will have as many roots ( $\alpha_k, \beta_k$ ) as its order, where the roots are defined by

$$\sum_{i=0}^N a_i \alpha_k^i = 0 \quad (2.1-3a)$$

$$\sum_{j=0}^M b_j \beta_k^j = 0 \quad (2.1-3b)$$

2.1-1

Because  $A_{CL}(\alpha_k) = 0$ , the  $\alpha_k$  are called the "zeros" of the closed loop transfer function; similarly because  $A_{CL}(\beta_k) = \infty$ , the  $\beta_k$  are the poles.

The poles and zeros can be either positive, negative, or complex conjugates. Considering a delta-function source function so that  $V_s(p) = 1$ , then the transform of the output voltage equals the closed-loop transfer function. The placement of the poles of this transfer function then determines the basic type of response of the circuit.

The denominator of the transfer function can be written as follows:

$$D(p) = \prod_{k=0}^M C_k (p - \beta_k) \quad (2.1-4)$$

explicitly denoting the fact that  $D(\beta_k) = 0$ . The inverse transform then assumes the form:

$$V_{out}(t) = \sum_{k=0}^M d_k \exp(\beta_k t) \quad (2.1-5)$$

where the  $d_k$  can be polynomials in  $t$  if equal poles are present. From this expression, five types of response are possible:

1. Decaying exponential -  $\beta_k$  negative
2. Decaying sinusoid -  $\beta_k$  complex with negative real part
3. Divergent exponential -  $\beta_k$  positive
4. Divergent sinusoid -  $\beta_k$  complex with positive real part
5. Steady sinusoid -  $\beta_k$  pure imaginary

Oscillators and regenerative circuits make use of cases 3 to 5 where the poles lie in the right half of the p-plane, including the imaginary axis. Cases 1 and 2 correspond to stable amplifiers with the poles lying in the left half plane. (Case 2 with large complex parts of  $\beta_k$  is usually not very desirable.)

## 2.2 Conditions for Oscillation

Although the conditions on the closed-loop transfer function separating amplifiers and oscillators appear straightforward, the practical problems of analyzing this function directly may be insuperable. Because the feedback factor (F) may be far easier to calculate, many attempts have been made to determine circuit response by examining the characteristics of F.

If the restriction to cases of resistors, capacitors and inductors or to active elements representable by the above is continued, then the feedback factor is also the quotient of two polynomials of finite order and real coefficients. The placement of the poles and zeros of this function can now be used to deduce the stability of the closed-loop system.

A divergent response or steady oscillation occurs only if the closed-loop transfer function ( $A_{CL}$ ) has poles in the right half of the p-plane, including the imaginary axis. If the open loop gain (A) and the feedback network ( $\beta$ ) result from stable systems, then they can have no poles in the right half plane. From equation 2.0-1, one then deduces that the only term possibly contributing to poles of  $A_{CL}$  in the right half plane is  $\frac{1}{1-F}$ . Thus, the only poles of  $A_{CL}$  in the right half plane result from zeros of  $1-F$ , which can have no poles in the right half plane because F has no poles there.

The feedback factor  $F$  as a function of the complex variable  $p$  can be viewed as a mapping of contours in the complex  $p$ -plane into contours in the complex  $F$ -plane. If  $F$  results from practical circuits employing at least one active element, it will tend to vanish at very large frequencies, so that

$$F \rightarrow 0$$

(2.2-1)

as  $|p| \rightarrow \infty$

A fundamental theorem of complex variable theory<sup>(1)</sup> holds that the mapping of a closed contour in the  $p$ -plane encircles the origin in the  $F$ -plane for every zero enclosed, if no poles are also enclosed. To investigate the stability of  $A_{CL}$ , the contour must contain the entire right half of the  $p$ -plane. Such a contour is the imaginary axis and a semi-circle with a radius approaching infinity. By translating the origin to  $(1,0)$ , the statement can be made that  $F$  will encircle the point  $(1,0)$  for every zero of  $1-F$  in the right half plane. Because  $F$  vanishes on the semi-circle, only values along the imaginary axis need be considered. Therefore, one is led to the Nyquist criterion for stability which states that an amplifier will be stable if  $F(j\omega)$  does not encircle the point  $(1,0)$  for all frequencies between  $-\infty$  and  $+\infty$ . The negative frequencies can be eliminated by the observation that

$$F(-j\omega) = F^*(j\omega)$$

(2.2-2)

because  $F$  contains polynomials with real coefficients.

A sufficient (but not necessary) condition that the Nyquist criterion be satisfied is that the amplitude of  $F$  always be less than one when the phase shift reaches  $180^\circ$ . Such a requirement

---

(1) Thomason, Linear Feedback Analysis, pp 133-142

excludes the positive real axis beyond (1,0), making encircling (1,0) impossible.

Because  $F$  can be written as the quotient of two finite order polynomials, then

$$F(j\omega) = -F_0 \frac{\prod_{j=0}^M (1 + j\omega\tau_j^0)}{\prod_{i=0}^N (1 + j\omega\tau_i^p)} \quad (2.2-3)$$

where  $F_0 = -F(0)$

and  $\tau_j^0 = \frac{-1}{\gamma_j}$   $\gamma_j = \text{zero of } F [\text{i.e. } F(\gamma_j) = 0]$

$\tau_i^p = \frac{-1}{\delta_i}$   $\delta_i = \text{pole of } F [\text{i.e. } F(\delta_i) = 0]$

From complex variable theory,  $F(j\omega)$  may also be written as

$$F(j\omega) = B(\omega) \exp \left[ j \left( \pi + \phi(\omega) \right) \right] \quad (2.2-4)$$

where  $B$  and  $\phi$  are real numbers given by

$$B(\omega) = F_0 \sqrt{\frac{\prod_{j=0}^M 1 + (\omega\tau_j^0)^2}{\prod_{i=0}^N 1 + (\omega\tau_i^p)^2}} \quad (2.2-5a)$$

$$\phi(\omega) = \sum_{j=0}^M \text{Arctan } \omega\tau_j^0 - \sum_{i=0}^N \text{Arctan } \omega\tau_i^p \quad (2.2-5b)$$

The stability requirement can then be expressed as

$$B(\omega_0) < 1 \quad (2.2-6)$$

where

$$\phi(\omega_0) = -\pi$$

Steady oscillation will occur if the phase shift reaches  $180^\circ$  at a frequency for which the amplitude is one. In this case some poles of  $A_{CL}$  lie on the imaginary axis. For larger values of  $A$ , complex poles with positive, real parts exist and give rise to divergent responses.

An asymptotic expansion of terms similar to those appearing in equation 2.2-5 can be performed as follows:

$$\left. \begin{array}{l} \sqrt{1 + (\omega\tau)^2} \approx 1 \\ \text{Arctan } \omega\tau \approx 0 \end{array} \right\} \text{ for } 1 > \omega\tau \quad (2.2-7a)$$

$$\left. \begin{array}{l} \sqrt{1 + (\omega\tau)^2} \approx \omega\tau \\ \text{Arctan } \omega\tau \approx \pi/2 \end{array} \right\} \text{ for } 1 < \omega\tau \quad (2.2-7b)$$

Then

$$B(\omega) \approx \frac{F_0}{\omega^k} \frac{\prod_{\substack{\text{For } \\ \omega\tau_j^0 > 1}} (\tau_j^0)}{\prod_{\substack{\text{For } \\ \omega\tau_i^p > 1}} (\tau_i^p)} \quad (2.2-8)$$

$$\phi(\omega) \approx \frac{-k\pi}{2}$$

where  $k$  = the number of poles with  $\omega\tau^p > 1$  minus the number of zeros with  $\omega\tau^o > 1$ .

In this approximation, a "frequency of gain cross-over" ( $\omega_c$ ) for which  $B = 1$  can be calculated according to

$$\omega_c = \left\{ F_o \frac{\prod_{\omega_c \tau_j^o > 1} \tau_j^o}{\prod_{\omega_c \tau_i^p > 1} \tau_i^p} \right\}^{1/k} \quad (2.2-9)$$

A corresponding time,  $t_c$ , is given by

$$t_c = \frac{1}{\omega_c} \quad (2.2-10)$$

The amplifier will only be stable if  $k \leq 2$  for  $\omega \leq \omega_c$ . The case for  $k = 2$  can be ambiguous because of additional phase shift neglected in this approximation coming from higher frequency poles.

The convenience of the asymptotic approximation becomes clearer if one considers the behavior of the logarithm of  $B(\omega)$  as a function of the logarithm of the frequency. If such a log-log plot is made, then only straight lines with slopes proportional to  $k$  are involved. As the frequency increases past a pole, the slope steepens, while a zero causes the curve to flatten. By using log-log paper for such plots, the added complexity of calculating logarithms is avoided. Usually it is also pointless to multiply the logarithm of  $B$  by 20 to obtain db or to divide  $\omega$  by  $2\pi$  to use frequency in Hertz. Because  $\tau$  is often directly calculated, the abscissa can sometimes

be conveniently plotted in units of time given by the reciprocal of  $\omega$ .

A typical case with two poles and one zero is given in Figure 2.2-1. From this type of graph, the influence of the "break points" at the poles and zeros is clearly illustrated.

## 2.3 Special Cases

The following special cases often result in practice either exactly or approximately.

### 2.3.1 Single Pole

Sometimes, at least for frequencies below gain cross-over, the feedback factor contains a single pole. Because this case never oscillates, the use of such a dominant time constant is a simple method of achieving amplifier stability. The feedback factor can then be written as

$$F = \frac{-F_o}{(1 + p\tau)} \quad (2.3.1-1)$$

and the closed loop gain becomes

$$A_{CL} = \frac{1}{\beta} \left\{ \frac{F}{1-F} \right\} = \frac{-1}{\beta} \left\{ \frac{F_o}{1+F_o} \right\} \left\{ \frac{1}{1+p\frac{\tau}{F_o+1}} \right\} \quad (2.3.1-2)$$

For  $F_o \gg 1$ ,  $A_{CL}$  becomes approximately

$$A_{CL} \cong \frac{-1}{\beta} \left\{ \frac{1}{1+pt_c} \right\} \quad (2.3.1-3)$$

where  $t_c = \text{gain cross-over time} = \frac{\tau}{F_o}$



$$F(p) = \frac{F_0(1 + p\tau_1^0)}{(1 + p\tau_1^p)(1 + p\tau_2^p)}$$

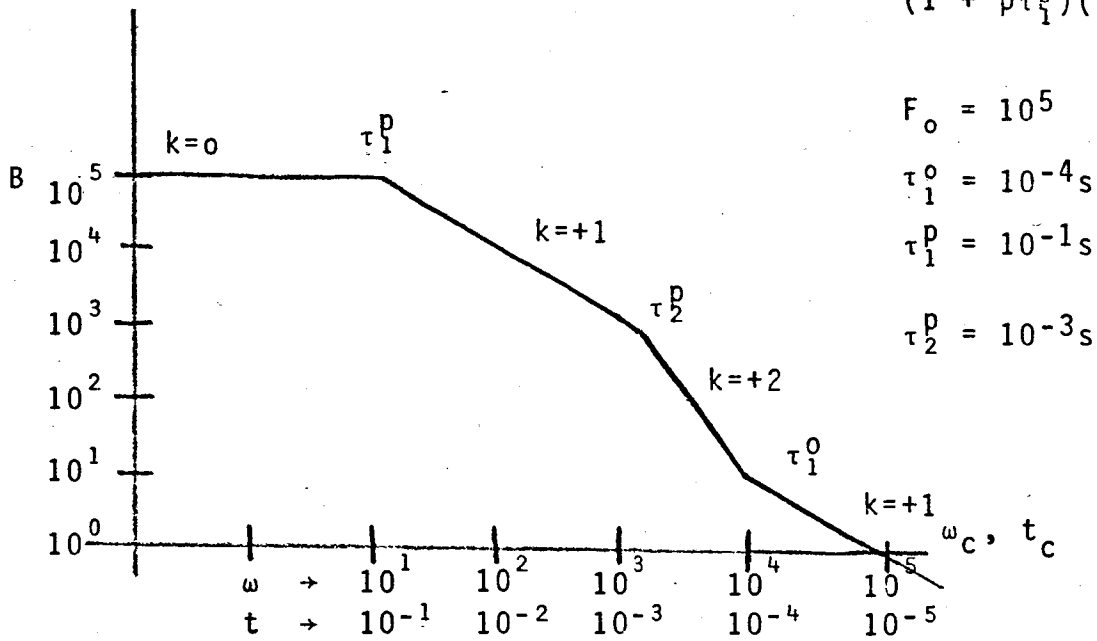


Figure 2.2-1 - Typical Asymptotic Response Plot

Thus, the rise-time of the closed-loop response is decreased from that of the open-loop response by the feedback factor - at least if the amplifier internally has sufficient current and voltage dynamic range to remain linear.

### 2.3.2 Two Poles

If the feedback factor possesses only two poles, oscillation still does not occur. In this case

$$F = \frac{-F_o}{(1+p\tau_A)(1+p\tau_B)} \quad (2.3.2-1)$$

and for  $F_o \gg 1$

$$A_{CL} \approx \frac{-1}{\beta} \left\{ \frac{1}{1 + p \left( \frac{\tau_A + \tau_B}{F_o} \right) + p^2 \frac{\tau_A \tau_B}{F_o}} \right\} \quad (2.3.2-2)$$

If this response is to be critically damped, then the roots must be real, implying

$$\tau_A^2 + \tau_B^2 = 4 F_o \tau_A \tau_B \quad (2.3.2-3)$$

Solving this equation for the case where  $\tau_A < \tau_B$ , one obtains

$$\tau_A \approx \tau_B / 4 F_o = \frac{t_c}{4} \quad (2.3.2-4)$$

where  $t_c$  = gain cross-over time =  $\frac{\tau_B}{F_o}$

The closed loop response becomes

$$A_{cL} = \frac{-1}{\beta} \left\{ \frac{1}{\left[ 1 + p \frac{t_c}{2} \right]^2} \right\} \quad (2.3.2-5)$$

For this case, the loop is still basically stabilized by a single dominant pole, because the no-ringing condition allows a second pole only to appear at frequencies above gain cross-over. However a slight improvement in rise time is achieved because two equal poles in the closed loop response at  $t_c/2$  replace a single pole at  $t_c$ . (Note: In general, the 10%-90% rise time for a multiple-pole system is given approximately by

$$T_R = 2.2 \sqrt{\sum_{i=1}^N \tau_i^2} \quad (2.3.2-6)$$

where the  $\tau_i$  are the  $N$  poles of the closed-loop transfer function.)

### 2.3.3 Two Poles and One Zero

Often bandwidth considerations do not permit one of two poles to be much larger than the other. A ringing response can still be avoided if a zero is placed near gain cross-over. For this case the feedback factor becomes

$$F = \frac{-F_o (1 + p\tau_o)}{(1 + p\tau_A)(1 + p\tau_B)} \quad (2.3.3-1)$$

and the closed loop gain can be written for  $F_o \gg 1$ :

$$A_{CL} = \frac{-1}{\beta} \left\{ \frac{1+p\tau_o}{1+p \left[ \tau_o + \frac{\tau_A + \tau_B}{F_o} \right] + p^2 \frac{\tau_A \tau_B}{F_o}} \right\} \quad (2.3.3-2)$$

The condition for critical damping is then

$$\left[ \tau_o + \frac{\tau_A + \tau_B}{F_o} \right]^2 = \frac{4\tau_A \tau_B}{F_o} \quad (2.3.3-3)$$

For  $F_o \gg \sim 10$  and the two poles not differing from each other by more than an order of magnitude, this condition becomes approximately

$$\tau_o \approx 2 \sqrt{\frac{\tau_A \tau_B}{F_o}} = 4t_c \quad (2.3.3-4)$$

where  $t_c = \text{gain cross-over time} = \frac{\tau_A \tau_B}{F_o \tau_o}$

The closed loop response is then

$$A_{CL} = \frac{-1}{\beta} \left\{ \frac{1+p4t_c}{(1+p2t_c)^2} \right\} \quad (2.3.3-5)$$

If  $\tau_A = \tau_B = \tau$ , then

$$\tau = 2t_c \sqrt{F_o} \quad (2.3.3-6)$$

compared to the single pole case where

$$\tau = t_c F_o \quad (2.3.3-7)$$

Thus, for the same cross-over time, the value of the stabilizing poles for the two pole system is considerably less than that for the single pole system if the feedback factor is large. Because standing current is often required to charge roll-off capacitors without rate limiting, the two pole - one zero system may achieve more bandwidth at less power than the use of a single, dominant pole.

A convenient method for generating the zero is to place a pole in the  $\beta$ -network. In this case:

$$\beta = \beta_o (1 + p\tau_o) \quad (2.3.3-8)$$

and  $A_{cL}$  becomes

$$A_{cL} = \frac{-1}{\beta_o} \left\{ \frac{1}{(+p2t_c)^2} \right\} \quad (2.3.3-9)$$

The inverse transform for a step function input is then the critically damped waveform

$$\frac{V_{out}}{V_s} = 1 - \left( 1 + \frac{t}{\tau} \right) \exp \left( -\frac{t}{\tau} \right) \quad (2.3.3-10)$$

where  $\tau = 2t_c$

If the  $\beta$ -network has no complex components, the inverse transform becomes

$$\frac{V_{out}}{V_s} = 1 - \left(1 - \frac{t}{\tau}\right) \exp\left(-\frac{t}{\tau}\right) \quad (2.3.3-11)$$

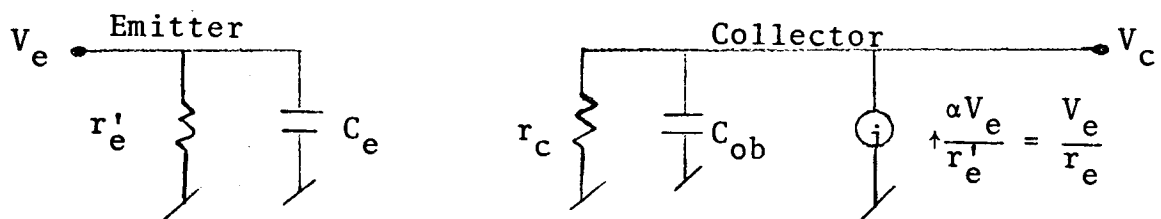
which has a maximum overshoot at  $t = 2\tau = 4t_c$  of 13.6%.

### 3.0 TRANSISTOR EQUIVALENT CIRCUITS

A transistor is a three terminal device. For analysis purposes, one of these terminals may be considered the reference or ground terminal, leaving four complex parameters to describe the behavior at the other two terminals. If the base is chosen as the ground terminal, one obtains the grounded-base equivalent circuit. This configuration is most amenable to analysis by basic transistor theory and forms the starting point for our calculations.

#### 3.1 Grounded Base

A simplified grounded base equivalent circuit is shown below.



$$r'_e = \frac{kT}{qI_e} \quad r_e = \frac{r'_e}{\alpha} = \frac{kT}{qI_c}$$

$$\tau_\alpha = \frac{1}{2\pi f_\alpha} = C_e r'_e$$

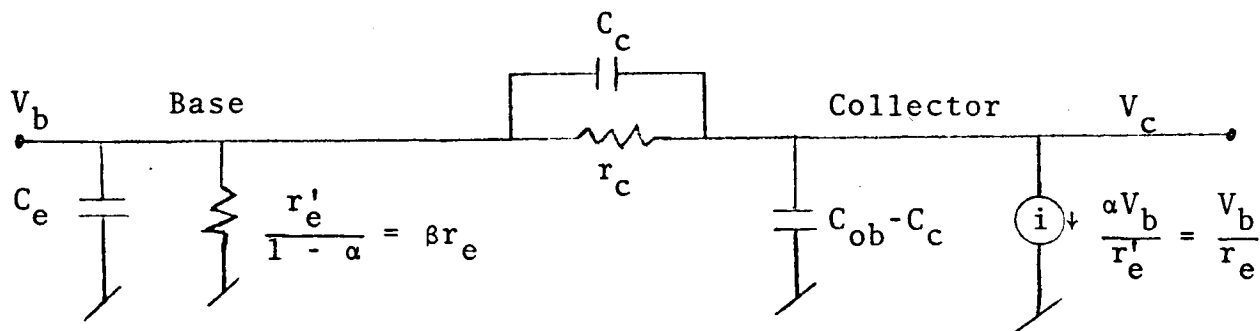
$C_{ob}$  = collector output capacity

The base spreading resistance referred to the emitter has been neglected as being small compared to  $r_e$ . This approximation is usually valid for collector or emitter currents ( $I_c, I_e$ ) less than 1 mA. The reverse voltage feedback from the collector to

the emitter has also been neglected because of the small coefficient (typically  $10^{-4}$ ). All the frequency dependences of the emitter-base junction have been lumped into a single time-constant ( $\tau_\alpha$ ), with such effects as diffusion time delay neglected. This transit time is usually of the order of 20% of  $\tau_\alpha$ .

### 3.2 Grounded Emitter

The grounded base equivalent circuit can be exactly manipulated to the grounded emitter configuration shown below.



$$\beta = \frac{\alpha}{1 - \alpha}$$

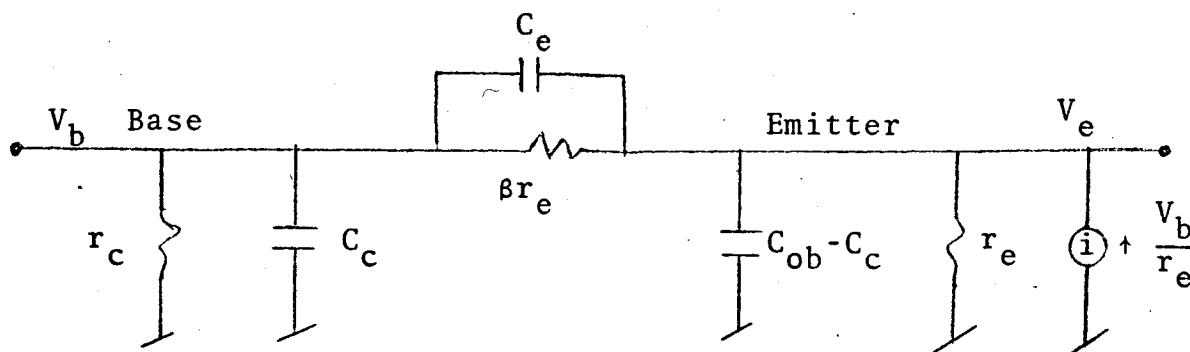
$C_c$  = collector-to-base capacity

The same approximations made in the grounded base configuration are still required here. Notice that the collector-to-base capacity is not exactly equal to  $C_{ob}$ , because  $C_{ob}$  includes stray capacity to the header and to the emitter, which is usually of the order of 1 pF.



### 3.3 Grounded Collector

The grounded emitter equivalent circuit can be exactly manipulated to the grounded collector configuration shown below.

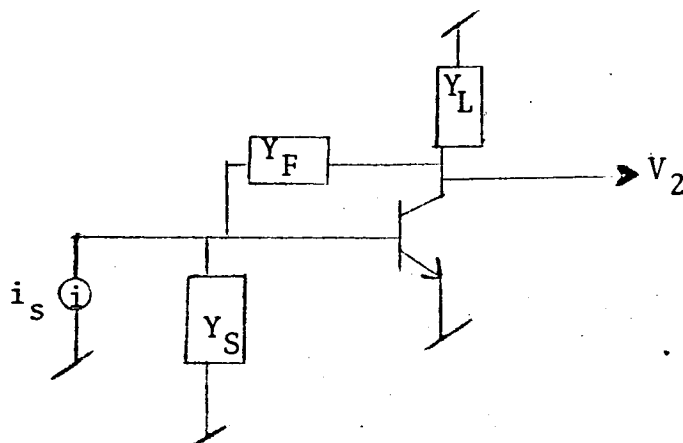


## 4.0 SINGLE TRANSISTOR AMPLIFIERS

Three simple amplifier circuits are analyzed in the following three sections. These circuits generally form the "building blocks" of more complicated systems.

### 4.1 The Grounded Emitter Amplifier

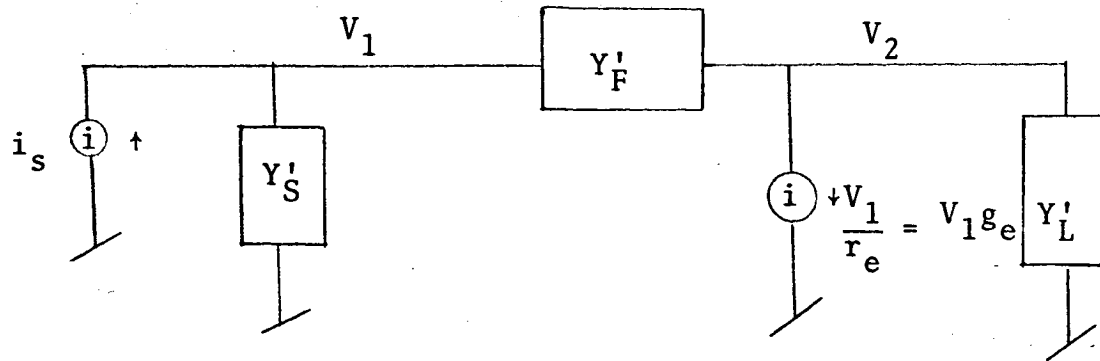
One of the simplest amplifier circuits is the single grounded emitter stage. In general such a stage can be represented as



where

$Y_S$	=	source admittance
$Y_F$	=	feedback admittance
$Y_L$	=	load admittance

Using the equivalent circuit for the transistor given on page 3.0-1, the circuit becomes



where

$$Y'_S = Y_S + \frac{1}{\beta r_e} + pC_e$$

$$Y'_F = Y_F + \frac{1}{r_c} + pC_c$$

$$Y'_L = Y_L + p(C_{ob} - C_c)$$

Setting up the node equations for the above, one obtains

$$i_s = V_1 [Y'_S + Y'_F] + V_2 [-Y'_F] \quad (4.1-1)$$

$$0 = V_1 [g_e - Y'_F] + V_2 [Y'_L + Y'_F]$$

The determinant then becomes

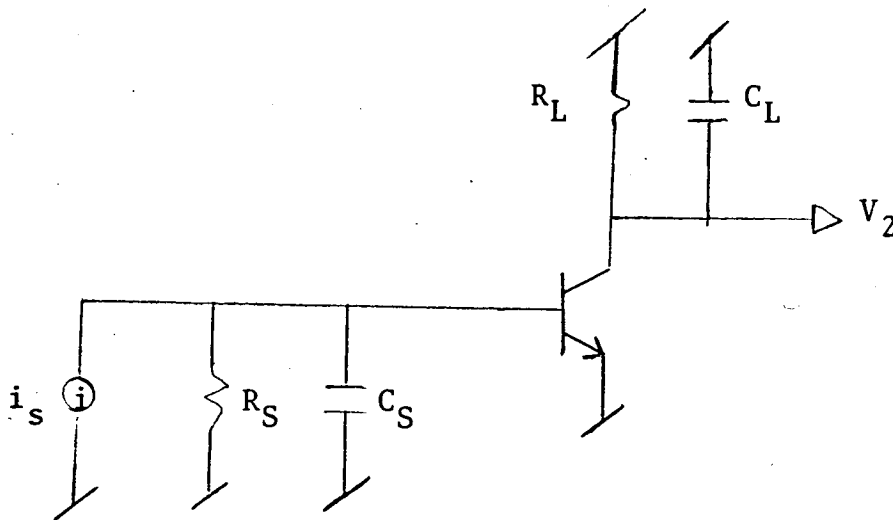
$$\Delta = \begin{vmatrix} Y'_S + Y'_F & -Y'_F \\ g_e - Y'_F & Y'_L + Y'_F \end{vmatrix} \quad (4.1-2)$$

$$\Delta = Y'_S Y'_L + Y'_S Y'_F + Y'_F Y'_L + Y'_F g_e$$

and the output voltage ( $V_2$ ) is related to the input current ( $i_s$ ) by

$$\frac{V_2}{i_s} = \frac{-(g_e - Y_F')}{Y_S' Y_L' + Y_S' Y_F' + Y_F' Y_L' + Y_F' g_e} \quad (4.1-3)$$

A typical condition for source and load admittances is shown below



If one defines the following quantities by

$$C_1 = C_S + C_e \quad (4.1-4)$$

$$g_1 = G_S + \frac{g_e}{\beta}$$

$$C_2 = C_{ob} - C_c + C_L$$

$$G_S = \frac{1}{R_S}$$

$$g_c = \frac{1}{r_c}$$

$$G_L = \frac{1}{R_L}$$

4.1-2

then

$$Y'_S = g_1 + pC_1 \quad (4.1-5)$$

$$Y'_F = g_c + pC_c$$

$$Y'_L = G_L + pC_2$$

Substituting these values into eq. 4.1-3, the transfer function becomes

$$\frac{V_2}{i_s} = \frac{\left[ g_e - g_c \right] \left[ 1 - pC_c r_e \left( \frac{1}{1 - r_e/r_c} \right) \right]}{\left[ g_1 g_c + g_1 G_L + g_c G_L + g_c g_e \right] \left[ 1 + pA + p^2 B \right]} \quad (4.1-6)$$

where

$$A = \frac{(g_1 + g_e + G_L) C_c + (g_c + G_L) C_1 + (g_1 + g_c) C_2}{g_1 g_c + g_1 G_L + g_c G_L + g_c g_e}$$

$$B = \frac{C_1 C_c + C_1 C_2 + C_c C_2}{g_1 g_c + g_1 G_L + g_c G_L + g_c g_e}$$

A useful set of approximations are the following

$$\begin{aligned} \beta &\gg 1 \\ R_S &\gg r_e & (G_S \ll g_e) \\ r_c &\gg R_S \parallel \beta r_e & (g_c \ll g_1) \end{aligned} \quad (4.1-7)$$

For this case

$$g_1 g_c + g_1 G_L + g_c G_L + g_c g_e \rightarrow g_1 G_L \left[ 1 + \frac{g_c g_e}{g_1 G_L} \right] \quad (4.1-8)$$

The transfer impedance then becomes

$$\frac{V_2}{i_s} \cong \left\{ \frac{M_i R_L}{1 + \frac{R_L M_i}{r_c}} \right\} \left\{ \frac{1 - p C_c r_e}{1 + p A + p^2 B} \right\} \quad (4.1-9)$$

where  $M_i$  = current gain into a zero-impedance load

$$M_i = \frac{g_e}{g_i} = \beta \frac{R_s}{R_s + \beta r_e}$$

The output impedance is reduced, compared to the grounded-base stage, by the current gain. This effect can be made explicit by writing equation 4.1-9 as

$$\frac{V_2}{i_s} = M_i \left\{ R_L \parallel \frac{r_c}{M_i} \right\} \left\{ \frac{1 - p C_c r_e}{1 + p A + p^2 B} \right\} \quad (4.1-10)$$

Thus, the output resistance ( $R_{out}$ ) given by

$$R_{out} = \frac{r_c}{M_i} \quad (4.1-11)$$

is reduced from the collector-base resistance ( $r_c$ ) by the current gain ( $M_i$ ). The reduction ( $k$ ) in effective current gain caused by the non-zero output resistance then becomes

$$k = \frac{1}{1 + \frac{R_L}{R_{out}}} = \frac{1}{1 + \frac{g_c g_e}{g_i G_L}} \quad (4.1-12)$$

and the transfer impedance becomes

$$\frac{V_2}{I_s} = kM_i R_L \left\{ \frac{1 - pC_c r_e}{1 + pA + p^2B} \right\} \quad (4.1-13)$$

The coefficients A and B are then given by

$$\begin{aligned} A &\cong k \left\{ (M_v C_c + C_1) R_1 + C_2 R_L \right\} \\ B &\cong kM_v R_1 r_e \left\{ C_1 C_c + C_1 C_2 + C_c C_2 \right\} \end{aligned} \quad (4.1-14)$$

where

$$R_1 = \frac{1}{g_1} = \text{zero-load input resistance}$$

$$R_1 = \frac{R_S \beta r_e}{R_S + \beta r_e}$$

$$M_v = \text{zero-source resistance voltage gain} = \frac{R_L}{r_e}$$

Although the roots of the denominator of equation 4.1-13 can be determined exactly using the quadratic formula, two cases where approximate factoring can be applied are particularly interesting. In the first case, the load time constant ( $C_2 R_L$ ) is assumed dominant so that

$$C_2 R_L \gg (M_v C_c + C_1) R_1 \quad (4.1-15)$$

Then, the two time constants ( $\tau_1, \tau_2$ ) implied by equation 4.1-13 become

$$\tau_1 \cong k C_2 R_L = C_2 (R_L || R_{out}) \quad (4.1-16)$$

$$\tau_2 \cong R_1 \left[ C_1 + C_c + \frac{C_1 C_c}{C_2} \right]$$

For the usual case where  $C_c \ll C_2$ , then

$$\tau_2 \cong R_1 [C_1 + C_c] \quad (4.1-17)$$

Thus, the input and output time constants are effectively separated as one would expect ignoring the Miller Effect.

In the second case the Miller Effect is assumed to be dominant so that

$$C_2 R_L \ll (M_V C_c + C_1) R_1 \quad (4.1-18)$$

and

$$\tau_1 \cong k R_1 (M_V C_c + C_1)$$

$$\tau_2 \cong r_e \left\{ \frac{C_c (C_1 + C_2) + C_1 C_2}{C_c + C_1 / M_V} \right\} \quad (4.1-19)$$

If also  $C_c \gg C_1/M_v$ , then

$$\tau_2 \approx r_e (C_1 + C_2) \quad (4.1-20)$$

#### 4.1.1 Input Admittance and Voltage Gain Representation

Often in the calculation of the transfer function for cascaded stages it is convenient to represent each stage by a voltage gain and by an input admittance. The parameters for such a representation can be simply obtained from equation 4.1-1.

The voltage gain is defined as the gain of the device when it is driven from a zero-impedance source. Thus

$$M_v = \lim_{Y_s \rightarrow \infty} \frac{V_2 Y_s}{i_2} \quad (4.1.1-1)$$

From equation 4.1-3

$$M_v = \frac{-(g_e - Y_F')}{Y_L' + Y_F'} \quad (4.1.1-2)$$

For the configuration shown on page 4.1-2,

$$M_v = - \left[ \frac{g_e - g_c}{G_L + g_c} \right] \left[ \frac{1 - p \frac{C_c}{g_e - g_c}}{1 + p \frac{C_c + C_2}{G_L + g_c}} \right] \quad (4.1.1-3)$$



For  $r_c \gg R_L$ ,

$$M_V \cong -\frac{R_L}{r_e} \left[ \frac{1 - pC_c r_e}{1 + p(C_c + C_2) R_L} \right] \quad (4.1.1-4)$$

The input admittance is given by

$$Y_{IN} = \frac{i_s}{V_1} = Y_S' + Y_F' \left[ \frac{Y_L' + g_e}{Y_L' + Y_F'} \right] \quad (4.1.1-5)$$

The term  $Y_S'$  is the admittance directly connected to the input. The term proportional to  $Y_F'$  results from the Miller effect and can be written as

$$Y_M = Y_F' \left[ \frac{Y_L' + g_e}{Y_L' + Y_F'} \right] = Y_F' (-M_V + 1) \quad (4.1.1-6)$$

For the configuration shown on page 4.1-2,

$$Y_M = \left[ g_c + pC_c \right] \left[ \frac{g_e + G_L}{g_c + G_L} \right] \left[ \frac{1 + p \frac{C_2}{G_L + g_e}}{1 + p \frac{C_c + C_2}{G_L + g_c}} \right] \quad (4.1.1-7)$$

For  $r_c \gg R_L$  and  $R_L \gg r_e$ ,

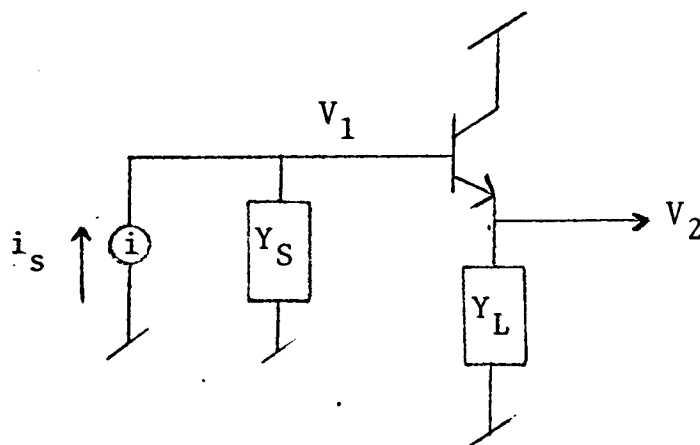
$$Y_M \cong \frac{(1 + pr_c C_c)}{r_c} \left[ \frac{R_L}{r_e} \right] \left[ \frac{1 + pC_2 r_e}{1 + p(C_2 + C_c) R_L} \right] \quad (4.1.1-8)$$

and

$$Z_M = \frac{1}{Y_M} \cong \left[ \frac{r_c}{1 + pr_c C_c} \right] \left[ \frac{r_e}{R_L} \right] \left[ \frac{1 + p(C_2 + C_c) R_L}{1 + pC_2 r_e} \right] \quad (4.1.1-9)$$

## 4.2 The Emitter Follower

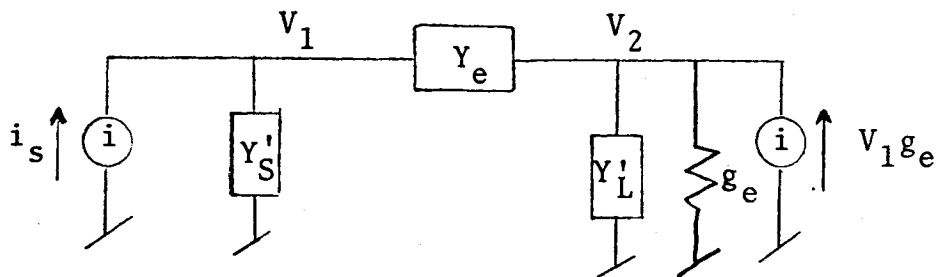
The emitter follower (grounded collector amplifier) is commonly used when signal inversion is not desired. Such a circuit can be represented by



where  $Y_S$  = source admittance

$Y_L$  = load admittance

Using the equivalent circuit for the transistor given in Section 3.3, the above circuit becomes



where

$$Y'_S = Y_S + \frac{1}{r_c} + pC_c = Y_S + g_c + pC_c$$

$$Y_e = \frac{1}{\beta r_e} + pC_e = \frac{g_e}{\beta} + pC_e$$

$$Y'_L = Y_L + p(C_{ob} - C_c) = Y_L + p(C_{ob} - C_c)$$

$$g_e = \frac{1}{r_e}$$

Setting up the node equations for the above, one obtains

$$i_s = V_1 \left[ Y'_S + Y_e \right] + V_2 \left[ -Y_e \right] \quad (4.2-1)$$

$$0 = V_1 \left[ -Y_e - g_e \right] + V_2 \left[ Y_e + Y'_L + g_e \right]$$

4.2-2

The determinant then becomes

$$\Delta = \begin{vmatrix} Y'_S + Y_e & -Y_e \\ -Y_e & -g_e \\ Y_e + Y'_L + g_e \end{vmatrix} \quad (4.2-2)$$

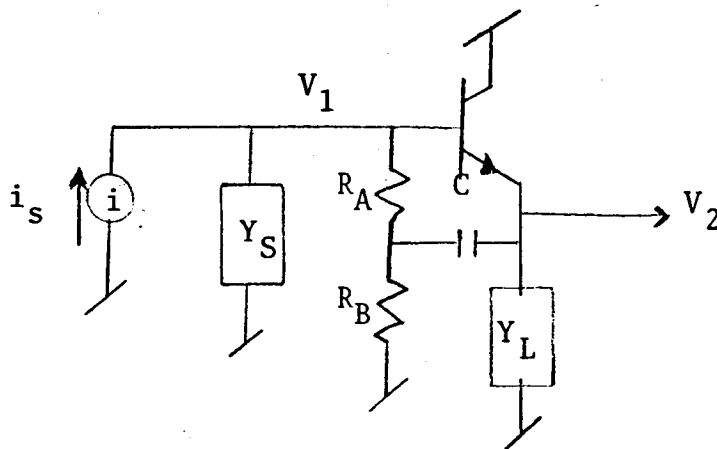
$$\Delta = Y'_S Y_e + Y'_S Y'_L + Y'_S g_e + Y_e Y'_L$$

and the output voltage ( $V_2$ ) is related to the input current ( $i_s$ ) by

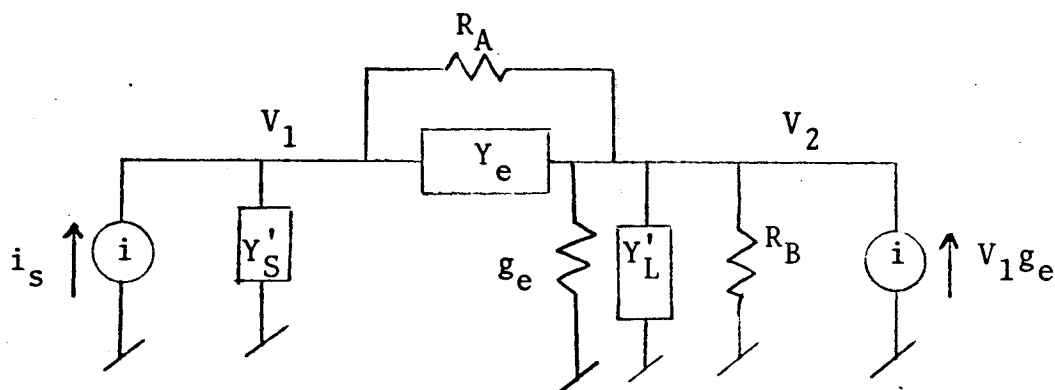
$$\frac{V_2}{i_s} = \frac{Y_e + g_e}{Y'_S Y_e + Y'_S Y'_L + Y'_S g_e + Y_e Y'_L} \quad (4.2-3)$$

#### 4.2.1 Bootstrapped Source Resistance

Often part of the source resistance is bootstrapped in order to obtain improved linearity, higher gain, and larger dynamic range. Such a circuit is



For the case where  $\frac{R_A R_B C}{R_A + R_B}$  is large compared to times of interest,  $C$  can be approximated by a short circuit, and the following equivalent circuit applies.



Equations (4.2-2) and (4.2-3) can be formally modified to include bootstrapping by replacing  $\beta$  with  $\beta'$  and  $Y_L'$  with  $Y_L''$ ,

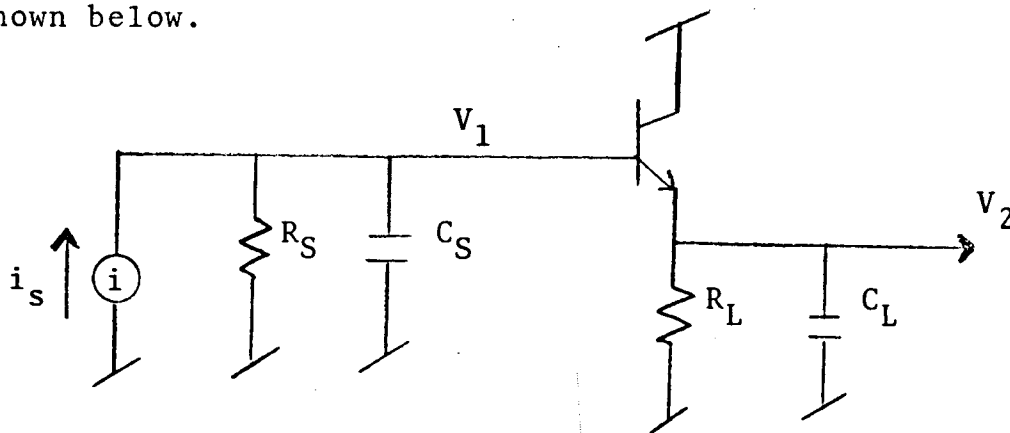
where

$$\beta' = \beta \frac{R_A}{\beta r_e + R_A} \quad (4.2.1-1)$$

$$Y_L'' = Y_L' + \frac{1}{R_B}$$

#### 4.2.2 Parallel RC Load and Source Impedances

A typical condition for source and load admittances is shown below.



if one defines the following quantities by

$$C_1 = C_S + C_c \quad (4.2.2-1)$$

$$C_2 = C_L + C_{ob} - C_c$$

$$G_1 = G_S + g_c$$

$$G_L = \frac{1}{R_L}$$

$$G_S = \frac{1}{R_S}$$

then

$$Y_S' = G_1 + pC_1 \quad (4.2.2-2)$$

$$Y_L' = G_L + pC_2$$

If the emitter follower is bootstrapped, the simple substitution discussed in Section 4.2.1 applies here also.

Substituting the above values into equation (4.2-3), one obtains for the transfer impedance, under the approximation that  $\beta \gg 1$ ,

$$\frac{V_2}{i_s} = R_S' \left\{ \frac{R_L}{R_L + R_{out}} \right\} \left\{ \frac{1 + p\tau_\alpha}{1 + pA + p^2B} \right\} \quad (4.2.2-3)$$

where

$$R_{out} = \text{output resistance}$$

$$= r_e + \frac{R_S \parallel r_c}{\beta}$$

$$\tau_\alpha = r_e C_e$$

$$A = \tau_\alpha \left\{ \frac{R_L + R_S'}{R_L + r_e + \frac{R_S'}{\beta}} \right\} + \tau_1 \left\{ \frac{R_L + r_e}{R_L + r_e + \frac{R_S'}{\beta}} \right\} + kC_2 R_{out}$$

$$B = k \left\{ \tau_\alpha \tau_1 + \tau_1 C_2 r_e + \tau_\alpha C_2 R_S' \right\}$$

$$k = \text{output resistance gain correction}$$

$$= \frac{1}{1 + \frac{R_{out}}{R_L}}$$



$$R_S' = R_S || r_c = \frac{R_S r_c}{R_S + r_c}$$

$$\tau_1 = \frac{C_1}{G_1}$$

A common application of an emitter follower is as a unity gain voltage amplifier. For this case one wants

$$k \approx 1 \quad (4.2.2-4)$$

$$R_S' \approx R_S$$

so that

$$R_{out} \ll R_L \quad (4.2.2-5)$$

which implies

$$r_e \ll R_L \quad (4.2.2-6)$$

$$R_S'/\beta \ll R_L$$

$$R_S \ll r_c.$$

For this case

$$A \approx \tau_\alpha \left\{ \frac{R_L + R_S}{R_L} \right\} + \tau_1 + C_2 R_{out} \quad (4.2.2-7)$$

$$B \approx \tau_\alpha \tau_1 \left\{ 1 + \frac{C_2}{C_e} + \frac{C_2}{C_1} \right\}$$

For the case where the source time constant is dominant so that

$$\tau_1 \gg C_2 R_{out} + \tau_\alpha \frac{R_L + R_S}{R_L} \quad (4.2.2-8)$$

Then the two roots of the denominator become approximately

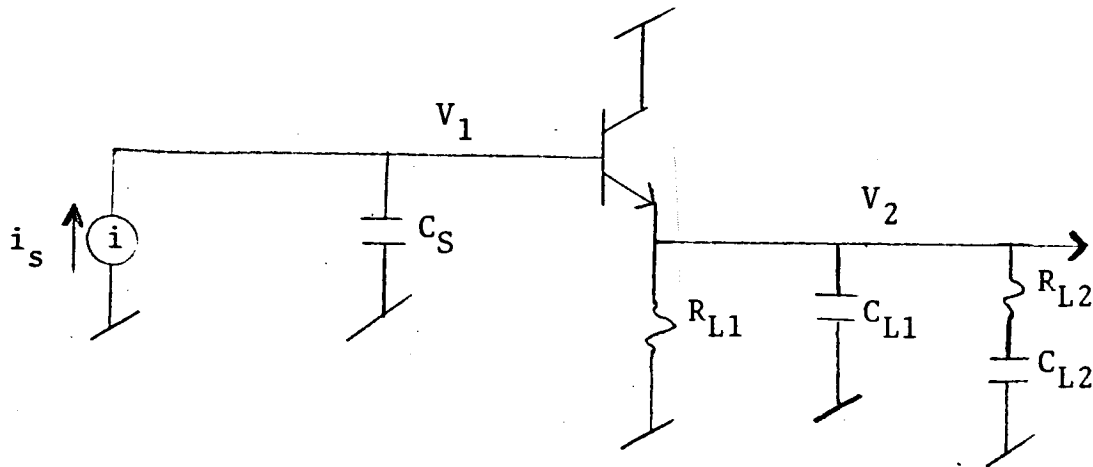
$$\tau_A \approx \tau_1 \quad (4.2.2-9)$$

$$\tau_B \approx \tau_\alpha \left[ 1 + \frac{C_2}{C_e} + \frac{C_2}{C_1} \right]$$

if also  $\tau_A \gg \tau_B$ .

#### 4.2.3 Series RC Load Impedance

In the case where a series RC component is present in load impedance, the circuit becomes for a capacitive source, such as when the emitter follower is bootstrapped



Then

$$Y_S' = pC_1 \quad (4.2.3-1)$$

$$Y_L = \frac{G_{L1}G_{L2} + p(C_{L1}G_{L2} + C_{L2}G_{L1} + C_{L2}G_{L2}) + p^2C_{L1}C_{L2}}{G_{L2} + pC_{L2}}$$

where

$$G_{L1} = \frac{1}{R_{L1}}$$

$$G_{L2} = \frac{1}{R_{L2}}$$

Then, substituting into equation (4.2-3), one obtains

$$\frac{V_2}{i_s} = \beta \frac{R_{L1} (1 + p\tau_\alpha)(1 + p\tau_{L2})}{1 + pA + p^2B + p^3C} \quad (4.2.3-2)$$

where

$$A = \beta(C_e + C_1) r_e + \tau_{L1} + \tau_{L2} + \beta C_1 R_{L1} + C_{L2} R_{L1}$$

$$B = \beta r_e (C_e + C_1) (\tau_{L1} + \tau_{L2} + C_{L2} R_{L1}) + \\ \beta C_1 R_{L1} (\tau_\alpha + \tau_{L2}) + \tau_{L1} \tau_{L2}$$

$$C = \beta r_e \tau_{L2} R_{L1} C_1 (C_e + C_{L1})$$

$$\tau_{L1} = R_{L1} C_{L1}$$

$$\tau_{L2} = R_{L2} C_{L2} \quad 4.2-9$$

For the case where

$$R_{L1} \gg r_e \quad (4.2.3-3)$$

$$\beta C_1 R_{L1} \gg \beta \tau_\alpha + \tau_{L1}$$

$$\tau_{L2} > \tau_{L1}$$

then

$$A \cong \beta C_1 R_{L1} + \tau_{L2} + C_{L2} R_{L1} \quad (4.2.3-4)$$

$$B \cong \beta C_1 R_{L1} (\tau_{L2} + C_{L2} r_e)$$

$$C \cong \beta C_1 R_{L1} r_e \tau_{L2} (C_e + C_{L1})$$

If the roots of the denominator of equation 4.2.3-2 are ordered such that

$$\tau_A \gg \tau_B \gg \tau_C \quad (4.2.3-5)$$

then

$$\tau_A \cong \beta C_1 R_{L1} + C_{L2} R_{L1} \quad (4.2.3-6)$$

$$\tau_B \cong \frac{C_{L2} (R_{L2} + r_e)}{1 + \frac{C_{L2}}{\beta C_1}}$$

$$\tau_C \cong r_e (C_e + C_{L1})$$

4.2-10

#### 4.2.4 Input Admittance and Voltage Gain Representation

Often it is convenient to treat the emitter follower as an impedance transfer device. In this notation the input admittance and the voltage gain become important.

The input admittance can be found by solving equation 4.2-1 for  $V_1$ . Thus

$$Y_{IN} = \frac{i_s}{V_1} = Y_S' + \frac{Y_e Y_L'}{Y_e + Y_L' + g_e} \quad (4.2.4-1)$$

The terms in  $Y_S$  and  $Y_C$  result from the admittances directly connected to the base. The remaining term is dependent on transistor parameters and on the load admittance, and represents the impedance transfer characteristic of the transistor. The input admittance can be written as

$$Y_{IN} = Y_S' + Y_Q \quad (4.2.4-2)$$

where  $Y_S' = Y_S + Y_C = Y_S + g_C + pC_C$

$$Y_Q = \frac{Y_e Y_L'}{Y_e + Y_L' + g_e}$$

The quantity  $Y_Q$  then becomes the term of further interest.

Inverting and simplifying gives

$$Z_Q = \frac{1}{Y_T} = \frac{1}{Y_e} + Z_L' \left[ 1 + \frac{g_e}{Y_e} \right] \quad (4.2.4-3)$$

where  $Z_L' = \frac{1}{Y_L'}$

Substituting for  $Y_e$  and assuming that  $\beta$  is large compared to unity, one obtains

$$Z_Q = \beta \frac{r_e + Z_L' (1 + p\tau_\alpha)}{1 + p\beta\tau_\alpha} \quad (4.2.4-4)$$

For the series RC load impedance discussed in Section 4.2.3,

$$Z_L' = R_{L1} \frac{1 + p\tau_{L2}}{1 + p \left[ \tau_{L1} + \tau_{L2} \left( 1 + \frac{R_{L1}}{R_{L2}} \right) \right] + p^2 \tau_{L1}\tau_{L2}} \quad (4.2.4-5)$$

where  $C_{ob} - C_c$  has been included in  $C_{L1}$ . Substituting this value, one obtains

$$Z_Q = \left\{ \frac{\beta(r_e + R_{L1})}{1 + p\beta\tau_\alpha} \right\} \left\{ \frac{1 + pE + p^2F}{1 + pH + p^2D} \right\} \quad (4.2.4-6)$$

where

$$H = \tau_{L1} + \tau_{L2} \left( 1 + \frac{R_{L1}}{R_{L2}} \right)$$

$$D = \tau_{L1}\tau_{L2}$$

$$E = R_p \left\{ C_{L1} + C_e + C_{L2} \left( 1 + \frac{R_{L2}}{r_e} + \frac{R_{L2}}{R_{L1}} \right) \right\}$$

$$F = C_{L2}R_{L2}R_p (C_e + C_{L1})$$

$$R_p = \frac{r_e R_{L1}}{r_e + R_{L1}} \quad 4.2-12$$

For  $H^2 \gg D$ , the denominator can be approximately factored such that

$$Z_Q \approx \left\{ \frac{R_{IN}}{1 + pC_{in} R_{in}} \right\} \left\{ \frac{1 + pE + p^2F}{(1 + p\beta\tau_\alpha)(1 + pD/H)} \right\} \quad (4.2.4-7)$$

where

$$R_{IN} = \beta(r_e + R_{L1})$$

$$C_{IN} = \frac{1}{\beta} \left[ \frac{R_{L1}}{R_{L1} + r_e} \right] \left[ C_{L1} + C_{L2} \left( 1 + \frac{R_{L2}}{R_{L1}} \right) \right]$$

Thus, to a first order approximation, the input resistance is increased over the load resistance by a factor of  $\beta$ , while the input capacitance is decreased by nearly the same factor.

For  $R_{L1} \gg R_{L2}$  and  $R_{L1} \gg r_e$ ,

$$C_{IN} \approx \frac{C_{L1} + C_{L2}}{\beta} \quad (4.2.4-8)$$

$$D/H \approx \frac{C_{L1} C_{L2} R_{L2}}{C_{L1} + C_{L2}} \quad (4.2.4-9)$$

$$E \approx r_e \left\{ C_{L1} + C_e + C_{L2} \left( 1 + \frac{R_{L2}}{r_e} \right) \right\} \quad (4.2.4-10)$$

$$F \approx r_e C_{L2} R_{L2} (C_e + C_{L1}) \quad (4.2.4-11)$$

The voltage gain can be found from equation 4.2-1 by solving for the limit

$$M_V = \lim_{Y_S \rightarrow \infty} \frac{V_2 Y_S}{i_S} = \frac{Y_e + g_e}{Y_e + g_e + Y_{L'}} \quad (4.2.4-12)$$

For  $\beta \gg 1$

$$M_V \cong \frac{1 + p\tau_\alpha}{1 + p\tau_\alpha + \frac{r_e}{Z_{L'}}} \quad (4.2.4-13)$$

For  $Z_{L'}$  given by equation 4.2.4-5,

$$M_V = \left\{ \frac{R_{L1}}{R_{L1} + r_e} \right\} \left\{ \frac{(1 + p\tau_\alpha)(1 + p\tau_{L2})}{1 + pM + p^2N} \right\} \quad (4.2.4-14)$$

where

$$M = \tau_{L2} + (C_{L1} + C_{L2} + C_e) R_p$$

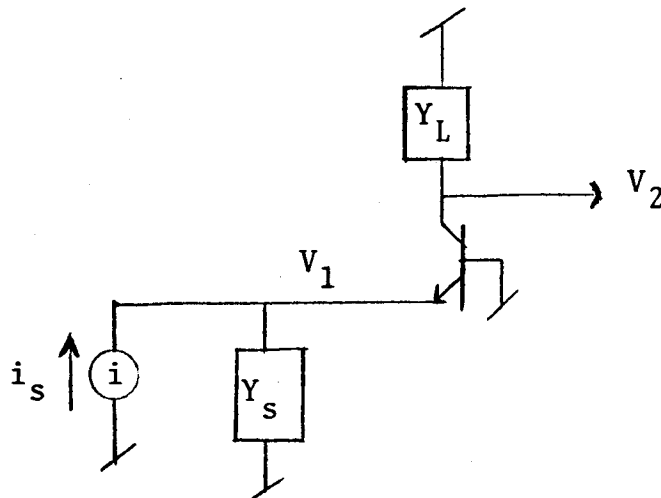
$$N = \tau_{L2} (C_e + C_{L1}) R_p$$

$$R_p = \frac{r_e R_{L1}}{r_e + R_{L1}}$$



### 4.3 The Grounded Base Amplifier

When a low input impedance and a high output impedance are required, a common configuration is the one shown below.

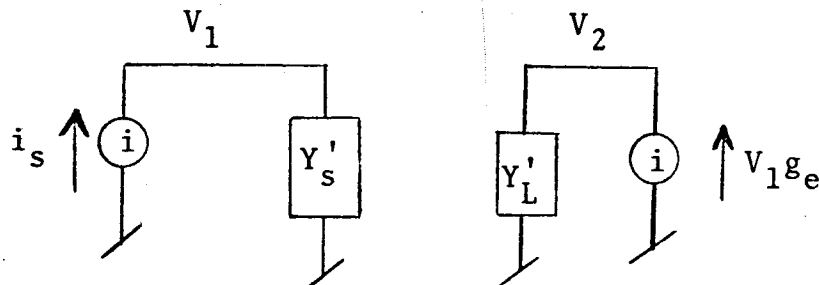


where

$Y_s$  = source admittance

$Y_L$  = load admittance

Using the equivalent circuit of Section 3.1, the above circuit becomes



where  $Y'_s = Y_s + g'_e + pC_e$

$Y'_L = Y_L + g_c + pC_e$

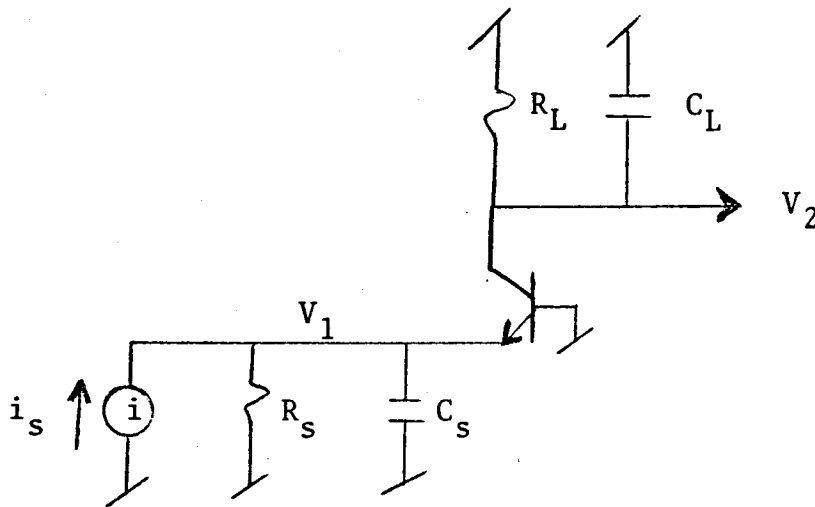
$g_e = 1/r_e$

$g'_e = g_e/\alpha$  4.3-1

The transfer impedance is easily found to be

$$\frac{V_2}{i_s} = \frac{g_e}{Y_s' Y_L'} \quad (4.3-1)$$

For the typical combination of load and source impedances shown below



the quantities of equation (4.3-1) become

$$Y_s' = G_s + g_e' + p(C_s + C_e) \quad (4.3-2)$$

$$Y_L' = G_L + g_c + p(C_L + C_c)$$

$$G_s = \frac{1}{R_s}$$

$$G_L = \frac{1}{R_L}$$

Equation (4.3-1) can then be written

$$\frac{V_2}{i_s} = \frac{g_e}{(G_s + g_e')(G_L + g_c)} \left[ 1 + p \frac{(C_s + C_e)}{G_s + g_e'} \right] \left[ 1 + p \frac{(C_L + C_c)}{G_L + g_c} \right] \quad (4.3-3)$$

With the approximation that

$$R_L \ll r_c \quad (4.3-4)$$

$$r_e' \ll R_s$$

Then

$$\frac{V_2}{i_s} \approx \frac{\alpha R_L}{\left[ 1 + p \tau_\alpha \left( 1 + \frac{C_e}{C_s} \right) \right] \left[ 1 + p (C_L + C_c) R_L \right]} \quad (4.3-5)$$

## 5.0 THE DOUBLE DIFFERENTIAL AMPLIFIER

A common configuration often used where dc stability is a requirement is the double-differential amplifier shown in Figure 5.0-1. The advantage of this configuration lies in the fact that the second stage can be used to balance the operating conditions of the first stage via an external feedback loop. High common mode rejection and dc stability determined only by the quality of the input transistor then result.

In this section we wish to calculate the transfer function of this amplifier in the differential mode. Common mode effects caused by  $R_{e1}$  and  $R_{e2}$  will be neglected in this analysis. The equivalent circuit of Figure 5.0-2 then results from the transistor circuit given in Section 3.2.

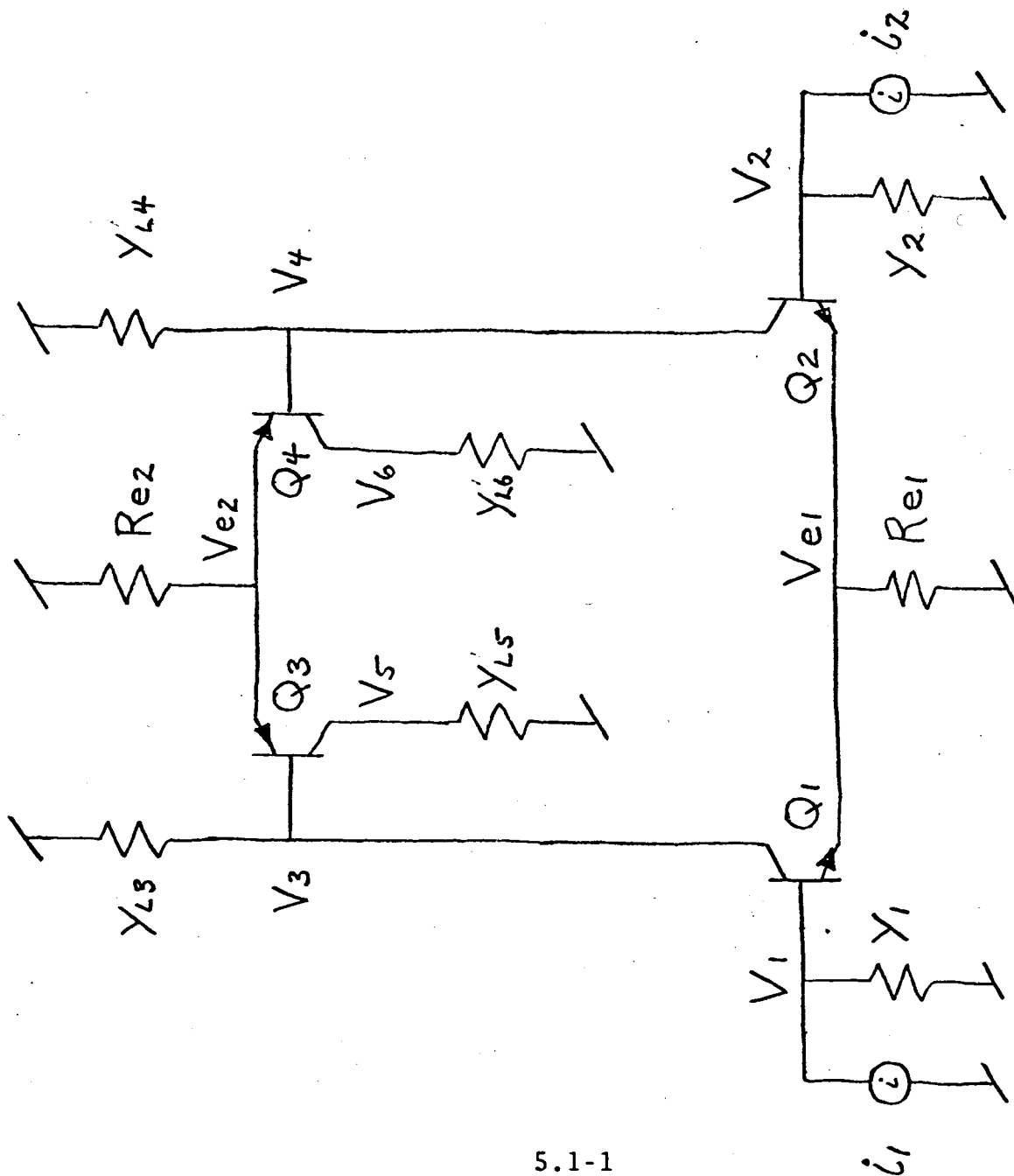
The analysis of this configuration in general is extremely tedious, and useful results can only be obtained by machine computation. However, in this report we will set up the equations in matrix form so that such computation could be performed if needed.

In usual practice this problem can be simplified because the amplifier is driven from a single-ended source, and one of the output collectors is grounded. If one also assumes a certain degree of symmetry, the calculations can be performed by hand. These results are given in Section 5.2.

### 5.1 General Solution

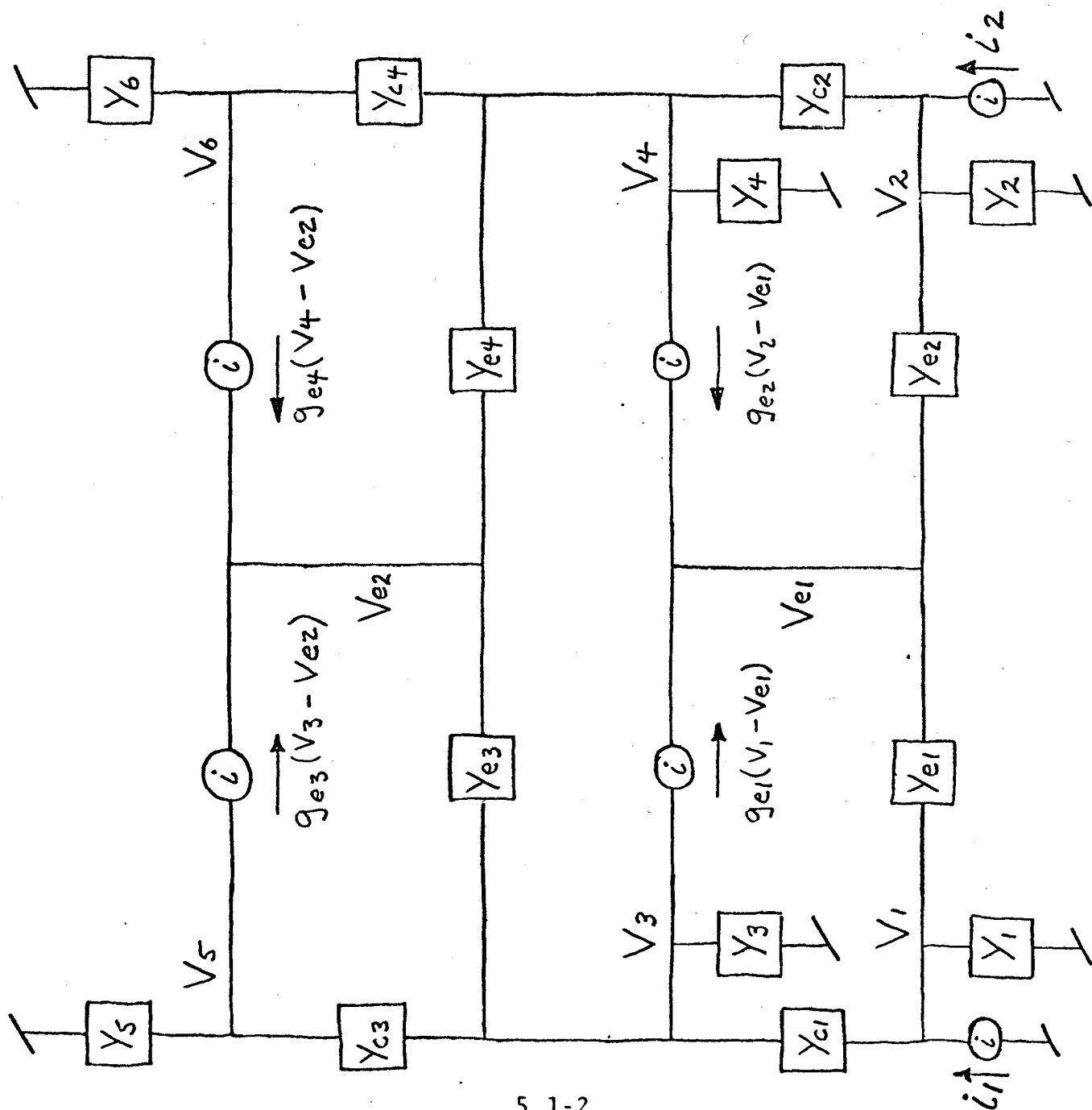
In linear circuit analysis, a complex set of equations can be written in the matrix form

$$I = YV \quad (5.1-1)$$



5.1-1

FIGURE 5.0-1: DOUBLE - DIFFERENTIAL AMPLIFIER



5.1-2

Figure 5.0-2: EQUIVALENT CIRCUIT

where for this case

$$I = (i_1, i_2, 0, 0, 0, 0, 0, 0)$$

$$V = \begin{pmatrix} V_1 \\ V_2 \\ V_3 \\ V_4 \\ V_5 \\ V_6 \\ V_{e1} \\ V_{e2} \end{pmatrix}$$

$Y = 8 \times 8$  matrix of admittances

From the equivalent circuit of Figure 5.0-2, Y becomes

$$Y = \begin{bmatrix} Y_1 + Y_{c1} + Y_{e1} & 0 & -Y_{c1} & 0 & 0 & 0 & -Y_{e1} & 0 \\ 0 & Y_2 + Y_{c2} + Y_{e2} & 0 & -Y_{c2} & 0 & 0 & -Y_{e2} & 0 \\ -Y_{c1} + g_{e1} & 0 & Y_3 + Y_{c1} + Y_{c3} + Y_{e3} & 0 & -Y_{c3} & 0 & -g_{e1} & -Y_{e3} \\ 0 & -Y_{c2} + g_{e2} & 0 & Y_4 + Y_{c2} + Y_{c4} + Y_{e4} & 0 & -Y_{c4} & -g_{e2} & -Y_{e4} \\ 0 & 0 & -Y_{c3} + g_{e3} & 0 & Y_5 + Y_{c3} & 0 & 0 & -g_{e3} \\ 0 & 0 & 0 & -Y_{c4} + g_{e4} & 0 & Y_6 + Y_{c4} & 0 & -g_{e4} \\ -Y_{e1} - g_{e1} & -Y_{e2} - g_{e2} & 0 & 0 & 0 & 0 & g_{e1} + g_{e2} + Y_{e1} + Y_{e2} & 0 \\ 0 & 0 & -Y_{e3} - g_{e3} & -Y_{e4} - g_{e4} & 0 & 0 & 0 & g_{e3} + g_{e4} + Y_{e3} + Y_{e4} \end{bmatrix}$$

(5.1-2)



In the usual manner, equation 5.1-1 can be solved for a given output voltage ( $V_i$ ) according to

$$V_i = \frac{|Y_i|}{|Y|} \quad (5.1-3)$$

where

$|Y|$  = determinant of  $Y$

$|Y_i|$  = determinant of  $Y$  with the  $i^{\text{th}}$  column replaced by  $I^T$ . ( $I^T$  = transpose of  $I$  =  $I$  written as a column vector.)

The determinants can be simplified by elementary operations and then expanded in cofactors. If rows one and two are added to row seven, then

$|Y| =$

$Y_1 + Y_{c1}$ $+Y_{e1}$	0	$-Y_{c1}$	0	0	0	$Y_1 + Y_{c1}$	0
0	$Y_2 + Y_{c2}$ $+Y_{e2}$	0	$-Y_{c2}$	0	0	$Y_2 + Y_{c2}$	0
$-Y_{c1}$ $+g_{e1}$	0	$Y_3 + Y_{c1}$ $+Y_{c3} + Y_{e3}$	0	$-Y_{c3}$	0	$-Y_{c1}$	$-Y_{e3}$
0	$-Y_{c2}$ $+g_{e2}$	0	$Y_4 + Y_{c2}$ $+Y_{c4} + Y_{e4}$	0	$-Y_{c4}$	$-Y_{c2}$	$-Y_{e4}$
0	0	$-Y_{c3}$ $+g_{e3}$	0	$Y_5$ $+Y_{c3}$	0	0	$-g_{e3}$
0	0	0	$-Y_{c4}$ $+g_{e4}$	0	$Y_6$ $+Y_{c4}$	0	$-g_{e4}$
$-Y_{e1}$ $-g_{e1}$	$-Y_{e2}$ $-g_{e2}$	0	0	0	0	0	0
0	0	$-Y_{e3}$ $-g_{e3}$	$-Y_{e4}$ $-g_{e4}$	0	0	0	$g_{e3} + g_{e4}$ $+Y_{e3} + Y_{e4}$

Expanding this determinant in cofactors, one obtains

$$|Y| = -\{Y_{e1} + g_{e1}\} |A_1| + \{Y_{e2} + g_{e2}\} |A_2| \quad (5.1-5)$$

where  $A_1$  and  $A_2$  are 7 x 7 matrices. Expanding  $A_1$  and  $A_2$  in cofactors:

$$|Y| = \{Y_{e1} + g_{e1}\} \{Y_{c1} |B_{11}| + (Y_1 + Y_{c1}) |B_{12}|\} \\ + \{Y_{e2} + g_{e2}\} \{Y_{c2} |B_{21}| + (Y_2 + Y_{c2}) |B_{22}|\} \quad (5.1-6)$$

where the B - matrices are given by

$$|B_{11}| = \begin{vmatrix} Y_2 + Y_{c2} & -Y_{c2} & 0 & 0 & Y_2 + Y_{c2} & 0 \\ +Y_{e2} & & & & & \\ 0 & 0 & -Y_{c3} & 0 & -Y_{c1} & -Y_{e3} \\ -Y_{c2} & Y_4 + Y_{c2} & 0 & -Y_{c4} & -Y_{c2} & -Y_{e4} \\ +g_{e2} & +Y_{c4} + Y_{e4} & & & & \\ 0 & 0 & Y_5 & 0 & 0 & -g_{e3} \\ & & +Y_{c3} & & & \\ 0 & -Y_{c4} & 0 & Y_6 & 0 & -g_{e4} \\ & +g_{e4} & & +Y_{c4} & & \\ 0 & -Y_{e4} & 0 & 0 & 0 & g_{e3} + g_{e4} \\ & -g_{e4} & & & & +Y_{e3} + Y_{e4} \end{vmatrix} \quad (5.1-7)$$

$|B_{12}| =$

$Y_2 + Y_{c2}$ $+Y_{e2}$	0	$-Y_{c2}$	0	0	0
0	$Y_3 + Y_{c1}$ $Y_{c3} + Y_{e3}$	0	$-Y_{c3}$	0	$-Y_{e3}$
$-Y_{c2}$ $+g_{e2}$	0	$Y_4 + Y_{c2}$ $Y_{c4} + Y_{e4}$	0	$-Y_{c4}$	$-Y_{e4}$
0	$-Y_{c3}$ $+g_{e3}$	0	$Y_5$ $+Y_{c3}$	0	$-g_{e3}$
0	0	$-Y_{c4}$ $+g_{e4}$	0	$Y_6$ $+Y_{c4}$	$-g_{e4}$
0	$-Y_{e3}$ $-g_{e3}$	$-Y_{e4}$ $-g_{e4}$	0	0	$g_{e3} + g_{e4}$ $Y_{e3} + Y_{e4}$

(5.1-8)

$|B_{21}| =$

$Y_1 + Y_{c1}$ $+Y_{e1}$	$-Y_{c1}$	0	0	$Y_1 + Y_{c1}$	0
$-Y_{c1}$ $+g_{e1}$	$Y_3 + Y_{c1}$ $Y_{c3} + Y_{e3}$	$-Y_{c3}$	0	$-Y_{c1}$	$-Y_{e3}$
0	0	0	$-Y_{c4}$	$-Y_{c2}$	$-Y_{e4}$
0	$-Y_{c3}$ $+g_{e3}$	$Y_5$ $+Y_{c3}$	0	0	$-g_{e3}$
0	0	0	$Y_6$	0	$-g_{e4}$
0	0	0	$Y_6$ $+Y_{c4}$	0	$-g_{e4}$
0	$-Y_{e3}$ $-g_{e3}$	0	0	0	$g_{e3} + g_{e4}$ $Y_{e3} + Y_{e4}$

(5.1-9)

$$B_{22} = \begin{vmatrix} Y_1 + Y_{c1} & -Y_{c1} & 0 & 0 & 0 & 0 \\ +Y_{e1} & & & & & \\ -Y_{c1} & Y_3 + Y_{c1} & 0 & -Y_{c3} & 0 & -Y_{e3} \\ +g_{e1} & Y_{c3} + Y_{e3} & & & & \\ 0 & 0 & Y_4 + Y_{c2} & 0 & -Y_{c4} & -Y_{e4} \\ & & Y_{c4} + Y_{e4} & & & \\ 0 & -Y_{c3} & 0 & Y_5 & 0 & -g_{e3} \\ & +g_{e3} & & +Y_{c3} & & \\ 0 & 0 & -Y_{c4} & 0 & Y_6 & -g_{e4} \\ & & +g_{e4} & & +Y_{c4} & \\ 0 & -Y_{e3} & -Y_{e4} & 0 & 0 & g_{e3} + g_{e4} \\ & -g_{e3} & -g_{e4} & & & Y_{e3} + Y_{e4} \end{vmatrix}$$

(5.1-10)

Further reduction of these matrices becomes overly tedious and will not be presented here for the general case.

In the foregoing analysis, the admittances were defined by Figures 5.0-1 and 5.0-2. They are related to the quantities used in Section 3.2 by

$$Y_e = \frac{g_e}{\beta} + pC_e \quad (5.1-11a)$$

$$Y_c = g_c + pC_c \quad (5.1-11b)$$

$$g_e = \frac{1}{r_e} \quad (5.1-11c)$$

$$g_c = \frac{1}{r_c} \quad (5.1-11d)$$

Also, the collector output capacitance,  $C_{ob} - C_c$ , was assumed to result principally from stray capacity to a grounded header. This capacitance was lumped into the appropriate load admittance, so that

$$Y_3 = Y_{L3} + p(C_{ob1} - C_{c1}) \quad (5.1-12a)$$

$$Y_4 = Y_{L4} + p(C_{ob2} - C_{c2}) \quad (5.1-12b)$$

$$Y_5 = Y_{L5} + p(C_{ob3} - C_{c3}) \quad (5.1-12c)$$

$$Y_6 = Y_{L6} + p(C_{ob4} - C_{c4}) \quad (5.1-12d)$$

## 5.2 Symmetrical, Single-Ended Double-Differential Amplifier

Often the double-differential amplifier is used in an inverting feedback configuration, resulting in the base of  $Q_1$  and the collector of  $Q_4$  being grounded. Thus,

$$V_1 = 0 \quad (5.2-1)$$

$$Y_1 = \infty$$

$$V_6 = 0$$

$$Y_6 = \infty$$

In addition, the bias conditions of  $Q_1$  and  $Q_2$  and of  $Q_3$  and  $Q_4$  are identical; and, when matched transistors are used, the following equalities are also valid:

$$g_{e1} = g_{e2} \quad (5.2-2)$$

$$Y_{e1} = Y_{e2}$$

$$Y_{c1} = Y_{c2}$$

$$Y_{c3} = Y_{c4}$$

Also, the interstage load admittances are made equal so that

$$Y_3 = Y_4 \quad (5.2-3)$$



With the above simplifications, the admittance matrix becomes

$$Y = \begin{pmatrix} Y_2 + Y_{e1} + Y_{c1} & 0 & -Y_{c1} & 0 & -Y_{e1} & 0 \\ 0 & Y_3 + Y_{e3} + Y_{c1} + Y_{c3} & 0 & -Y_{c3} & -g_{e1} & -Y_{e3} \\ -Y_{c1} + g_{e1} & 0 & Y_3 + Y_{e3} + Y_{c1} + Y_{c3} & 0 & -g_{e1} & -Y_{e3} \\ 0 & -Y_{c3} + g_{e3} & 0 & Y_5 + Y_{c3} & 0 & -g_{e3} \\ -Y_{e1} - g_{e1} & 0 & 0 & 0 & 2Y_{e1} + 2g_{e1} & 0 \\ 0 & -Y_{e3} - g_{e3} & -Y_{e3} - g_{e3} & 0 & 0 & 2Y_{e3} + 2g_{e3} \end{pmatrix}$$

(5.2-4)

and the voltage and current vectors simplify to

$$V = \begin{pmatrix} V_2 \\ V_3 \\ V_4 \\ V_5 \\ V_{e1} \\ V_{e2} \end{pmatrix} \quad (5.2-5)$$

$$I = (i_2, 0, 0, 0, 0, 0) \quad (5.2-6)$$

The determinant can be simplified by factoring out  $2Y_{e1} + 2g_{e1}$  from the fifth row and  $2Y_{e3} + 2g_{e3}$  from the sixth row. Also, multiply the new fifth row by  $Y_{e1}$  and add it to the first row, and by  $g_{e1}$  and add to the third row. The resultant determinant then becomes

$$|Y| = (2Y_{e1} + 2g_{e1})(2Y_{e3} + 2g_{e3}) \begin{vmatrix} Y_2 + Y_{c1} + Y_{e1}/2 & 0 & -Y_{c1} & 0 & 0 & 0 \\ 0 & Y_3 + Y_{e3} & 0 & -Y_{c3} & -g_{e1} & -Y_{e3} \\ & Y_{c1} + Y_{c3} & & & & \\ g_{e1}/2 & 0 & Y_3 + Y_{e3} & 0 & 0 & -Y_{e3} \\ -Y_{c1} & & Y_{c1} + Y_{c3} & & & \\ 0 & -Y_{c3} & 0 & Y_5 + Y_{c3} & 0 & -g_{e3} \\ & +g_{e3} & & & & \\ -1/2 & 0 & 0 & 0 & 1 & 0 \\ 0 & -1/2 & -1/2 & 0 & 0 & 1 \end{vmatrix} \quad (5.2-7)$$

5.2-3

Expanding the determinant by cofactors, one obtains

$$|Y| = K \left\{ \left( Y_2 + Y_{c1} + \frac{Y_{e1}}{2} \right) |A_1| - Y_{c1} \left( \frac{|A_2|}{2} + |A_3| \right) \right\} \quad (5.2-8)$$

where  $K = 4(Y_{e1} + g_{e1})(Y_{e3} + g_{e3})$  and  $A_1$ ,  $A_2$ , and  $A_3$  are 4 x 4 matrices given by

$$|A_1| = \begin{vmatrix} Y_3 + Y_{e3} & 0 & -Y_{c3} & -Y_{e3} \\ Y_{c1} + Y_{c3} & Y_3 + Y_{e3} & 0 & -Y_{e3} \\ 0 & Y_{c1} + Y_{c3} & 0 & -Y_{e3} \\ -Y_{c3} & 0 & Y_5 & -g_{e3} \\ +g_{e3} & +Y_{c3} & +Y_{c3} & \\ -1/2 & -1/2 & 0 & 1 \end{vmatrix} \quad (5.2-9)$$

$$|A_2| = \begin{vmatrix} Y_3 + Y_{e3} & -Y_{c3} & -g_{e1} & -Y_{e3} \\ Y_{c1} + Y_{c3} & -Y_{c3} & -g_{e1} & -Y_{e3} \\ 0 & 0 & 0 & -Y_{e3} \\ -Y_{c3} & Y_5 & 0 & -g_{e3} \\ +g_{e3} & +Y_{c3} & 0 & -g_{e3} \\ -1/2 & 0 & 0 & 1 \end{vmatrix} \quad (5.2-10)$$

$$|A_3| = \begin{vmatrix} 0 & Y_3 + Y_{e3} & -Y_{c3} & -Y_{e3} \\ Y_{c1} + Y_{c3} & 0 & 0 & -Y_{e3} \\ g_{e1/2} & -Y_{c1} & 0 & -Y_{e3} \\ 0 & -Y_{c3} & Y_5 + Y_{c3} & -g_{e3} \\ 0 & -1/2 & 0 & 1 \end{vmatrix} \quad (5.2-11)$$

Evaluating the determinants of the A-matrices gives

$$\begin{aligned} |A_1| = & \frac{Y_{e3} Y_{c3}^2}{2} + \frac{g_{e3} Y_{c3}}{2} (Y_3 + Y_{c1} + Y_{c3}) \\ & + (Y_3 + Y_{c1})(Y_3 + Y_{e3} + Y_{c1} + Y_{c3})(Y_5 + Y_{c3}) \\ & + Y_5 Y_{c3} (Y_3 + Y_{e3} + Y_{c1} + Y_{c3}) \end{aligned} \quad (5.2-12)$$

$$|A_2| = \frac{g_{e1} Y_{e3} (Y_5 + Y_{c3})}{2} \quad (5.2-13)$$

$$\begin{aligned}
|A_3| = & \left\{ Y_{c1} - \frac{g_{e1}}{2} \right\} \left\{ (Y_5 + Y_{c3}) \left( Y_3 + \frac{Y_{e3}}{2} + Y_{c1} + Y_{c3} \right) \right. \\
& \left. + Y_{c3} \left( \frac{g_{e3}}{2} - Y_{c3} \right) \right\} \quad (5.2-14)
\end{aligned}$$

Combining terms then yields for the determinant of the admittance matrix

$$\begin{aligned}
|Y| = & K \left[ \left\{ Y_2 + \frac{Y_{e1}}{2} + Y_{c1} \right\} \cdot \left\{ \left[ Y_3 + Y_{e3} + Y_{c1} + Y_{c3} \right] \right. \right. \\
& \left[ (Y_3 + Y_{c1}) (Y_5 + Y_{c3}) + Y_5 Y_{c3} \right] \\
& + \frac{g_{e3} Y_{c3}}{2} (Y_3 + Y_{c1} + Y_{c3}) + \frac{Y_{e3} Y_{c3}^2}{2} \left. \right\} \\
& + \frac{g_{e1} Y_{c1}}{2} \left\{ (Y_3 + Y_{c1}) (Y_5 + Y_{c3}) + Y_5 Y_{c3} + \frac{g_{e3} Y_{c3}}{2} \right\} \\
& + Y_{c1} \left\{ Y_{c1} Y_{c3}^2 - \frac{Y_{c3} g_{e3} Y_{c1}}{2} \right. \\
& \left. - (Y_3 + \frac{Y_{e3}}{2} + Y_{c1} + Y_{c3}) Y_{c1} (Y_5 + Y_{c3}) \right\} \left. \right] \quad (5.2-15)
\end{aligned}$$

We now proceed to calculate the transfer admittance by determining the dependence of  $V_5$  on  $i_2$ . The matrix for  $V_5$  is given by

$|Y_{V5}|$

=

$Y_2 + Y_{e1}$ $+ Y_{c1}$	0	$-Y_{c1}$	$i_2$	$-Y_{e1}$	0
0	$Y_3 + Y_{e3}$ $Y_{c1} + Y_{c3}$	0	0	$-g_{e1}$	$-Y_{e3}$
$-Y_{c1}$ $+ g_{e1}$	0	$Y_3 + Y_{e3}$ $Y_{c1} + Y_{c3}$	0	$-g_{e1}$	$-Y_{e3}$
0	$-Y_{c3}$ $+ g_{e3}$	0	0	0	$-g_{e3}$
$-Y_{e1}$ $- g_{e1}$	0	0	0	$2Y_{e1}$ $+ 2g_{e1}$	0
0	$-Y_{e3}$ $- g_{e3}$	$-Y_{e3}$ $- g_{e3}$	0	0	$2Y_{e3}$ $+ 2g_{e3}$

Performing similar elementary operations as used in reducing  $|Y|$ , one can simplify equation 5.2-16 to

$$|Y_{V5}| = K \left\{ \frac{|B_1|}{2} + |B_2| \right\} i_2 \quad (5.2-17)$$

where  $B_1$  and  $B_2$  are 4 x 4 matrices given by

$$|B_1| = \begin{vmatrix} Y_3 + Y_{e3} & 0 & -g_{e1} & -Y_{e3} \\ Y_{c1} + Y_{c3} & Y_3 + Y_{e3} & 0 & -Y_{e3} \\ 0 & Y_{c1} + Y_{c3} & 0 & -Y_{e3} \\ -Y_{c3} & 0 & 0 & -g_{e3} \\ +g_{e3} & 0 & 0 & -g_{e3} \\ -1/2 & -1/2 & 0 & 1 \end{vmatrix} \quad (5.2-18)$$

$$|B_2| = \begin{vmatrix} 0 & Y_3 + Y_{e3} & 0 & -Y_{e3} \\ Y_{c1} + Y_{e3} & 0 & Y_3 + Y_{e3} & -Y_{e3} \\ -Y_{c1} + g_{e1}/2 & 0 & Y_{c1} + Y_{c3} & -Y_{e3} \\ 0 & -Y_{c3} + g_{e3} & 0 & -g_{e3} \\ 0 & -1/2 & -1/2 & 1 \end{vmatrix} \quad (5.2-19)$$

Evaluating these determinants one obtains

$$|Y_{V5}| = - \frac{i_2 K g_{e1} g_{e3} Y_3}{2} \left\{ 1 + \frac{Y_{c1} + Y_{c3}}{Y_3} \right\} \left\{ 1 - X_N \right\} \quad (5.2-20)$$

where  $X_N$  is a non-minimum phase term given by

$$X_N = \frac{Y_{c1}}{g_{e1}} + \frac{Y_{c3}}{g_{e3}} + \left( \frac{Y_{c1}}{g_{e1}} \right) \left( \frac{Y_{c3}}{g_{e3}} \right) \frac{Y_{e3}}{Y_3 + Y_{c1} + Y_{c3}} \quad (5.2-21)$$



The transfer admittance then becomes

$$Z_T = \frac{V_5}{I_2} = \frac{-g_{e1} g_{e3} (Y_3 + Y_{c1} + Y_{c3})(1 - X_N)}{2|Y'|} \quad (5.2-22)$$

where

$$|Y'| = \frac{|Y|}{K}$$

Combining terms, one obtains for the determinant

$$\begin{aligned} \frac{|Y'|}{Y_3'} &= Y_2' \left\{ Y_5' Y_3'' + Y_{c3} \left[ \frac{g_{e3}}{2} - Y_{c3} \left( 1 - \frac{Y_{e3}}{2Y_3'} \right) \right] \right\} \\ &\quad + \frac{g_{e1} Y_{c1}}{2} \left\{ Y_5' \left[ 1 + \frac{Y_{c1}}{Y_3' g_{e1}} \left( Y_{e3} - 2Y_3'' \right) \right] \right. \\ &\quad \left. + \frac{Y_{c3} g_{e3}}{2Y_3'} \left[ 1 - \frac{2Y_{c1}}{g_{e1}} - \frac{2Y_{c3}}{g_{e3}} \left( 1 - \frac{2Y_{c1}}{g_{e1}} \right) \right] \right\} \end{aligned} \quad (5.2-23)$$

where

$$Y_2' = Y_2 + \frac{Y_{e1}}{2} + Y_{c1}$$

$$Y_5' = Y_5 + Y_{c3}$$

$$Y_3' = Y_3 + Y_{c1} + Y_{c3}$$

$$Y_3'' = Y_3 + Y_{c1} + Y_{c3} + Y_{e3}$$

If

$$2Y_{c1} \ll g_{e1} \quad (5.2-24)$$

$$2Y_{c3} \ll g_{e3} \quad (5.2-25)$$

$$Y_{c1} \left( \frac{Y_{e3}}{Y_3'} \right) \ll g_{e1} \quad (5.2-26)$$

then

$$Z_T \approx \frac{-g_{e1} g_{e3}}{2 \left\{ Y_2' \left[ Y_5' Y_3'' + \frac{Y_{c3} g_{e3}}{2} \right] + \frac{g_{e1} Y_{c1}}{2} \left[ Y_5' + \frac{Y_{c3} g_{e3}}{2 Y_3'} \right] \right\}} \quad (5.2-27)$$

### 5.2.1 Input Admittance and Voltage Gain Representation

The voltage gain, defined by

$$M_V = \lim_{Y_2 \rightarrow \infty} \frac{V_5 Y_2}{i_2}, \quad (5.2.1-1)$$

can be found directly from equations 5.2-22 and 5.2-15. In this case the equations simplify to

$$M_V = \frac{-g_{e1} g_{e3} Y_3 \left( 1 + \frac{Y_{c1} + Y_{c3}}{Y_3} \right) (1 - X_N)}{2|Y'|} \quad (5.2.1-2)$$

$$\text{where } |Y'| = \left[ Y_3 + Y_{e3} + Y_{c1} + Y_{c3} \right] \left[ (Y_3 + Y_{c1})(Y_5 + Y_{c3}) + Y_5 Y_{c3} \right] + \frac{g_{e3} Y_{c3}}{2} \left[ Y_3 + Y_{c1} + Y_{c3} \right] + \frac{Y_{e3} Y_{c3}^2}{2}$$

For the same substitutions as made in simplifying equation 5.2-23,

$$M_V = \frac{-g_{e1} g_{e3} (1 - X_N)}{2 \left\{ Y_5' Y_3'' + \frac{g_{e3} Y_{c3}}{2} - Y_{c3}^2 \left( 1 + \frac{Y_{e3}}{2Y_3'} \right) \right\}} \quad (5.2.1-3)$$

If

$$2Y_{c3} \left( 1 + \frac{Y_{e3}}{2Y_3'} \right) \ll g_{e3} \quad (5.2.1-4)$$

and if

$$Y_{c1} \ll g_{e1} \quad (5.2.1-5)$$

then

$$M_V \cong \frac{-g_{e1} g_{e3}}{2 \left\{ Y_5' Y_3'' + \frac{g_{e3} Y_{c3}}{2} \right\}} \quad (5.2.1-6)$$

In addition to the voltage gain, one generally also needs the input admittance, defined by

$$Y_{IN} = \frac{i_2}{V_2} \quad (5.2.1-7)$$

The determinant for  $V_2$  obviously becomes

$$|Y_{V2}| = K|A_1|i_2 \quad (5.2.1-8)$$

where  $|A_1|$  is given by equation 5.2-9. Because

$$V_2 = \frac{|Y_{V2}|}{|Y|}, \quad (5.2.1-9)$$

then

$$Y_{IN} = \frac{i_2 |Y|}{|Y_{V2}|} = Y_2 + Y_{c1} + \frac{Y_{e1}}{2} - Y_{c1} \left\{ \frac{\frac{|A_2|}{2} + |A_3|}{|A_1|} \right\} \quad (5.2.1-10)$$

The first three terms result from the admittances hung directly on the input. The last term, proportional to  $Y_{c1}$ , results from the Miller effect, motivating us to define  $Y_{M1}$  by

$$Y_{IN} = Y_2 + Y_{c1} + \frac{Y_{e1}}{2} + Y_{M1} \quad (5.2.1-11)$$

where

$$Y_{M1} = M_{V1} Y_{c1}$$

$$M_{V1} = - \frac{\frac{|A_2|}{2} + |A_3|}{|A_1|}$$

The numerator of the equation for the first-stage voltage gain  $M_{V1}$  can be simplified using equations 5.2-13 and 5.2-14, which imply that

$$\begin{aligned} - \left\{ \frac{|A_2|}{2} + |A_3| \right\} &= \frac{g_{e1}}{2} \left[ (Y_5 + Y_{c3})(Y_3 + Y_{c1}) + Y_{c3} Y_5 \right. \\ &\quad \left. + \frac{g_{e3} Y_{c3}}{2} \right] - Y_{c1} \left[ (Y_5 + Y_{c3})(Y_3 + \frac{Y_{e3}}{2} \right. \\ &\quad \left. + Y_{c1} + Y_{c3}) + Y_{c3} \left( \frac{g_{e3}}{2} - Y_{c3} \right) \right] \\ &= \left\{ \frac{g_{e1}}{2} - Y_{c1} \right\} \left\{ Y_5' Y_3' + \frac{Y_{c3}}{2} (g_{e3} - 2Y_{c3}) \right\} \\ &\quad - \frac{Y_{c1} Y_5' Y_{e3}}{2} \end{aligned} \quad (5.2.1-12)$$

Similarly,

$$|A_1| = Y_3' \left\{ Y_{c3} \left( \frac{g_{e3}}{2} - Y_{c3} \right) + Y_5' Y_3'' \right\} - \frac{Y_{c3}^2 Y_{e3}}{2} \quad (5.2.1-13)$$

$$\text{If } 2Y_{c1} \ll g_{e1} \quad (5.2.1-14)$$

$$2Y_{c3} \ll g_{e3} \quad (5.2.1-15)$$

$$Y_{c1} \ll \frac{Y_3'}{Y_{e3}} g_{e1} \quad (5.2.1-16)$$

$$Y_{c3} \ll \frac{Y_3'}{Y_{e3}} g_{e3} \quad (5.2.1-17)$$

then

$$M_{V1} \cong \frac{g_{e1}}{2 \left\{ Y_3' + \frac{Y_{e3}}{1 + \frac{Y_{c3} g_{e3}}{2Y_3' Y_5'}} \right\}} \quad (5.2.1-18)$$

## Appendix B

### Pulse Shaping in Pulse-Height Analyzer Systems

Pulse Shaping in  
Pulse-Height Analyzer Systems

by

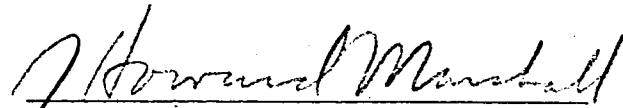
J. Howard Marshall

ATC Internal Report No. 2

26 July 1966

Analog Technology Corporation  
3410 East Foothill Boulevard  
Pasadena, California

Approved by:

A handwritten signature in dark ink, appearing to read "J. Howard Marshall", is written over a horizontal line.

J. Howard Marshall  
Vice President  
Advanced Planning



ATC INTERNAL REPORT NUMBER 2  
PULSE SHAPING IN PULSE-HEIGHT ANALYZER SYSTEMS

Table of Contents

	<u>Page No.</u>
1.0 INTRODUCTION	1
2.0 ERRORS RESULTING FROM RANDOM EVENTS	1
2.1 Statistical Distributions	2
2.1.1 Rounding Errors	7
2.2 Errors from Variable Counting Rates	8
2.2.1 Coincidence-Gated System	11
2.2.2 Open-Gate System	22
3.0 NOISE	47
3.1 Typical Noise Sources	50
3.1.1 Resistor Noise	50
3.1.2 Shot Noise	51
3.1.3 Junction-Transistor Noise	54
3.1.4 Field-Effect Transistor Noise	57
3.2 The Charge-Sensitive Amplifier	61
3.2.1 Field-Effect Transistor Input Stage	78
3.3 Noise Counting Rates	84
3.3.1 Photomultiplier Tube System	98

## List of Figures and Tables

	<u>Page No.</u>
Figure 2.2-1 Pulse-Height Analyzer System	10
2.2.2-1 Typical Sequence of Pulses	29
3.1.3-1 Transistor Noise Model	55
3.1.4-1 Grounded-Source Equivalent Noise Circuit	58
3.2.1 Noise Equivalent Circuit	62
3.2.1-1 Typical FET Amplifier Configuration	79
3.3-1 Discriminator Response	85
3.3.1-1 X-Ray Detector System	99
Table 1 Noise and Peak Values for Optimized Shaping Using Simple Poles	77
2 Typical Solid-State Detector System Noise Levels	83
3 Noise Counting Rate Parameters	95
4 Typical Noise Counting Rates	97
5 Typical Noise Counting Rates	106

## ATC INTERNAL REPORT NUMBER 2

### PULSE SHAPING IN PULSE-HEIGHT ANALYZER SYSTEMS

J. H. Marshall

July 26, 1966

#### 1.0 INTRODUCTION

The choice of the correct pulse shape in pulse-height analyzer systems is often a series of involved compromises between such factors as statistics, noise, accuracy and complexity. In order to avoid the small chance that random choices will converge on an optimum system in the presence of so many interrelating factors, an analytical approach is essential. To provide a basis for such an analytical design, a theoretical treatment of the effect of pulse shaping on pile-up and noise is given here.

#### 2.0 ERRORS RESULTING FROM RANDOM EVENTS

In addition to systematic errors such as gain drifts or bias changes, many experiments are subject to various forms of random errors. For example, the number of radioactive decays occurring during a fixed time interval is not uniquely predictable. Similarly, the number of pulses generated by thermal noise during a fixed time interval can only be determined on the average.

Extensive analysis of the statistical theory of such random behavior is available in the literature<sup>(1)</sup>. It will be possible here only to summarize some of the main points of this theory relevant to particle-counting experiments.

---

(1) Harold Cramer, Mathematical Methods of Statistics, (Princeton University Press, 1958).

## 2.1 Statistical Distributions

Many experiments involve the repeated sampling of a random variable. In such experiments, the experimenter usually wishes to know relevant parameters of the statistical distributions describing the phenomena in which he is interested. For example, he might wish to determine the average rate of a radioactive decay or the average number of solar X-rays lying within a given energy range. A powerful theorem of statistical analysis, called the central limit theorem, states that nearly all distributions describing such physical phenomena approach the normal distribution as the number of observations becomes sufficiently large. The frequency function for the normal distribution is given by

$$P(x) = \frac{1}{\sqrt{2\pi}\sigma} \exp \frac{-(x-m)^2}{2\sigma^2} \quad (2.1-1)$$

where  $P(x_0) dx$  represents the probability that the variable  $x$  lies within  $dx$  of  $x_0$ . This function has a mean value of  $m$  and a standard deviation of  $\sigma$ , where  $m$  and  $\sigma$  are defined by

$$m = \int_{-\infty}^{\infty} x P(x) dx \quad (2.1-2)$$

$$\sigma^2 = \int_{-\infty}^{\infty} (x-m)^2 P(x) dx \quad (2.1-3)$$

and  $P(x)$  is obviously normalized so that

$$1 = \int_{-\infty}^{\infty} P(x) dx \quad (2.1-4)$$

The normal distribution contains only two parameters,  $m$  and  $\sigma$ . If one knows that the phenomena being measured are normally distributed, then the purpose of an experiment becomes the determination of  $m$  and  $\sigma$  at various times or under changing conditions. Even for non-normal distributions, the mean and root-mean-square width will be good estimators for the properties of the actual distribution. For example, in an experiment to determine a counting rate, the best estimate of the rate is the total number of counts divided by the total time during which they were accumulated. Similarly, the average energy of a particle providing a peak in a pulse-height spectrum lying between channels  $n$  and  $k$  can be calculated from

$$\bar{E} = \frac{\sum_{i=n}^k N_i E_i}{\sum_{i=n}^k N_i} \quad (2.1-5)$$

where

$N_i$  = number of counts in the  $i^{\text{th}}$  channel

$E_i$  = equivalent energy of the  $i^{\text{th}}$  channel

If the rms width of the peak is  $\sigma_1$ , then the accuracy with which the mean input energy can be determined is

$$\sigma = \frac{\sigma_1}{\sqrt{N}} \quad (2.1-6)$$

where  $N$  = number of counts in the peak. Thus, repeated measurements of a noisy distribution can improve the accuracy of the determination of the input signal. In order for this technique to be fully effective, gain drifts, offset changes, or other purely systemic effects must be constant during the period of measurement. These concepts can also be generalized to include continuous functions. In this case the mean becomes

$$m = \lim_{T \rightarrow \infty} \frac{1}{2T} \int_{-T}^T f(t) dt \quad (2.1-7)$$

with a variance given by

$$\sigma^2 = \lim_{T \rightarrow \infty} \frac{1}{2T} \int_{-T}^T f^2(t) dt - m^2 \quad (2.1-8)$$

One of the most common distributions present in counting experiments occurs when one considers the result of multiple trials of an experiment which may either succeed or fail. For

example, when tossing coins, the coin may come up heads or tails. Similarly, a given particle may or may not have an energy in excess of a predetermined amount. If the probability of success on one trial is  $p$ , then the probability of  $r$  successes in  $n$  trials is given by

$$P_r = \binom{n}{r} p^r (1-p)^{n-r} \quad (2.1-9)$$

where

$$\binom{n}{r} = \text{Binomial coefficient} = \frac{n(n-1)\cdots(n-r+1)}{r!} = \frac{n!}{(n-r)!r!}$$

This distribution has a mean value and standard deviation given by

$$m = np \quad (2.1-10)$$

$$\sigma = \sqrt{np(1-p)}$$

In the limit where  $n$  becomes large and the probability of success is small but not vanishing, then

$$P_r \rightarrow P(x) = \frac{1}{\sqrt{2\pi m}} \exp \left[ -\frac{(x-m)^2}{2m} \right] \quad (2.1-11)$$

This limit shows that, as implied by the central limit theorem, the binomial distribution approaches a normal distribution with a standard deviation equal to the square root of the mean number

of counts accepted. This fact is the basis for the usual statement that the statistical error equals the square root of the number of counts. (Note that when the probability of success is not small, the exact formula [2.1-10] must be used.) By dividing the standard deviation by the mean, one obtains the fractional error given by

$$\frac{\sigma}{m} = \frac{1}{\sqrt{m}} \quad (2.1-12)$$

Thus, by accumulating more counts, the experimenter can improve the accuracy of his measurement.

Another interesting limit of 2.1-9 results when

$$p = \lambda/n \quad (2.1-13)$$

so that  $p \rightarrow 0$  as  $n \rightarrow \infty$ . In this case the binomial distribution approaches the Poisson distribution, given by

$$P_r = \frac{\lambda^r}{r!} e^{-\lambda} \quad (2.1-14)$$

with a mean value of  $\lambda$  and a standard deviation of  $\sqrt{\lambda}$ .

This distribution results when one considers the probability that one or more random pulses occur in a given time interval immediately following another pulse. In this case the parameter  $\lambda$  becomes  $Rt$ , where  $R$  is the mean counting rate and  $t$  is the measuring interval. The parameter  $r$  is the number of pulses in the interval, and the probability  $P_r$  becomes

$$P_r = \frac{(Rt)^r}{r!} e^{-Rt} \quad (2.1-15)$$



The probability that the first pulse occurs at  $t$  is then

$$1 - P_0 = 1 - e^{-Rt} \quad (2.1-16)$$

The probability that the first pulse occurs at a time  $t$  within  $dt$  then results from differentiating 2.1-16,

$$P(t)dt = Re^{-Rt}dt \quad (2.1-17)$$

Several applications of the above general principles will be given in the following sections. The problem for the instrument designer is then to choose the parameters of his system so as to prevent these statistical effects from unnecessarily contributing to measurement errors.

### 2.1.1 Rounding Errors

Often digital data compression techniques are applied to reduce unnecessary use of limited data transmission facilities. When such techniques are used, rounding errors occur. The addition of these errors to over-all system accuracy can be calculated as follows.

The distribution that describes a rounding error is the rectangular distribution defined by

$$P(x) = \begin{cases} 1/C & -C/2 < x < C/2 \\ 0 & \text{otherwise} \end{cases} \quad (2.1.1-1)$$

where  $C$  is the total resolution of the digital system. The mean of  $P(x)$  is

$$m = \int_{-\infty}^{\infty} xP(x) dx = 0 \quad (2.1.1-2)$$

and thus one should take the center of the interval as the best estimate. The error given by

$$\sigma = \sqrt{\int_{-\infty}^{\infty} x^2 P(x) dx} = \frac{C}{2\sqrt{3}} \quad (2.1.1-3)$$

should be added to other system errors as the square root of the sum of the squares.

## 2.2 Errors from Variable Counting Rates

Because the percentage error decreases with an increasing number of counts (see equation 2.1-12), the experimenter often will choose to accumulate as many counts as possible. If the measuring time is limited, then high counting rates may result. These high rates can cause errors in addition to those discussed in Section 2.1, because of dead-time or amplitude shifts in the signal processing system. A poorly designed signal processing system can unnecessarily compound these errors.

Before embarking on a detailed analysis of rate-dependent effects on a linear analyzer system, we wish to remark that poorly designed systems can have non-linearities that significantly increase the purely statistical errors. For example, if pulse amplifiers do not have sufficient dynamic range and linearity, base-line shifts occurring at high rates can produce gain changes<sup>(2)</sup>. The need for good linearity then not only becomes necessary for ease of data analysis, but also is necessary to eliminate rate-dependent gain shifts. Such linearity usually can be achieved by the use of sufficient negative

---

(2) Fairstein and Hahn, Nucleonics 23, (July, September, November 1965 and January, March 1966).

feedback and by intelligent design of circuits handling large signals. This sophistication is also required to provide independence of temperature and aging of active elements.

A typical pulse-height analyzer system is shown in Figure 2.2-1. Pulses from a particle detector enter an amplifier containing pulse-shaping elements. The amplifier output signal then passes through a linear gate into an analog-to-digital converter. For this analysis we will assume that these latter circuits are direct-coupled and fast enough so that all pulse shaping is effectively performed before the linear gate. The gate is opened and closed in response to coincidence or busy signals generated in external logic circuits.

Experiments in which such pulse-height analyzers are used typically require the measurement of pulse-height distributions for particular events in the presence of a random background of uninteresting pulses. The desired events are often selected by coincidence logic or by the presence of a distinguishing feature in the pulse-height spectrum, such as a peak. Not only may the background make the selection of the desired events difficult, but it may also distort their pulse-height spectrum. This distortion may appear both as a variation in the average measured amplitude for the desired events and as a smearing of sharp features, such as peaks, in the pulse-height spectrum. These effects result from the fact that at high rates an appreciable probability exists that the sum of two or more pulses may be analyzed concurrently, so that each event cannot be treated as a separate entity. The presence of capacitative coupling compounds this problem, because it may be possible to supply an average charge to the

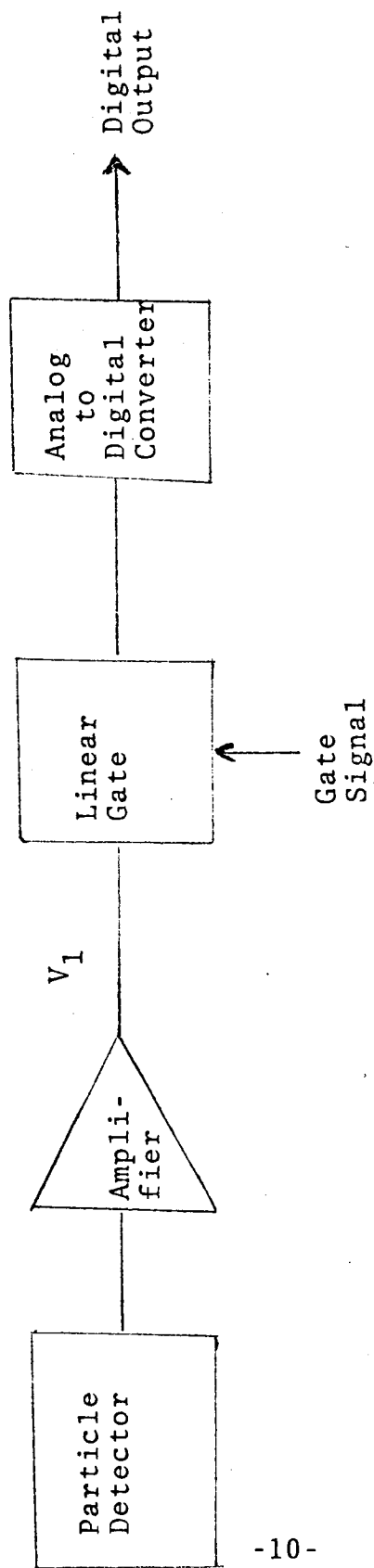


Figure 2.2-1: Pulse-Height Analyzer System

14

coupling capacitor, resulting in the shift of a critical baseline voltage.

We will consider two modes of control of the linear gate which result in significantly different statistical errors. In the first mode, the events of interest are selected from a random background by external coincidence logic or by the fact that the signal of interest has a very much larger amplitude than the background. The linear gate remains constantly closed except when the interesting event occurs. In the second mode, the gate remains constantly open, except during busy periods for the analyzer, and events are analyzed on a first-come, first-served basis.

#### 2.2.1 Coincidence-Gated System

In a coincidence-gated system a typical problem is to measure the amplitude produced by a particular event selected by external means. If there is no correlation between the times that the gate is opened and the background events, then the background pulses are being randomly sampled. If the maximum variation of the signal peak lies within the linear region of analyzer operation and does not overlap any additional signal peaks, then the best estimate of a given peak is found by calculating the mean channel number (or equivalent input energy) for events in the peak. Similarly, the peak width can be measured by calculating the root-mean-square value. Both these quantities can vary with increasing counting rate, and this variation can be estimated as follows:

Let the amplifier pulse shaping be independent of amplitude so that the contribution to the amplifier output level ( $V_1$ ) from the  $i^{\text{th}}$  pulse at a time  $t$  is:

$$V_{1i} = V_{oi} f(t-t_i) \quad (2.2.1-1)$$

where

$V_{oi}$  = peak value of the  $i^{\text{th}}$  pulse

$f$  = pulse-shape function normalized to a value of one at the peak

$t_i$  = time of arrival of the  $i^{\text{th}}$  particle, ignoring any pure delay effects

If particles began arriving at the detector at a time  $T_1$  and  $N_1$  particles have arrived between time  $T_1$  and time zero, with  $N_2$  particles between time zero and time  $t$ , then the total output voltage at a time  $t$  becomes:

$$V_1(t) = \sum_{i=1}^{N_1} V_{oi} f(t-t_i) + \sum_{i=N_1+1}^{N_2(t)} V_{oi} f(t-t_i) \quad (2.2.1-2)$$

If the linear gate opens occasionally at random times starting at time zero, then an average peak shift given by the average value of  $V_1(t)$  occurs. This average can be calculated from

$$\bar{V}_1 = \lim_{T_2 \rightarrow \infty} \frac{1}{T_2} \int_0^{T_2} V_1(t) dt \quad (2.2.1-3)$$

Substituting from equation 2.2.1-2 for  $V_1(t)$ , one obtains

$$\bar{V}_1 = \lim_{T_2 \rightarrow \infty} \frac{1}{T_2} \left\{ \sum_{i=1}^{N_1} V_{oi} \int_0^{T_2} f(t-t_i) dt + \sum_{i=N_1+1}^{N_2(T_2)} V_{oi} \int_0^{T_2} f(t-t_i) dt \right\} \quad (2.2.1-4)$$

The integral can be evaluated as follows:

$$\int_0^{T_2} f(t-t_i) dt = \int_0^{T_2-t_i} f(t') dt' \quad (2.2.1-5)$$

where

$$t' = t - t_i$$

and

$$f(t') = 0 \text{ for } t' < 0$$

In the limit that  $T_2$  approaches infinity and if the integral converges to  $K_1$ , then

$$\lim_{T_2 \rightarrow \infty} \int_0^{T_2} f(t-t_i) dt = \int_0^{\infty} f(t') dt' = K_1 \quad (2.2.1-6)$$

Because the integral in the limit is independent of  $t_i$ , it can be factored out of equation 2.2.1-4 leaving

$$\bar{V}_1 = K_1 \lim_{T_2 \rightarrow \infty} \frac{1}{T_2} \left\{ \sum_{i=N_1+1}^{N_2(T_2)} V_{oi} \right\} \quad (2.2.1-7)$$

The average value of the peak amplitude of the background spectrum can be written as

$$\bar{V}_0 = \lim_{T_2 \rightarrow \infty} \left\{ \frac{\sum_{i=N_1+1}^{N_2(T_2)} V_{oi}}{N_2(T_2) - N_1} \right\} \quad (2.2.1-8)$$

If the pulses arrive at an average rate  $R$ , then on the average

$$N_2(T_2) - N_1 = RT_2 \quad (2.2.1-9)$$

and equation 2.2.1-7 becomes

$$\bar{V}_1 = K_1 R \bar{V}_0 \quad (2.2.1-10)$$

Notice that  $K_1$  can be determined directly from the Fourier transform of  $f(t)$ . This transform is given by

$$F(j\omega) = \int_{-\infty}^{\infty} f(t) e^{-j\omega t} dt \quad (2.2.1-11a)$$

with an inverse transform of

$$f(t) = \frac{1}{2\pi} \int_{-\infty}^{\infty} F(j\omega) e^{j\omega t} d\omega \quad (2.2.1-11b)$$



so that

$$K_1 = \int_0^{\infty} f(t) dt = \frac{1}{2\pi} \int_0^{\infty} \int_{-\infty}^{\infty} F(j\omega) e^{j\omega t} d\omega dt \quad (2.2.1-12)$$

Inverting the order of integration and remembering that

$$\int_{-\infty}^{\infty} e^{j\omega t} dt = 2\pi \delta(\omega) \quad (2.2.1-13)$$

Then

$$K_1 = F(0) \quad (2.2.1-14)$$

Similarly one can calculate the root-mean-square variation of  $V_1$  from the above mean. The variance is given by

$$\sigma^2 = \overline{(V_1(t) - \bar{V}_1)^2} \quad (2.2.1-15)$$

Performing the squaring and averaging operations, one obtains

$$\sigma^2 = \overline{V_1^2(t)} - \bar{V}_1^2 \quad (2.2.1-16)$$

Substituting for  $V_1(t)$  from equation 2.2.1-2 and squaring,

$$V_1^2(t) = \sum_{i=1}^{N_2(t)} \sum_{j=1}^{N_2(t)} V_{oi} V_{oj} f(t-t_i) f(t-t_j) \quad (2.2.1-17)$$

Again averaging over a time period from zero to  $T_2$  and letting  $T_2$  approach infinity,

$$\overline{V_1^2} = \lim_{T_2 \rightarrow \infty} \frac{1}{T_2} \left\{ \int_0^{T_2} \sum_{i,j=1}^{N_2(T_2)} V_{oi} V_{oj} f(t-t_i) f(t-t_j) dt \right\} \quad (2.2.1-18)$$

Arranging terms,

$$\overline{V_1^2} = \lim_{T_2 \rightarrow \infty} \frac{1}{T_2} \left\{ \sum_{i,j=1}^{N_2(T_2)} V_{oi} V_{oj} \int_0^{T_2} f(t-t_i) f(t-t_j) dt \right\} \quad (2.2.1-19)$$

Recognizing that  $f(t)$  vanishes for negative times and separating the cross-terms from the squared terms,

$$\begin{aligned} \overline{V_1^2} = & \lim_{T_2 \rightarrow \infty} \frac{1}{T_2} \left\{ \sum_{i=N_1+1}^{N_2(T_2)} V_{oi}^2 \int_{-\infty}^{T_2} f^2(t') dt' \right\} \\ & + \lim_{T_2 \rightarrow \infty} \frac{1}{T_2} \left\{ \sum_{\substack{i,j=N_1+1 \\ j>i}}^{N_2(T_2)} 2 V_{oi} V_{oj} \int_{-\infty}^{T_2} f(t') f(t'+t_i-t_j) dt' \right\} \end{aligned} \quad (2.2.1-20)$$

The above integrals are autocorrelation integrals and obey several well-known laws<sup>(3)</sup>. For example, a simple relationship exists between the integral and the Fourier transform  $F(j\omega)$  of the pulse response.

$$\phi(t_{ij}) = \int_{-\infty}^{\infty} f(t) f(t+t_{ij}) dt = \frac{1}{2\pi} \int_{-\infty}^{\infty} |F(j\omega)|^2 e^{-j\omega t_{ij}} d\omega$$

(2.2.1-21)

where

$$t_{ij} = t_i - t_j$$

[This result can be simply proved by substituting the definition of  $F(j\omega)$  from equation 2.2.1-11, integrating over  $t$  applying equation 2.2.1-13 and using the fact that  $F(-j\omega) = F^*(j\omega)$ .]  
In the limit of infinite  $T_2$ , equation 2.2.1-20 becomes

$$\overline{V_1^2} = RK_2 \overline{V_0^2} + \lim_{T_2 \rightarrow \infty} \frac{1}{T_2} \sum_{\substack{i,j=N_1+1 \\ j>i}}^{N_2(T_2)} 2V_{oi} V_{oj} \phi(t_{ij})$$

(2.2.1-22)

where

$$K_2 = \phi(0) = \int_0^{\infty} f^2(t) dt = \frac{1}{2\pi} \int_{-\infty}^{\infty} |F(j\omega)|^2 d\omega$$

---

(3) Y. W. Lee, Statistical Theory of Communication, (John Wiley and Sons, Inc., New York).

$$\overline{V_o^2} = \lim_{N_2 \rightarrow \infty} \left\{ \frac{\sum_{i=N_1+1}^{N_2} V_{oi}^2}{N_2 - N_1} \right\}$$

The second term of equation 2.2.1-22 can be written as

$$\lim_{T_2 \rightarrow \infty} \frac{1}{T_2} \sum_{i=N_1+1}^{N_2(T_2)} 2 V_{oi} \sum_{j=i+1}^{N_2(T_2)} V_{oj} \phi(t_{ij}) \quad (2.2.1-23)$$

In the limit of infinite  $T_2$ , many values of  $t_{ij}$  and  $V_{oj}$  appear, allowing the second factor in 2.2.1-23 to be simplified by averaging over  $t_{ij}$  and  $V_{oj}$ . Applying the same techniques used in simplifying 2.2.1-4, one obtains

$$\lim_{T_2 \rightarrow \infty} \sum_{j=i+1}^{N_2(T_2)} V_{oj} \phi(t_{ij}) = \bar{V}_o R \int_0^\infty \phi(t_{ij}) dt_{ij} \quad (2.2.1-24)$$

Replacing  $\phi(t_{ij})$  by its Fourier transform given in 2.2.1-21, interchanging the order of integrations over  $t_{ij}$  and  $\omega$ , and using the delta-function relation of 2.2.1-13, then

$$\lim_{T_2 \rightarrow \infty} \sum_{j=i+1}^{N_2(T_2)} V_{oj} \phi(t_{ij}) = \frac{\bar{V}_o R |F(0)|^2}{2} \quad (2.2.1-25)$$

Substituting this expression in equation 2.2.1-23 and remembering that  $F(0)$  is real and equal to  $K_1$ ,

$$\overline{V_1^2} = RK_2 \overline{V_o^2} + (R\bar{V}_o K_1)^2 = RK_2 \overline{V_o^2} + \bar{V}_1^2 \quad (2.2.1-26)$$

and the variance becomes

$$\sigma^2 = RK_2 \overline{V_o^2} \quad (2.2.1-27)$$

The results given in equations 2.2.1-10 and 2.2.1-27 are special cases of Campbell's theorem<sup>(4)</sup>.

The above analysis is important in determining the optimal pulse shaping for an analyzer system operating at high counting rates. The average peak shift should be made to vanish by choosing  $f(t)$  such that  $K_1$  is zero. This requirement is equivalent to choosing a wave shape with a vanishing Fourier transform at zero frequency. Thus, if RC pulse shaping is used and if the time dependence of the detector signal can be approximated by a delta-function, then at least two differentiating time constants are required - that is:

$$F(j\omega) = \frac{j\omega\tau_1 C}{(1+j\omega\tau_1)(1+j\omega\tau_2)} \quad (2.2.1-28)$$

This function obviously satisfies  $F(0) = 0$ , so that  $K_1$  also vanishes and no shifts of average peak position should occur in a well-designed, linear system.

The reduction of peak spreading requires several considerations. Obviously, the pulse width should be as short as possible, limited by the detector output pulse width, available circuit elements and system power constraints. Notice that in evaluating the limit of infinite  $T_2$ , the period during

---

(4) S. O. Rice, "Mathematical Analysis of Random Noise" from Selected Papers on Noise and Stochastic Processes, edited by N. Wax (Dover Publications, Inc., New York, 1954).

which averaging was performed had to be long compared to any variations in  $f(t)$ . If the count rate is also variable because of a pulsed particle source or a rotating spacecraft, no time constants in  $f(t)$  of the order of the time for appreciable rate variations should be present. Otherwise, the averaging technique performed above will not be valid, resulting in unexpected peak shifts and increased line widths<sup>(4)</sup>. Thus, when RC pulse shaping is used, the optimal system requires that all time constants be roughly equal and short compared to the average spacing between pulses.

If the ultimate is required in negligible effects at high rates, "inspection" circuits are often employed. Such a circuit allows the linear gate to open only when no background signal is present at the input. In this way peak smearing is reduced at the expense of increased dead time. Again short time constants are required to prevent pile-up and baseline shifts which could cause large and unnecessary increases in dead time.

As an example of the above techniques, consider the double-differentiated, double-integrated function given in Laplace transform by

$$F(p) = \left[ \frac{p\tau}{(1+p\tau)^4} \right] \left[ \frac{1}{0.131} \right] \quad (2.2.1-29)$$

---

(4) Rice, Loc. Cit.

with an inverse transform of

$$f(t) = \frac{\left(\frac{t}{\tau}\right)^2 \left(3 - \frac{t}{\tau}\right) \exp\left(-\frac{t}{\tau}\right)}{0.786}, \quad (2.2.1-30)$$

which is normalized to a value of unity at the peak. This wave-shape provides moderate independence of detector or amplifier open-loop rise times, while still being easy to mechanize. Also for many applications nearly optimal noise performance can be achieved by a proper choice of the shaping time constant  $\tau$ .

The Fourier transform obviously vanishes at zero frequency so that  $K_1 = 0$ , and no shifts of the mean peak positions should occur. The peak broadening can be calculated from equation 2.2.1-27:

$$\sigma^2 = \frac{\overline{RV_o^2}}{2\pi} \int_{-\infty}^{\infty} |F(j\omega)|^2 d\omega \quad (2.2.1-31)$$

$$\sigma = 1.35 \sqrt{\overline{V_o^2}} \sqrt{R\tau}$$

An estimate of the order of magnitude of these peak broadening effects can be generated by considering a 256 channel analyzer operating at an average rate of  $10^4$  counts/second. If the rms value of the background were 20% of the signal peak, then, for  $\tau = 1 \mu s$ , the rms peak broadening would be 2.7%, or 6.9 channels, for a signal peak in channel 255.

A wave-shape often used for high counting rate systems is the "double delay-line clipped" function, given by

$$V(t) = \begin{cases} V_0 & 0 < t < \tau \\ -V_0 & \tau < t < 2\tau \\ 0 & \text{otherwise} \end{cases} \quad (2.2.1-32)$$

This function also has a zero mean and a standard deviation given by

$$\sigma = 1.41 \sqrt{V_0^2} \sqrt{R\tau} \quad (2.2.1-33)$$

According to these criteria, the pulse shapes of equations 2.2.1-30 and 2.2.1-32 are nearly equivalent. The double delay-line clipped technique is not recommended for spacecraft use because of problems involving size, temperature stability and ringing of delay lines.

### 2.2.2 Open-Gate System

As the average time between gate openings approaches the analyzer dead time or if the gate remains continually open except during an analysis period, the computation of the mean shift given in the previous section breaks down. Because of the methods of construction of most analyzers and because of fundamental limitations in the data analysis, not all portions of the input pulse can be treated identically in calculating



the mean peak shift. This statistical bias will result in a shift in the mean value of a portion of the pulse-height spectrum, even though the average pulse amplitude vanishes.

Most pulse-height analyzers use some form of peak detection to begin the analysis and actually measure the peak value of the pulse. A dead time then results during which the analyzer processes the event. For analyzers employing the capacitive-rundown technique, this dead time is roughly proportional to the input amplitude. For binary-search or stacked-discriminator analyzers, the dead time is nearly independent of the input pulse height.

This dead time results in the loss of an event which follows an analyzed event in a time less than the dead time. The probability that a particle actually is emitted during this period results from the analysis of the Poisson distribution. From equation 2.1-15, the probability that no particles are lost becomes

$$P_0 = \exp (-RT) \quad (2.2.2-1)$$

where

$R$  = average rate

$T$  = dead time

The average number of lost particles per discriminator triggering is given by

$$\bar{N}_{\text{LOST}} = \sum_{r=1}^{\infty} r P_r(T) = m(T) = RT \quad (2.2.2-2)$$

Although this dead-time loss may be large, accurate data corrections can be made if the dead time itself is well known. Such corrections are complicated if the dead time is a function of the amplitude of the triggering pulse, because then both the pulse-height spectrum and the average counting rate must be included in generating a rate correction. If the dead time is principally determined by a discriminator pulse width and if this pulse width is independent of the rate and of the triggering amplitude, then only the average rate of discriminator triggering ( $R'$ ) need be known. This rate can then be used to find the true average rate from

$$R = \frac{R'}{1 - R'T} \quad (2.2.2-3)$$

In order to reduce the dependence of the dead time on the pulse-height spectrum, the amplifier pulse width must be considerably less than that of the discriminator. Also, the discriminator threshold should rapidly recover to its nominal value after the output returns to its quiescent state.

The usual capacitive-rundown analyzer does not satisfy the requirement that the dead time is independent of the triggering amplitude. However, an estimate of dead-time losses can often be made by using an average dead time produced by the average event in the pulse-height spectrum.

In addition to causing events to be lost, this dead time contributes to statistical biases producing peak shifts. These biases primarily result from slowly varying "tails" on the amplifier output pulses.

The typical amplifier-analyzer system usually possesses both primary and secondary pulse shaping networks<sup>(2)</sup>. The primary networks principally determine the pulse shape and amplitude for short times and result in a transient response which is rapidly varying with large amplitudes. This network provides most of the bandpass shaping required for proper analyzer operation and noise performance. Often secondary pulse-shaping networks are also present caused by capacitive couplings between amplifier stages. These time constants generally produce slowly varying signals with amplitudes for short times small compared to those from the primary networks. However, the large amplitude primary transient rapidly decays, so that for longer times the slowly varying secondary network response dominates.

These considerations motivate the division of the amplifier output pulse into two time regions such that

$$f(t) = f_1(t) + f_2(t) \quad (2.2.2-4)$$

where  $f_1(t)$  is rapidly varying and contains the pulse-height information, and  $f_2(t)$  is slowly varying and results from secondary capacitive couplings. Included in  $f_1(t)$  are the effects of the primary pulse-shaping networks, and the amplitude of  $f_1(t)$  for short times is usually much larger than that of  $f_2(t)$ . Typically  $f_1(t)$  lasts for times very short compared to the time required to analyze an event, while  $f_2(t)$  lasts for times comparable to or greater than this analysis time.

In the analysis of Section 2.2.1, the response of the analyzer and data analysis to  $f_1(t)$  and to  $f_2(t)$  was assumed

---

(2) Fairstein and Hahn, Loc. Cit.

identical when these signals resulted from background events. For high rates of analysis and for an open-gate system, this assumption fails to be valid for several reasons.

In the open-gate system it is usually necessary to select events of interest by the position and shape of their pulse-height spectrum. Several interesting types of events, together with an uninteresting background, may be present in the same pulse-height spectrum. The mean value of a portion of the spectrum can no longer be determined by averaging over the entire spectrum, as implied in the analysis of Section 2.2.1, because of the distorting effects from the other events. These events are no longer excluded from the spectrum by external coincidence logic, and the problem becomes more complicated than just calculating the accidental coincidence between background and interesting events.

Furthermore, the first-come, first-served nature of the analyzer complicates the nature of the pile-up of the positive portion of  $f_1(t)$ . (For definiteness, the peaks of the pulses being analyzed are assumed to be positive.) Most analyzers detect the change in sign of the slope of the input pulse and measure the value of the concurrent maximum. Almost immediately after this maximum is detected, the gate is closed and further pulses are excluded until the analyzer is finished processing the event. Therefore, when two pulses add with relative timing such as not to change the peak value, the analyzer will not generate a distorted output even though the average value of the positive portion may change. For example, a pulse just following a detected pulse at a time greater than that required for gate closure will not effect the analysis of the first pulse. Because the typical analyzer has a dead time long compared to the duration of  $f_1(t)$  and because the first

pulse to produce a maximum is always analyzed, except when the analyzer happens to be busy with a previous event, it is improbable that the portions of  $f_1(t)$  following the maximum contribute to spectral distortions.

In addition, unless very high rates are present, accidental pile-up of the rapidly varying portions of the amplifier pulse is improbable because of the small width of these pulses. When such pile-up does occur, the resulting sum is usually very different from the value of either pulse alone because the amplitudes in  $f_1(t)$  are of the same order as the maximum. Pile-up of these pulses then results in errors approaching a factor of two<sup>(2)</sup>, and often results in an analysis which is excluded as being outside the amplitude range of interest.

Therefore, if one selects a narrow portion of the pulse-height spectrum and performs an average over this portion in order to determine, say, the energy produced by some process of interest, then the above arguments imply that pile-up effects resulting from the primary pulse shaping will be quite different from those calculated from a simple average of  $f_1(t)$ . In fact practically all of  $f_1(t)$  for times larger than the time for the maximum will contribute negligibly to spectral distortions. The contribution of the early parts of  $f_1(t)$  depend strongly on the particular pulse shape and on the method of data analysis. Clearly the probability of finding just the correct portion of  $f_1(t)$  to shift the maximum significantly without shifting it completely out of the range of interest will be small, unless the average spacing between pulses approaches the width of  $f_1(t)$ . Therefore, in the following analysis of peak shifts only the pile-up of the tails will be considered.

---

(2) Fairstein and Hahn, Loc. Cit.

The procedure for calculating the tail pile-up is as follows. Define  $t = 0$  as the time of arrival of a pulse analyzed by the system. The gate then closes from  $t = 0$  to  $t = T$ , where  $T$  is the analyzer dead time. (The time from the pulse arrival to the closing of the gate has been assumed small compared to the dead time, and these small differences have been neglected.) The effect of tail pile up at a time  $t$ , where  $t > T$ , will be found by averaging over all possible cases. Notice that the fact that a pulse was analyzed at  $t = 0$  implies that no pulses occurred in the interval  $(0, -T)$ , unless the analyzer was busy during this interval. The probability that the gate was closed during  $(0, -T)$  will be neglected in this analysis. This approximation is valid if the average time between gate closures is small compared to the gate width. For rapidly decaying pulses this approximation becomes even more valid because of the decay of effects during  $(0, -T)$  in the interval  $(0, T)$ . For the purpose of simplicity, an average over pulse amplitude and dead time is implied so that all pulses can be considered to have the same amplitude and dead time.

Consider Figure 2.2.2-1, which illustrates the effect of  $n + 1$  pulses in the interval  $(0, T)$  and  $m$  pulses in the interval  $(-T, -\infty)$  on the base line at  $t$ , where  $t > T$ . If a pulse were to arrive at time  $t$ , then the baseline shift at this time would be

$$f_{nm}(t; t_1 \dots t_n, s_1 \dots s_m) = \sum_{i=0}^n f(t-t_i) + \sum_{j=1}^m f(t+s_j) \quad (2.2.2-5)$$

where

$$s \equiv -t$$

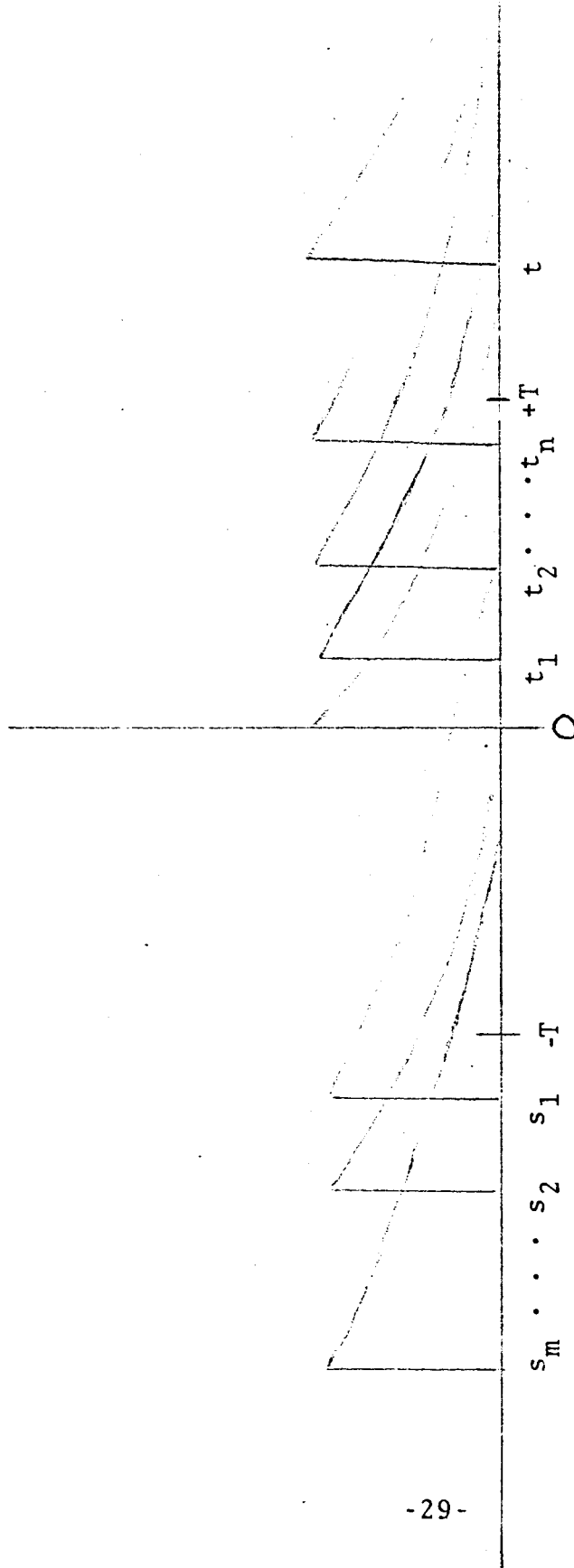


Figure 2.2.2-1  
Typical Sequence of Pulses

We then average over all times of occurrence of the next analyzed pulse to obtain

$$\bar{f}_{nm}(t_1 \dots t_n, s_1 \dots s_m) = \int_T^\infty P(t-t_n) f_{nm}(t) dt \quad (2.2.2-6)$$

where  $P(t-t_n) dt$  = probability that the next pulse occurs at  $t$  within  $dt$  when the last pulse occurred at  $t_n$ .

If we also average over the  $t_i$  and the  $s_j$ ,

$$\bar{f}_{nm} = \int_T^\infty \int_0^T \int_{t_1}^T \dots \int_{t_{n-1}}^T \int_T^\infty \int_T^{s_m} \dots \int_T^{s_2} \left[ \sum_{i=0}^n f(t-t_i) + \sum_{j=1}^m f(t+s_j) \right]$$

$$\times \prod_{i=1}^n P(t_i - t_{i-1}) \prod_{j=1}^m P(s_j - s_{j-1}) P(t - t_n)$$

$$\times ds_1 \dots ds_m dt_n \dots dt_1 dt \quad (2.2.2-7)$$

where  $t_0 = 0$

$$s_0 = T$$

16/



From equation 2.1-17 for the Poisson distribution and from the fact that no pulses occur in the interval  $(0, -T)$ , then

$$P(t_i - t_{i-1}) = R \exp -R(t_i - t_{i-1}) \quad (2.2.2-8)$$

$$P(s_j - s_{j-1}) = R \exp -R(s_j - s_{j-1})$$

where

$R$  = the average rate of pulses.

The above product of probabilities then reduces to

$$R^{n+m+1} \exp -R(t + s_m - T) \quad (2.2.2-9)$$

so that  $\bar{f}_{nm}$  becomes

$$\bar{f}_{nm} = R^{n+m+1} \int_T^\infty \int_0^T \int_{t_1}^T \cdots \int_{t_{n-1}}^T \int_T^\infty \int_T^{s_m} \cdots \int_T^{s_2} \left[ \sum_{i=0}^n f(t-t_i) + \sum_{j=1}^m f(t+s_j) \right]$$

$$\times \exp -R(t+s_m-T) ds_1 \cdots ds_m dt_n \cdots dt_1 dt \quad (2.2.2-10)$$

In order to average over all values of  $n$  and  $m$ , we must allow  $s_m$  to extend into the infinite past and also sum over all possible numbers of pulses in the interval  $(0, T)$ . Thus,

$$\bar{F} = \lim_{m \rightarrow \infty} \sum_{n=0}^{\infty} \bar{F}_{nm} \quad (2.2.2-11)$$

For the integration and summation over  $i$ , the only dependence on the  $s_j$  is through the exponential term, which becomes

$$\begin{aligned} & R^m \int_T^{\infty} \int_T^{s_m} \dots \int_T^{s_2} \exp -R (s_m - T) ds_1 \dots ds_m \\ &= \int_T^{\infty} R^{-1} \frac{[R(s_m - T)]^{m-1}}{(m-1)!} \exp -R(s_m - T) ds_m \\ &= 1 \end{aligned} \quad (2.2.2-11)$$

Similarly the summation and integration over the  $j$  terms can be simplified by factoring out the integral over  $t_i$ , which becomes

$$\int_0^T \int_{t_1}^T \dots \int_{t_{n-1}}^T dt_n \dots dt_1 = \frac{T^n}{n!} \quad (2.2.2-12)$$

The integral then is given by

$$\begin{aligned}
 \bar{f}_{nm} = & R^{n+1} \int_T^\infty \int_0^T \int_{t_1}^T \cdots \int_{t_{n-1}}^T \left[ \sum_{i=0}^n f(t-t_i) \right] \\
 & \times \exp -Rt \, dt_n \cdots dt_1 \, dt \\
 & + \frac{R^{n+m+1} T^n \exp Rt}{n!} \int_T^\infty \int_T^\infty \int_T^{s_m} \cdots \int_T^{s_2} \left[ \sum_{j=1}^m f(t-s_j) \right] \\
 & \times \exp -R(t+s_m) \, ds_1 \cdots ds_m \, dt \quad (2.2.2-13)
 \end{aligned}$$

If one replaces  $f(t)$  by its Fourier integral transform, given in equation 2.2.1-11b, then

$$f(t-t_i) = \frac{1}{2\pi} \int_{-\infty}^{\infty} F(j\omega) \exp [j\omega(t-t_i)] \, d\omega \quad (2.2.2-14)$$

and the sum over  $i$  can be written

$$\begin{aligned}
 & \frac{R^{n+1}}{2\pi} \int_{-\infty}^{\infty} F(j\omega) \int_T^{\infty} \exp[-t(R-j\omega)] dt \\
 & \times \int_0^T \int_{t_1}^T \cdots \int_{t_{n-1}}^T \left[ 1 + \sum_{i=1}^n \exp(-j\omega t_i) \right] dt_n \cdots dt_1 d\omega \\
 & = \frac{R^{n+1} \exp -RT}{2\pi} \int_{-\infty}^{\infty} \frac{F(j\omega) \exp j\omega T}{R - j\omega} \int_0^T \int_{t_1}^T \cdots \int_{t_{n-1}}^T \left[ 1 + \sum_{i=1}^{n+1} \exp(-j\omega t_i) \right] dt_n \cdots dt_1 d\omega \\
 & = \frac{T^n R^{n+1} \exp -RT}{2\pi n!} \int_{-\infty}^{\infty} \frac{F(j\omega) \exp j\omega T d\omega}{R - j\omega} \\
 & + \frac{R^n \exp -RT}{2\pi (-j\omega)^n} \int_{-\infty}^{\infty} \frac{RF(j\omega)}{R - j\omega} \int_0^{-j\omega T} \int_0^{t_1'} \cdots \int_0^{t_{n-1}'} \sum_{i=1}^{n+1} \exp(-t_i') dt_n' \cdots dt_1' d\omega
 \end{aligned}$$

(2.2.2-15)

where the  $t_i$  variables were changed to  $t'_i$  given by

$$t'_i = j\omega (T - t_i)$$

It can be shown that

$$\int_0^y \int_0^{x_n} \dots \int_0^{x_2} \sum_{i=1}^{n \geq 1} \exp \alpha X_i dX_1 \dots dX_n = \frac{y^{n-1}}{\alpha(n-1)!} (e^{\alpha y} - 1)$$

(2.2.2-16)

(This relation can be proved by mathematical induction as follows:

Assume that

$$\int_0^{x_n} \dots \int_0^{x_2} \sum_{i=1}^{n-1} \exp \alpha X_i dX_1 \dots dX_{n-1} = \frac{x_n^{n-2} [\exp (\alpha x_n) - 1]}{\alpha(n-2)!}$$

(2.2.2-17)

Then one needs to prove that the above also holds for the addition of one more variable so that the integration is also carried out over  $X_n$ , that is

$$\begin{aligned}
 & \int_0^{X_{n+1}} \int_0^{X_n} \cdots \int_0^{X_2} \left[ \exp \alpha X_n + \sum_{i=1}^{n-1} \exp \alpha X_i \right] dX_1 \dots dX_{n-1} dX_n \\
 &= \int_0^{X_{n+1}} \frac{X_n^{n-1} \exp (\alpha X_n) dX_n}{(n-1)!} + \int_0^{X_{n+1}} \frac{X_n^{n-2} (e^{\alpha X_n} - 1)}{\alpha (n-2)!} dX_n \\
 &= \frac{X_{n+1}^{n-1} \exp \alpha X_{n+1}}{\alpha (n-1)!} - \frac{1}{\alpha (n-2)!} \int_0^{X_{n+1}} X_n^{n-2} \exp (\alpha X_n) dX_n \\
 &\quad + \int_0^{X_{n+1}} \frac{X_n^{n-2} \exp \alpha X_n}{\alpha (n-2)!} dX_n - \frac{X_{n+1}^{n-1}}{\alpha (n-1)!} \\
 &= \frac{X_{n+1}^{n-1}}{\alpha (n-1)!} (\exp \alpha X_{n+1} - 1) \qquad (2.2.2-17)
 \end{aligned}$$

The relation is trivially proved for  $n = 1$ , which completes the induction.)

Substituting equation 2.2.2-16 into equation 2.2.2-15 and realizing that the proof of 2.2.2-15 does not depend on the order of integration, then the sum over  $i$  becomes

$$\begin{aligned} & \frac{(RT)^n \exp -RT}{2\pi n!} \int_{-\infty}^{\infty} \frac{RF(j\omega) \exp j\omega T}{R-j\omega} d\omega \\ & + \frac{(RT)^{n-1} \exp -RT}{2\pi (n-1)!} \int_{-\infty}^{\infty} \frac{R^2 F(j\omega) [\exp j\omega T - 1]}{j\omega (R-j\omega)} d\omega \\ & n \geq 1 \end{aligned} \quad (2.2.2-18)$$

If the sum over  $n$  shown in equation 2.2.2-11 is also performed and recognizing that

$$\exp RT = \sum_{i=0}^{\infty} \frac{(RT)^n}{n!} \quad (2.2.2-19)$$

Then the sum over  $i$  becomes

$$\frac{R}{2\pi} \int_{-\infty}^{\infty} \frac{F(j\omega)}{R-j\omega} \left[ \left( 1 + \frac{R}{j\omega} \right) \exp j\omega T - \frac{R}{j\omega} \right] d\omega \quad (2.2.2-20)$$

This integral is most easily performed as a contour integral given by

$$\frac{R}{2\pi j} \oint_C \frac{F(Z)}{R-Z} \left[ \left( 1 + \frac{R}{Z} \right) \exp^{ZT} - \frac{R}{Z} \right] dZ \quad (2.2.2-21)$$

where the closed contour C includes the imaginary axis  $(-j\infty, j\infty)$  and an infinite semi-circle surrounding the negative half-plane. Notice that the integral vanishes on the semi-circle so that the value of the integral along the imaginary axis (eq. 2.2.2-20) just equals  $2\pi j$  times the sum of the residues at poles in the negative half-plane. (This contour excludes the pole at  $Z = R$  and, unless  $F(Z)$  has a pole at the origin, the limit as  $Z \rightarrow 0$  shows that the remainder of the expression is finite there. Thus, the only relevant poles are those of  $F(Z)$ .)

The sum over  $j$  can be written as

$$\frac{(RT)^n \exp^{-RT}}{2\pi n!} \int_0^\infty \int_0^\infty \int_0^{s'_m} \dots \int_0^{s'_2} \left[ \sum_{j=1}^m f\left(\frac{t'+s'_j}{R} + 2T\right) \right]$$

$$\times \exp^{-(t'+s'_m)} ds'_1 \dots ds'_m dt' \quad (2.2.2-22)$$

where

$$t' = R(t-T)$$

$$s'_j = R(s_j - T)$$



Performing the sum over  $n$  and substituting the Fourier transform for  $f(t)$ , one obtains

$$\begin{aligned} & \frac{1}{2\pi} \int_{-\infty}^{\infty} F(j\omega) \exp j\omega 2T \left[ \int_0^{\infty} \exp -t' \left( 1 - \frac{j\omega}{R} \right) dt' \right] \\ & \times \int_0^{\infty} \int_0^{s'_m} \cdots \int_0^{s'_2} \left[ \sum_{j=1}^m \exp \frac{j\omega s'_j}{R} \right] \exp -s'_m ds'_1 \cdots ds'_m d\omega \end{aligned} \quad (2.2.2-23)$$

Applying the relation given in equation 2.2.2-16, then the above term becomes

$$\frac{R}{2\pi} \int_{-\infty}^{\infty} \frac{F(j\omega) \exp j\omega 2T}{j\omega (1 - j\frac{\omega}{R})} \left[ \frac{1}{(1 - \frac{j\omega}{R})^m} - 1 \right] d\omega \quad (2.2.2-24)$$

Taking the limit of infinite  $m$  and using a contour integral with the same contour as in equation 2.2.2-21, one obtains

$$\frac{R}{2\pi j} \oint_C \frac{F(Z) \exp 2TZ}{(R-Z)(Z-\epsilon)} dz \quad (2.2.2-25)$$

where the  $Z - \epsilon$  term implies that the pole at the origin should not be included in the sum of the residues, because the limit of the term in brackets of equation 2.2.2-24 as  $\omega \rightarrow 0$  is finite. (The quantity  $\epsilon$  is an infinitesimal real-number which formally prevents the denominator of the integrand from vanishing at the origin but negligibly influences the residues at other poles.)

Combining equations 2.2.2-21 and 2.2.2-25, the total baseline shift becomes

$$\bar{f} = \frac{R}{2\pi j} \oint_C \frac{F(Z)}{R-Z} \left\{ \exp ZT - \frac{R}{Z-\epsilon} \left[ \exp 2ZT - \exp ZT + 1 \right] \right\} dZ \quad (2.2.2-26)$$

where  $C$  surrounds the negative half-plane, including the imaginary axis, and  $Z-\epsilon$  implies that a pole exists at the origin only if  $F(Z)$  has a pole there.

According to a fundamental theorem of complex variable theory, the integral of a function satisfying certain general requirements around a closed contour is related to the "residues" at the  $m$  poles contained within the contour by

$$\oint_C G(Z) dZ = 2\pi j \sum_{k=1}^m a_k \quad (2.2.2-27)$$

where  $a_k$  is the residue at the  $k^{\text{th}}$  pole at  $Z = Z_k$  and, for a pole of order  $n$ , is given by

$$a_k = \frac{1}{(n-1)!} \frac{d^{n-1}}{dZ^{n-1}} \left[ G(Z) (Z-Z_k)^n \right]_{Z=Z_k} \quad (2.2.2-28)$$

This theorem can be used to evaluate simply the integral of equation 2.2.2-26 to obtain

$$\bar{F} = R \sum_{k=1}^m a_k \quad (2.2.2-29)$$

where the  $a_k$  are given by

$$a_k = \frac{1}{(n-1)!} \frac{d^{n-1}}{dZ^{n-1}} \left[ (Z-Z_k)^n \left\{ \frac{F(Z)}{R-Z} \left[ \exp ZT - \frac{R}{Z} (\exp 2ZT - \exp ZT + 1) \right] \right\} \right]_{Z=Z_k} \quad (2.2.2-30)$$

and where  $Z_k$  is a value of  $Z$  producing a pole of order  $n$  in  $F(Z)$  and lying in the left half-plane. The summation in equation 2.2.2-29 is carried out over all  $m$  poles of  $F(Z)$  lying in the left half-plane. ( $F(Z)$  has a pole of order  $n$  at  $Z_k$  if and only if  $\lim_{Z \rightarrow Z_k} (Z-Z_k)^{n-1} F(Z)$  is infinite, but  $\lim_{Z \rightarrow Z_k} (Z-Z_k)^n F(Z)$  is finite.)

In order to illustrate the implication of the above results, consider the case where one secondary time constant ( $\tau_s$ ) is used in a system with equal primary integrating and differentiating time constants ( $\tau_p$ ). The Laplace transform, normalized to unit peak amplitude, is

$$F(p) = \frac{A_1 p \tau_s \tau_p}{(1+p\tau_p)^2(1+p\tau_s)} \quad (2.2.2-31)$$

where for  $\tau_s \gg \tau_p$

$$A_1 \approx 2.73 \quad (2.2.2-32)$$

This transform contains a double pole at  $Z = -1/\tau_p$ , leading to  $f_1(t)$ , and a single pole at  $Z = -1/\tau_s$ , leading to  $f_2(t)$ . The total baseline shift can be written as

$$\bar{f} = Ra_1 + Ra_2 \quad (2.2.2-33)$$

where  $a_1 = \text{residue at } Z = -1/\tau_p$

$a_2 = \text{residue at } Z = -1/\tau_s$

For the case where the dead time ( $T$ ) is long compared to  $\tau_p$  so that

$$\frac{T}{\tau_p} \exp(-T/\tau_p) \ll 1 \quad (2.2.2-34)$$

$$\exp(-T/\tau_p) \ll 1$$

and for  $\tau_p \ll \tau_s$ , then

$$Ra_1 \approx 2A_1 (R\tau_p)^2 \left[ \frac{1 + 1/2 R\tau_p}{(1 + R\tau_p)^2} \right] \quad (2.2.2-35)$$

An exact evaluation of the residue at  $Z = -1/\tau_s$  gives

$$Ra_2 = \frac{-A_1 R \tau_p}{\left(1 - \frac{\tau_p}{\tau_s}\right)} \left[ \frac{R \tau_s}{1 + R \tau_s} \right] \left[ 1 + \exp \frac{-2T}{\tau_s} - \exp \frac{-T}{\tau_s} + \frac{1}{R \tau_s} \exp \frac{-T}{\tau_s} \right] \quad (2.2.2-36)$$

which reduces to

$$Ra_2 \approx \frac{-A_1 \tau_s}{\tau_p} \left[ \frac{(R \tau_p)^2}{1 + R \tau_s} \right] \left[ 1 + \exp \frac{-2T}{\tau_s} - \exp \frac{-T}{\tau_s} + \frac{1}{R \tau_s} \exp \frac{-T}{\tau_s} \right] \quad (2.2.2-37)$$

when  $\tau_p \ll \tau_s$ .

If  $T$  is sufficiently small compared to  $\tau_s$  to justify a first order expansion for the exponentials, then

$$Ra_2 \approx -A_1 R \tau_p \left( 1 - \frac{T}{\tau_s} \right) \quad (2.2.2-38)$$

For the case where

$$\begin{aligned} \tau_p &= 1 \text{ } \mu\text{s} \\ \tau_s &= 25 \text{ } \mu\text{s} \\ R &= 10,000 \text{ counts/second} \end{aligned} \quad (2.2.2-39)$$

then

$$\begin{aligned} Ra_1 &= 0.055\% \\ Ra_2 &= 0.767\% \end{aligned} \quad (2.2.2-40)$$

The large contribution to the peak shift resulting from the secondary differentiating network has long been recognized<sup>(2)</sup>. For this reason, double differentiation is often used for the primary pulse shaping. If double integration is also used, and if a single secondary differentiation is present, then the Laplace transform becomes

$$F(p) = \frac{A_3 p^2 \tau_s \tau_p^2}{(1 + p \tau_p)^4 (1 + p \tau_s)} \quad (2.2.2-41)$$

A fourth order pole at  $-1/\tau_p$  and a first order pole at  $-1/\tau_s$  are present in  $F(Z)$ . The residue at  $-1/\tau_p$  under the approximations given in equation 2.2.2-34 becomes

$$R_1 a_1 \approx \frac{A_3 (R\tau_p)^2}{(1+R\tau_p)^4} \quad (2.2.2-42)$$

where

$$A_3 \approx 7.64$$

and an exact evaluation of the residue at  $-1/\tau_s$  gives

$$Ra_2 = \frac{A_3 (R\tau_p)^2}{\left(1 - \frac{p}{\tau_s}\right)^4 (1+R\tau_s)} \left[ 1 + \exp \frac{-2T}{\tau_s} - \exp \frac{-T}{\tau_s} + \frac{1}{R\tau_s} \exp \frac{-T}{\tau_s} \right] \quad (2.2.2-43)$$

When  $\tau_p$  is small compared to  $\tau_s$ , this residue reduces to

$$Ra_2 \approx \frac{A_3 (R\tau_p)^2}{(1+R\tau_s)} \left[ 1 + \exp \frac{-2T}{\tau_s} - \exp \frac{-T}{\tau_s} + \frac{1}{R\tau_s} \exp \frac{-T}{\tau_s} \right] \quad (2.2.2-44)$$

and for  $T$  sufficiently small compared to  $\tau_s$  to permit a first order expansion of the exponentials,

$$Ra_2 \approx A_3 \left( \frac{\tau_p}{\tau_s} \right) R\tau_p \left( 1 - \frac{T}{\tau_s} \right) \quad (2.2.2-45)$$

For the case given in equation 2.2.2-39, then

$$Ra_1 = 0.0764\%$$

(2.2.2-46)

$$Ra_2 = 0.0858\%$$

The reduction by nearly an order of magnitude in  $Ra_2$  indicates the advantage of the double-differentiated primary waveform.

Examination of equations 2.2.2-42 and 2.2.2-45 shows that a large value of  $\tau_s$  is required to minimize tail pile-up. Even when the ratio of  $\tau_s$  to  $\tau_p$  is 25:1, the pile-up from  $f_2(t)$  is greater than that from  $f_1(t)$  at rates of  $10^4$  counts/ second. At lower rates the relative effect of  $\tau_s$  becomes even more severe. Thus, values of  $\tau_s$  in the range of 100 times  $\tau_p$  appear required for optimal operation of a high-rate system.

However, such large values of  $\tau_s$  can produce other adverse effects. For example, peak shifts can occur if the counting rate changes appreciably during times for which  $f_2(t)$  is not negligibly small.<sup>(4)</sup> If  $\tau_s$  were made 250  $\mu s$ , then a time of nearly 1 ms would be required for the transients caused by an abrupt rate change to decay. Thus, an analyzer used with a pulsed particle source, for example, should not

---

(4) Rice, Loc. Cit.

possess secondary time constants comparable to the period of the particle burst.

Furthermore, Fairstein<sup>(2)</sup> has shown that, if an amplifier is overloaded, dead times and periods of non-linear or inaccurate operation occur for times of the order of the secondary time constant. Thus, an analyzer system operating with large numbers of overload-producing input signals should not possess secondary differentiating time constants larger than typical analyzer dead times.

Usually a compromise between tail pile-up and rate shift or overload dependent effects is made by choosing secondary time constants in the 25 to 100  $\mu$ s time range. This choice often is not particularly satisfactory if a truly optimum, general purpose system is desired. A more effective approach appears to be to direct couple the amplifier-analyzer system so that the only differentiating time constants are those involved in the primary pulse shaping networks. In this way all pile-up from secondary coupling networks is eliminated, and recovery from overload or rate changes is determined by the fast primary networks.



### 3.0 NOISE

Because noise is generated by random fluctuations of the energy in various noise producing systems, the same basic statistical analysis applied in Section 2 can be used to calculate the effect of pulse shaping on amplifier or detector noise sources. The central limit theorem, discussed in Section 2.1, implies that the distribution in amplifier output voltage (or current) caused by noise will be approximately Gaussian. This result follows from the fact that the output noise signal at any given time is the composite of the amplifier response to input noise impulses during a large number of previous intervals. Because the number of noise impulses during one interval is not determined by the number during any other interval, the result for each interval can be considered an independent random variable. The central limit theorem says that the distribution of the sum of many random variables approaches the normal distribution, with a mean ( $m$ ) and standard deviation ( $\sigma$ ) given by

$$m = \sum_{i=1}^n m_i \quad (3.0-1)$$

$$\sigma^2 = \sum_{i=1}^n \sigma_i^2 + \sum_{\substack{i,j=1 \\ i \neq j}}^n \gamma_{ij} \sigma_i \sigma_j \quad (3.0-2)$$

where

$m, \sigma$ , = parameters of the distribution of the sum of  $n$  variables, each with mean  $m_i$  and standard deviation  $\sigma_i$

$\gamma_{ij}$  = correlation coefficient between variables  $i$  and  $j$ .

Except for dc systems, the mean value is of no consequence, since it will be eliminated by any ac couplings. If the mean exists, it will represent an offset in the system.

The fluctuations in the output signals, related to the rms values, are usually defined as the noise signal. The rms noise voltage (or equivalent input signal) is sometimes specified directly. More commonly in pulse-height analyzer systems, the full-width-at-half-maximum of the pulse-height distribution produced by a noiseless input signal is specified because of its ease of measurement. The differential pulse-height spectrum for Gaussian noise is given by

$$P(V_o) = \frac{1}{\sqrt{2\pi} \sigma} \exp - \frac{V_o^2}{2\sigma^2} \quad (3.0-3)$$

where  $P(V_o)dV$  represents the probability that  $V$  lies within  $dV$  of  $V_o$ , and the mean value has been assumed to be zero. From 3.0-3, the full-width-at-half-maximum (FWHM) is related to the rms value by

$$\text{FWHM} = (2\sqrt{2\ln 2}) \sigma = 2.35 \sigma \quad (3.0-4)$$

The remaining problem is the calculation of  $\sigma$ . From the rule for adding variances given by equation 3.0-2, and from the fact that different frequencies can be treated as independent variables, which follows from the orthogonality of the Fourier transform, the average square of the output noise voltage becomes

$$\overline{V_1^2} = \frac{1}{2\pi} \int_0^\infty |F(j\omega)|^2 \left[ \sum_{i=1}^n \overline{e_i^2} + \sum_{\substack{i,j=1 \\ i \neq j}}^n \gamma_{ij} \sqrt{\overline{e_i^2}} \sqrt{\overline{e_j^2}} \right] d\omega \quad (3.0-5)$$

where  $F(j\omega)$  = Fourier transform of the amplifier  
current impulse response

$\overline{e_i^2}$  = square average of the equivalent current  
input noise per unit bandwidth (in Hertz)  
for noise from the  $i^{\text{th}}$  source

$\gamma_{ij}$  = correlation coefficient between the  $i^{\text{th}}$   
and  $j^{\text{th}}$  noise source

Notice that if two noise sources are totally uncorrelated,  
 $\gamma = 0$ , and they add as the sum of the squares. If they are  
completely correlated,  $\gamma = 1$ , and they add directly. An equa-  
tion similar to 3.0-5 can be written using the Fourier trans-  
form of the voltage impulse response and equivalent input  
voltage noise sources. The representation used in a given pro-  
blem becomes a matter of computational convenience.

### 3.1 Typical Noise Sources

The choice of an optimal pulse shape depends upon the nature of the noise voltages and currents mentioned in Section 3.0. Several of these sources will be discussed here.

#### 3.1.1 Resistor Noise

One of the most common sources of noise is thermal energy in a resistor. For an ideal resistor, this noise is independent of frequency or current flowing in the resistor and can be calculated from fundamental theorems involving the equal partition of energy.

Resistor noise may be expressed in either of two equivalent ways using either a noise current or a noise voltage generator. In both cases, the available noise power is constant as a function of frequency and resistance and is given by:

$$P_R = 4kT = \frac{\overline{e_n^2}}{R} = \overline{i_n^2} R \quad (3.1.1-1)$$

where  $P_R$  = noise power per unit bandwidth (in Hz)

$\overline{e_n^2}$  = mean-square noise voltage =  $4kTR$   
per unit bandwidth

$\overline{i_n^2}$  = mean-square noise current =  $\frac{4kT}{R}$   
per unit bandwidth

$k$  = Boltzman's constant

$T$  = absolute temperature

Some resistors may have noise levels considerably in excess of that calculated by equation 3.1.1-1, which represents a lower limit. High quality metal-film resistors generally deviate negligibly from the above calculated noise level.

### 3.1.2 Shot Noise

A common type of noise, present in most particle detectors and amplifier elements, is shot noise. For example, if a leakage current from such sources as photomultiplier dark current or solid-state detector leakage is present at the amplifier input, statistical variations of this current contribute to the system noise. This noise arises because current flow is really the motion of individual electrons. Thus, a current can be written as

$$i(T) = \sum_{i=1}^{N(T)} q \delta(t-t_i) \quad (3.1.2-1)$$

where  $q$  = electronic charge

$t_i$  = time of the  $i^{\text{th}}$  impulse

and on the average

$$\bar{I} = \frac{Nq}{T} \quad (3.1.2-2)$$

Applying the same techniques as in Section 2.2.1, the mean effect of  $i$  on the amplifier output becomes

$$\bar{V}_1 = \lim_{T \rightarrow \infty} \frac{1}{T} \int_0^T \sum_{i=1}^{N(T)} q \delta(t-t_i) f(t-t_i) dt \quad (3.1.2-3)$$

$$V_1 = \bar{I} F(0) \quad -51-$$

For the usual case where at least one ac coupling is present  $F(0) = 0$ , then  $\bar{V}_1$  vanishes. The variance then becomes

$$\overline{V_1^2} = \lim_{T \rightarrow \infty} \frac{q^2}{T} \int_0^T \sum_{i,j=1}^{N(T)} f(t-t_i) f(t-t_j) dt \quad (3.1.2-4)$$

which can be reduced to

$$\begin{aligned} \overline{V_1^2} = & \frac{\bar{i}q}{2\pi} \int_{-\infty}^{\infty} |F(j\omega)|^2 d\omega \\ & + \lim_{T \rightarrow \infty} \frac{1}{2\pi T} \sum_{\substack{i,j=1 \\ j>i}}^{N(T)} |F(j\omega)|^2 e^{-j\omega t_{ij}} d\omega \end{aligned} \quad (3.1.2-5)$$

Because  $t_{ij}$  is often small compared to the pulse width, the summation over  $j$  can be replaced by an integral. Thus, in the limit of infinite  $T$ , the second term of 3.1.2-5 becomes

$$\sum_{i=1}^{\infty} \int_0^{\infty} f(t) \int_0^{\infty} f(t') dt' dt \quad (3.1.2-6)$$

The integral over  $t'$  is just the mean of  $f(t)$ , which we have assumed to vanish. Therefore, the rms output noise voltage resulting from a current  $\bar{I}$  is

$$\sqrt{\overline{V_1^2}} = \sqrt{\int_0^\infty \frac{\bar{I}q}{\pi} |F(j\omega)|^2 d\omega} \quad (3.1.2-7)$$

resulting in the usual formula that the rms current noise per unit bandwidth (in hertz) is

$$\sqrt{\overline{i_N^2}} = \sqrt{2iq} \quad (3.1.2-8)$$

### 3.1.3 Junction-Transistor Noise

The noise sources involved in the typical junction transistor are basically extensions of the principles mentioned in the previous two sections. One exception to this rule is the  $1/f$  noise, which is poorly understood but probably results from surface leakage effects and from ohmic leakage across the collector-base junction<sup>(5)</sup>.

A mid-frequency noise model<sup>(6)</sup> of a bipolar transistor is given in Figure 3.1.3-1, which uses the grounded base configuration. The various noise sources given in this figure are:

$e_{Ne}$  = collector-current shot noise per unit bandwidth

$i_{Nb}$  = base-current shot noise per unit bandwidth

$i_{Nc}$  = collector leakage current shot noise per unit bandwidth

$e_{Nb}$  = base-spreading resistance noise per unit bandwidth

From Section 3.1.2, the shot-noise components per unit bandwidth are related to the relevant currents by

$$\overline{e_{Ne}^2} = 2qI_c r_e^2 \quad (3.1.3-1)$$

$$\overline{i_{Nb}^2} = 2qI_b \quad (3.1.3-2)$$

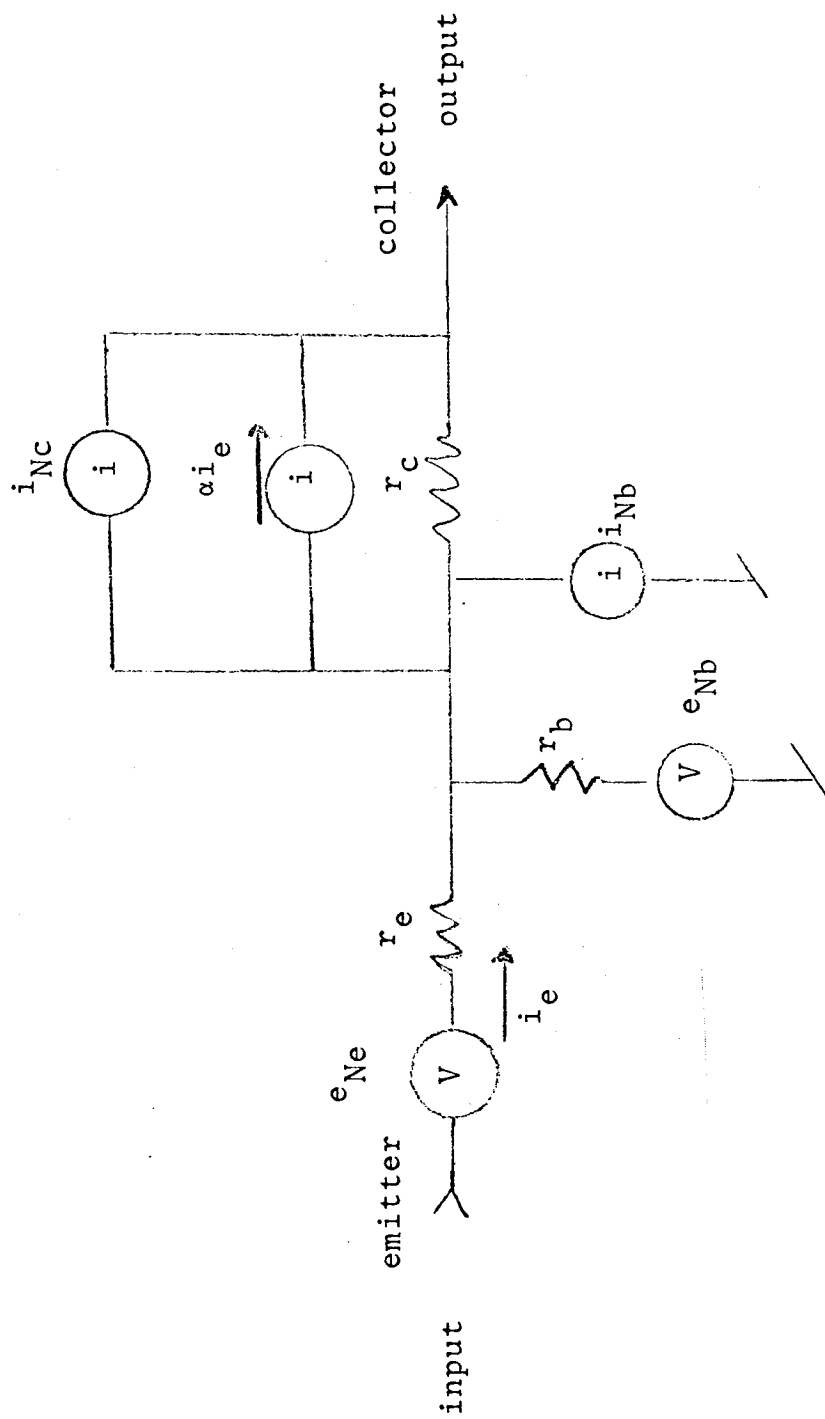
$$\overline{i_{Nc}^2} = 2qI_{co} \quad (3.1.3-3)$$

---

(5) W. H. Fonger, "A Determination of  $1/f$  Noise Sources in Semiconductor Diodes and Triodes," Transistors I, RCA Laboratories, Princeton, N.J., 1956.

(6) A. G. Di Loreto: Noise Optimization Techniques for Linear Transistor Amplifiers U.S. Naval Ordnance Test Station, China Lake, Calif., Oct. 1963 NAVWEPS Report 8381.





$r_e$  = grounded-base emitter input resistance

$r_b$  = base-spreading resistance

$\alpha$  = grounded-base current gain

$r_c$  = collector-base resistance

Figure 3.1.3-1: Transistor Noise Model

where:

$I_c$  = collector current

$I_b$  = base current

$I_{co}$  = collector leakage current

$q$  = charge on the electron

The transistor has the usual relations between the parameters of equations 3.1.3-1, -2, and -3; namely

$$I_b = \frac{I_c}{\beta} \quad (3.1.3-4)$$

$$r_e = \frac{kT}{qI_c} \quad (3.1.3-5)$$

where  $\beta$  = grounded-emitter current gain

$k$  = Boltzmann's constant

$T$  = absolute temperature

The noise sources can then be written

$$\overline{e_{Ne}^2} = 2kTr_e = \frac{2(kT)^2}{qI_c} \quad (3.1.3-6)$$

$$\overline{i_{Nb}^2} = \frac{2qI_c}{\beta} \quad (3.1.3-7)$$

$$\overline{i_{Nc}^2} = 2qI_{co} \quad (3.1.3-8)$$

$$\overline{e_{Nb}^2} = 4kTr_b \quad (3.1.3-9)$$

where the usual formula for resistive noise was used in equation 3.1.3-9.

In addition to the above relations, one must realize that base and collector shot noise may be highly correlated because they both result basically from the same current. Thus, the correlation factor  $\gamma$  between  $\overline{i_{Ne}^2} = \frac{e_{Ne}^2}{r_e^2}$  and  $\overline{i_{Nb}^2}$  is often taken to be unity. Moreover,  $1/f$  noise, which so far has been neglected, adds directly to  $e_{Ne}$ , so that a component in addition to pure shot noise exists for this generator.

#### 3.1.4 Field-Effect Transistor Noise

A noise equivalent circuit for a field-effect transistor is shown in Figure 3.1.4-1. For mid-band frequencies Van der Ziel<sup>(7,8)</sup> has shown that the noise sources are given approximately by

$$\overline{i_{Ng}^2} \approx 2qI_g + \frac{4kT}{g_m} \omega^2 C_{gs}^2 ab \quad (3.1.4-1)$$

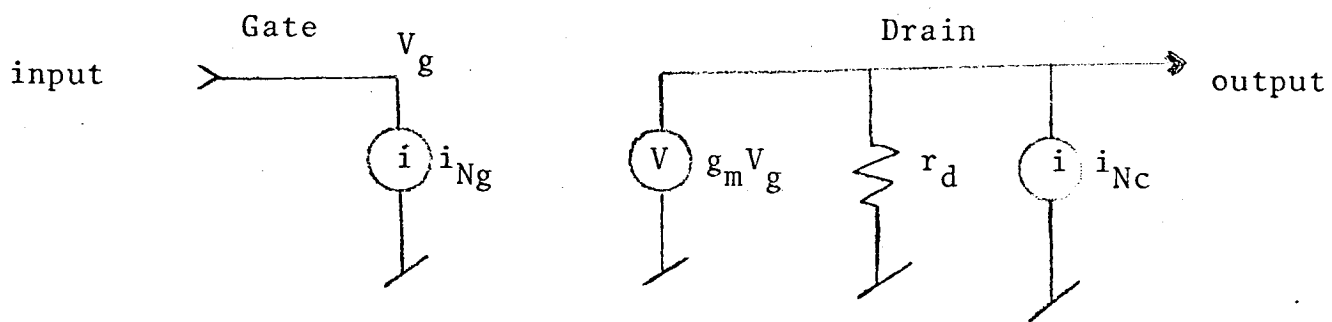
$$\overline{i_{Nc}^2} \approx 4kTg_m a \quad (3.1.4-2)$$

where  $\overline{i_{Ng}^2}$  = square average noise current per unit bandwidth resulting from gate leakage current ( $I_g$ ).

---

(7) A. Van der Ziel, "Thermal Noise in Field-Effect Transistors," Proc. IRE, 50, p 1808, August 1962.

(8) A. Van der Ziel, "Gate Noise in Field-Effect Transistors at Higher Frequencies," Proc. IRE, 51, p 461, March 1963.



$g_m$  = transconductance

$r_d$  = drain output resistance

Figure 3.1.4-1: Grounded-Source Equivalent Noise Circuit

$\overline{i_{Nc}^2}$  = square average noise current per unit bandwidth resulting from thermal channel noise.

$C_{gs}$  = gate-source capacity.

$\omega$  = angular frequency.

$I_g$  = gate leakage current.

$a$  = coefficient dependent on bias conditions and specific device. Theoretical optimum value<sup>(7)</sup> is of the order of 0.7.

$b$  = coefficient dependent on bias and specific device. Typically<sup>(8)</sup>  $b$  ranges between 0.35 and 0.40.

The result for the gate leakage current noise follows directly from the analysis of shot noise given in Section 3.1.2. The thermal channel noise results primarily from the fact that the channel is resistive. The dependence of the gate noise current on frequency arises from capacitive coupling to the channel thermal noise. This noise is correlated to the thermal noise source such that

$$\overline{i_{Ng}^* i_{Nc}} = ac\sqrt{b} 4 kT \omega C_{gs} \quad (3.1.4-3)$$

$c$  = complex correlation coefficient dependent on bias and specific device. Typically<sup>(8)</sup>  $c$  ranges between  $j 0.39$  and  $j 0.42$ .

The thermal channel noise source is sometimes represented by a noise voltage generator between the source and ground. In this representation, the equivalent noise voltage per unit

---

(7) Van der Ziel, Loc. Cit.

(8) Van der Ziel, Loc. Cit.

196

bandwidth becomes

$$e_{Nc}^2 = \frac{4kTb}{g_m} \quad (3.1.4-4)$$

The above model fails to be accurate for frequencies below 100 Hz where 1/f noise becomes important. In this region, the channel noise component rises with decreasing frequency.

### 3.2 The Charge-Sensitive Amplifier

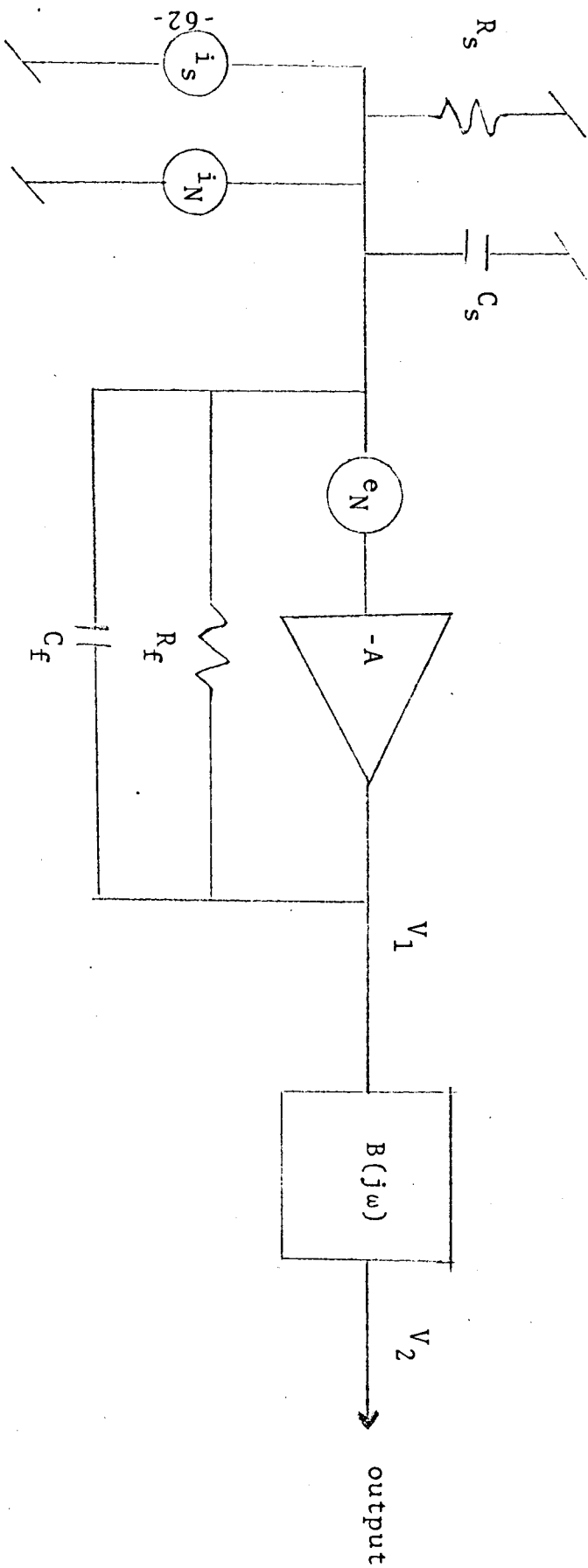
One of the severe noise problems in the design of nuclear pulse amplifiers arises when small signals from solid-state detectors or from photomultiplier tubes must be amplified. For reasons beyond the scope of this section, the charge-sensitive amplifier configuration shown in Figure 3.2-1 is generally employed. The calculation of the system noise for such a configuration forms a useful example of the general principles stated above.

The basic configuration consists of an operational amplifier, followed by additional pulse-shaping networks  $[B(j\omega)]$ . The noise sources at the input represent the total rms equivalent noise per unit bandwidth from both amplifier and external sources. In the following discussion the amplifier gain  $(-A)$  will be assumed infinitely large so that the transfer impedance is totally determined by the feedback and input networks  $(R_f, C_f, R_s, C_s)$ . Under this approximation the output noise voltage caused by input noise current  $(V_{2i})$  becomes:

$$V_{2i}^2 = \int_0^\infty \frac{|B(j\omega)|^2 \overline{i_N^2} R_f^2 d\omega}{2\pi (1 + \omega^2 R_f^2 C_f^2)} \quad (3.2-1)$$

The voltage component is given by

$$V_{2v}^2 = \int_0^\infty \frac{|B(j\omega)|^2 \overline{e_N^2} \left\{ 1 + \left[ \frac{(C_f + C_s) R_f R_s \omega}{R_f + R_s} \right]^2 \right\} \left[ \frac{R_s + R_f}{R_s} \right]^2 d\omega}{2\pi (1 + \omega^2 R_f^2 C_f^2)} \quad (3.2-2)$$



$i_s$  = signal current  
 $i_N$  = input noise current per unit bandwidth  
 $e_N$  = input noise voltage per unit bandwidth  
 $B(j\omega)$  = postamplifier shaping network =  $V_2/V_1$

Figure 3.2-1: Noise Equivalent Circuit



Under the usual approximation that

$$\left[ (C_f + C_s) \left( \frac{R_f R_s}{R_f + R_s} \right) \right]^2 \gg \left[ R_f C_f \right]^2 \quad (3.2-3)$$

equation 3.2-3 reduces to

$$V_{2v}^2 = \int_0^\infty \frac{|B(j\omega)|^2 \overline{e_N^2} R_f^2 (C_f + C_s)^2 \omega^2 d\omega}{2\pi (1 + \omega^2 R_f^2 C_f^2)} \quad (3.2-4)$$

Similarly, if a correlation  $\gamma$  exists between  $e_N$  and  $i_N$ , this component of output noise becomes

$$V_{2c}^2 = \int_0^\infty \frac{|B(j\omega)|^2 \gamma \sqrt{\overline{e_N^2} \overline{i_N^2}} \left\{ \frac{(R_s + R_f) R_f}{R_s} \right\} \left\{ \sqrt{1 + \frac{[(C_f + C_s) R_f R_s \omega]^2}{R_f + R_s}} \right\} d\omega}{2\pi (1 + \omega^2 R_f^2 C_f^2)} \quad (3.2-5)$$

Under the approximation given in equation 3.2-3, then

$$V_{2c}^2 \cong \int_0^\infty \frac{|B(j\omega)|^2 \gamma \sqrt{\overline{e_N^2} \overline{i_N^2}} R_f^2 (C_f + C_s) \omega d\omega}{2\pi (1 + \omega^2 R_f^2 C_f^2)} \quad (3.2-6)$$

If the noise sources  $e_N$  and  $i_N$  are approximately independent of frequency, the total output noise becomes

$$V_{2N}^2 = \frac{\tau_1^2}{2\pi C_f^2} \left\{ \overline{i_N^2} \int_0^\infty \frac{|B(j\omega)|^2 d\omega}{(1+\omega^2\tau_1^2)} + \gamma \sqrt{\overline{e_N^2} \overline{i_N^2}} (C_f + C_s) \int_0^\infty \frac{|B(j\omega)|^2 \omega d\omega}{(1+\omega^2\tau_1^2)} + \overline{e_N^2} (C_f + C_s)^2 \int_0^\infty \frac{|B(j\omega)|^2 \omega^2 d\omega}{(1+\omega^2\tau_1^2)} \right\} \quad (3.2-7)$$

where

$$\tau_1 \equiv R_f C_f$$

Suppose that the pulse shaping networks are restricted to simple RC or LR circuits so that  $B(j\omega)$  becomes the product of terms of the form  $\frac{1}{1+j\omega\tau}$  and  $\frac{j\omega\tau}{1+j\omega\tau}$ . Then, we can write

$$B(j\omega) = \prod_{i=2}^m \frac{j\omega\tau_i}{1+j\omega\tau_i} \prod_{i=m+1}^{m+n} \frac{1}{1+j\omega\tau_i} \quad (3.2-8)$$

where there are  $m-1$  differentiating networks in  $B(j\omega)$  and  $n$  integrating networks, and  $\tau_i = \tau_1$  is reserved for the

preamplifier. The total system current impulse response then becomes

$$F(j\omega) = \frac{1}{j\omega C_f} \prod_{i=1}^m \frac{j\omega\tau_i}{1+j\omega\tau_i} \prod_{i=m+1}^n \frac{1}{1+j\omega\tau_i} \quad (3.2-9)$$

The pulse shape corresponding to this frequency response can be obtained from the following contour integral

$$f(t) = \frac{Q}{2\pi C_f} \left[ \prod_{i=1}^m \tau_i \right] \oint_C \frac{p^{m-1} e^{pt} dp}{\prod_{i=1}^{n+m} (1+p\tau_i)} \quad (3.2-10)$$

where the contour surrounds the negative half plane. The above expression is based on the assumption that the detector produces a charge  $Q$  during a time short compared to the  $\tau_i$ , so that

$$i_s \cong Q \delta(t) \quad (3.2-11)$$

In order to compare various amplifier configurations, the output noise voltage (eq. 3.2-7) is divided by the peak of the impulse response (eq. 3.2-10) to obtain an equivalent input noise energy. The square of the equivalent input noise energy then becomes

$$\begin{aligned} \overline{E_N^2} = & \frac{1}{2\pi Q^2 g_M^2(\tau_1, \tau_2, \dots, \tau_{n+m})} \left\{ \overline{i_N^2} \int_0^\infty \frac{\omega^{2m-2} d\omega}{\prod_{i=1}^{n+m} (1+\omega^2\tau_i^2)} \right. \\ & + \gamma \overline{e_N^2} \overline{i_N^2} (C_f + C_s) \int_0^\infty \frac{\omega^{2m-1} d\omega}{\prod_{i=1}^{n+m} (1+\omega^2\tau_i^2)} \\ & \left. + \overline{e_N^2} (C_f + C_s)^2 \int_0^\infty \frac{\omega^{2m} d\omega}{\prod_{i=1}^{n+m} (1+\omega^2\tau_i^2)} \right\} \quad (3.2-12) \end{aligned}$$

502

where  $Q$  is the energy-to-charge conversion factor of the detector and where  $g_M$  is the maximum value of  $g(t; \tau_1, \tau_2, \dots, \tau_{n+m})$ . The function of  $g(t)$  is given by

$$g(t) = \frac{1}{2\pi j} \oint_C \frac{p^{m-1} e^{pt} dp}{\prod_{i=1}^{n+m} (1+p\tau_i)} \quad (3.2-13)$$

If the noise currents and voltages ( $\overline{e_N^2}$ ,  $\overline{i_N^2}$ ) do not depend on the shaping time constants ( $\tau_i$ ), the equivalent input noise energy is a completely symmetric function in the  $\tau_i$ . Therefore, the minimum value of  $\overline{E_N^2}$  will occur when all the  $\tau_i$  are equal. The remainder of the analysis will be restricted to calculating the noise for this optimal case. (The use of the preamplifier feedback network as one of the primary pulse-shaping time constants gives less than optimal noise performance because of the noise produced by  $R_f$ . However, this increase is often negligibly small, so that the problems at high rates caused by larger secondary differentiators can be avoided by using  $R_f C_f$  as one of the primary pulse shaping networks. Where low noise is the prime consideration,  $R_f$  is often made as large as possible.)

For the case where all  $\tau_i$  are equal, then

$$g(t) = \frac{1}{2\pi j} \oint_C \frac{p^{m-1} e^{pt} dp}{(1+p\tau)^{n+m}} \quad (3.2-14)$$

Changing variables to

$$Z = p\tau \quad (3.2-15)$$

$$t' = t/\tau$$

then one obtains

$$g(t') = g(t/\tau) = \frac{\tau^m}{2\pi j} \oint_C \frac{z^{m-1} e^{zt'} dz}{(1+z)^{n+m}} \quad (3.2-16)$$

A similar variable change in the integrals of equation 3.2-12 results in

$$\begin{aligned} \overline{E_N^2} = & \frac{1}{2\pi Q^2 h_M^2} \left\{ \overline{i_N^2} \tau \int_0^\infty \frac{x^{2m-2} dx}{(1+x^2)^{n+m}} \right. \\ & + \gamma \sqrt{\overline{e_N^2} \overline{i_N^2}} (C_f + C_s) \int_0^\infty \frac{x^{2m-1} dx}{(1+x^2)^{n+m}} \\ & \left. + \frac{\overline{e_N^2} (C_f + C_s)^2}{\tau} \int_0^\infty \frac{x^{2m} dx}{(1+x^2)^{n+m}} \right\} \quad (3.2-17) \end{aligned}$$

where  $h_M$  is the maximum value of

$$h(t') = h(t/\tau) = \frac{1}{2\pi j} \oint_C \frac{z^{m-1} e^{zt'} dz}{(1+z)^{n+m}} \quad (3.2-18)$$

Notice that  $h_M$  is not a function of  $\tau$ , which only gives the general scale factor for time.

The optimum value for  $\tau$  is obviously given by the condition that the  $\overline{i_N^2}$  and  $\overline{e_N^2}$  components of equation 3.2-17 are equal. Thus

$$\tau_{\text{opt}} = (C_s + C_f) \sqrt{\frac{\overline{e_N^2}}{\overline{i_N^2}}} \sqrt{\frac{\int_0^\infty \frac{X^{2m} dX}{(1+X^2)^{n+m}}}{\int_0^\infty \frac{X^{2m-2} dX}{(1+X^2)^{n+m}}}} \quad (3.2-19)$$

with a corresponding minimum noise energy

$$\begin{aligned} \overline{E_N^2}_{\text{opt}} = & \frac{(C_s + C_f) \sqrt{\overline{e_N^2} \overline{i_N^2}}}{2\pi Q^2 h_M^2} \left\{ \gamma \int_0^\infty \frac{X^{2m-1} dX}{(1+X^2)^{n+m}} \right. \\ & \left. + 2 \sqrt{\left[ \int_0^\infty \frac{X^{2m-2} dX}{(1+X^2)^{n+m}} \right] \left[ \int_0^\infty \frac{X^{2m} dX}{(1+X^2)^{n+m}} \right]} \right\} \quad (3.2-20) \end{aligned}$$

The integrals involved in the above two equations are tabulated<sup>(9)</sup>

(9) Dwight, "Tables of Integrals and other Mathematical Data," (The Macmillan Co., New York, N.Y.)

205

and their evaluation gives

$$\int_0^{\infty} \frac{x^{2m-1} dx}{(1+x^2)^{n+m}} = \frac{(m-1)!(n-1)!}{2(m+n-1)!} \quad (3.2-21)$$

$$\int_0^{\infty} \frac{x^{2m-2} dx}{(1+x^2)^{n+m}} = \frac{1}{2} B(m-\frac{1}{2}, n+\frac{1}{2}) \quad (3.2-22)$$

$$\int_0^{\infty} \frac{x^{2m} dx}{(1+x^2)^{n+m}} = \frac{1}{2} B(m+\frac{1}{2}, n-\frac{1}{2}) \quad (3.2-23)$$

where

$$B(a, b) = \frac{\Gamma(a) \Gamma(b)}{\Gamma(a+b)}$$

$$\Gamma(a) = (a-1)! \text{ for } a = \text{integer}$$

$$\Gamma(a+\frac{1}{2}) = \frac{1 \cdot 3 \cdot 5 \cdots (2a-3)(2a-1) \sqrt{\pi}}{2^a} \text{ for } a = \text{integer}$$

$$\Gamma(a+1) = a \Gamma(a)$$

Substituting these values one obtains

$$\tau_{\text{opt}} = (C_s + C_f) \sqrt{\frac{e_N^2}{i_N^2}} \sqrt{\frac{2m-1}{2n-1}} \quad (3.2-24)$$

$$E_N^2, \text{opt} = \frac{(C_s + C_f) \sqrt{e_N^2 i_N^2}}{Q^2 h_M^2 (n+m-1)!} \left\{ \frac{\gamma}{4\pi} (m-1)!(n-1)! + \frac{[1 \cdot 3 \cdot 5 \cdots (2m-1)] [1 \cdot 3 \cdot 5 \cdots (2n-1)]}{2^{n+m} \sqrt{(2n-1)(2m-1)}} \right\} \quad (3.2-25)$$

The evaluation of  $h_M$  can be aided by observing that equation 3.2-18 can be written as

$$h(t') = \frac{1}{2\pi j} \frac{d^{m-1}}{dt'^{m-1}} \oint_C \frac{e^{Zt'} dZ}{(1+Z)^{n+m}} \quad (3.2-26)$$

The residue at the pole at  $Z = -1$  is easily evaluated to give

$$h(t') = \frac{d^{m-1}}{dt'^{m-1}} \left[ \frac{t'^{n+m-1} e^{-t'}}{(n+m-1)!} \right] \quad (3.2-27)$$

where as before  $t' = t/\tau$ . The peak value of  $h(t')$  can be obtained by differentiating equation 3.2-27 again with respect



to  $t'$  and evaluating  $h(t')$  for the time at which the derivative vanishes.

Two cases for the differentiation networks will be considered here - namely, single and double differentiation. These cases correspond to  $m = 1$  and  $m = 2$ , respectively. For single differentiation one obtains

$$h_1(t') = \frac{t'^n e^{-t'}}{n!} \quad (3.2-28)$$

$$h_{M1} = \frac{n^n e^{-n}}{n!} \quad (3.2-29)$$

with the peak occurring at a time

$$T_{p1} = n\tau \quad (3.2-30)$$

The optimum time constant and noise are given by

$$\tau_{opt,1} = (C_s + C_f) \sqrt{\frac{e_N^2}{i_N^2}} \frac{1}{\sqrt{2n-1}} \quad (3.2-31)$$

$$T_{p1} = (C_s + C_f) \sqrt{\frac{e_N^2}{i_N^2}} \frac{n}{\sqrt{2n-1}} \quad (3.2-32)$$

$$\overline{E_{N,1}^2} = \frac{(C_s + C_f) \sqrt{e_N^2 i_N^2} (n!)^2}{Q^2 (n^n e^{-n})^2} \left\{ \frac{\gamma}{4\pi n} + \frac{[1 \cdot 3 \cdot 5 \dots (2n-1)]}{n! 2^{n+1} \sqrt{2n-1}} \right\} \quad (3.2-33)$$

As the value of  $n$  is increased (i.e. as more integrating networks are used), the equivalent noise energy decreases slowly. The optimum value is produced by letting  $n$  approach infinity. In this case, the pulse response approaches a Gaussian, given by

$$\lim_{n \rightarrow \infty} h_1(t') = \frac{1}{\sqrt{2\pi n}} \exp - \left[ \frac{(t' - n)^2}{2n} \right] \quad (3.2-34)$$

This result was proved by Fairstein and Hahn<sup>(2)</sup>, who recognized that equation 3.2-28 was formally identical to the Poisson distribution, which, by the central limit theorem, approaches the normal distribution for infinite  $n$ . The value of  $h_M$  follows directly from 3.2-34 or from Stirling's approximation for the factorial, namely

$$\lim_{n \rightarrow \infty} n! = \sqrt{2\pi n} \, n^n e^{-n} \left[ 1 + \frac{1}{12n} \right] \quad (3.2-35)$$

$$\lim_{n \rightarrow \infty} h_{M1} = \frac{1}{\sqrt{2\pi n}} \quad (3.2-36)$$

Applying Stirling's approximation to equation 3.2-33, one obtains for the minimum noise energy under the assumptions of simple RC or LR shaping and of a single differentiator

$$\begin{aligned} E_{N^2, \text{MIN } 1} &= \frac{(C_s + C_f) \sqrt{e_N^2 i_N^2}}{Q^2} \left[ \frac{\gamma}{2} + \sqrt{\frac{\pi}{2}} \right] \\ &= \frac{(C_s + C_f) \sqrt{e_N^2 i_N^2}}{Q^2} \left[ 0.5 \gamma + 1.25 \right] \end{aligned} \quad (3.2-37)$$

---

(2) Fairstein and Hahn, Loc. Cit.

For no correlation the rms noise becomes

$$\sqrt{E_{N^2, \text{MIN}}^2} = \frac{1.12}{Q} \sqrt{(C_s + C_f) \sqrt{e_N^2} \sqrt{i_N^2}} \quad (3.2-38)$$

As shown in Section 2, minimizing baseline shifts requires that at least two differentiating networks be employed. This fact motivates the following calculation of the noise for the case of  $m = 2$ . In this case the transient response becomes

$$h_2(t') = \frac{t'^n (n+1-t') e^{-t'}}{(n+1)!} \quad (3.2-39)$$

with a maximum at  $T_p$  given by

$$h_{M2} = \frac{\sqrt{n+1}}{(n+1)!} \left[ (n+1) - \sqrt{n+1} \right]^n e^{-[n+1-\sqrt{n+1}]} \quad (3.2-40)$$

$$T_{p2} = (n+1 - \sqrt{n+1}) \tau \quad (3.2-41)$$

The optimum time constant and noise become

$$\tau_{\text{opt},2} = (C_s + C_f) \sqrt{\frac{e_N^2}{i_N^2}} \sqrt{\frac{3}{2n-1}} \quad (3.2-42)$$

$$T_{p2} = (C_s + C_f) \sqrt{\frac{e_N^2}{i_N^2}} \sqrt{\frac{3}{2n-1}} (n+1 - \sqrt{n+1}) \quad (3.2-43)$$

$$\begin{aligned} \overline{E_N^2}, \text{opt}, 2 = & \frac{(C_s + C_f) \sqrt{e_N^2 i_N^2} (n+1!)^2}{Q^2 (n+1) [(n+1) - \sqrt{n+1}]^{2n} e^{-2} [n+1 - \sqrt{n+1}]} \\ & \times \left\{ \frac{\gamma}{4\pi n(n+1)} \frac{\sqrt{3}}{4} (n+1)! 2^n \frac{1 \cdot 3 \cdot 5 \cdots (2n-1)}{\sqrt{2n-1}} \right\} \end{aligned} \quad (3.2-44)$$

In this case the noise has a minimum at  $n = 2$  and then increases with increasing  $n$ . The limiting transient response can be found from differentiating equation 3.2-34 to obtain

$$\lim_{n \rightarrow \infty} h_2(t') = \frac{n-t'}{n \sqrt{2\pi n}} \exp - \left[ \frac{(t' - n)^2}{2n} \right] \quad (3.2-45)$$

with a maximum given by

$$\lim_{n \rightarrow \infty} h_{M2} = \frac{1}{n \sqrt{2\pi e}} \quad (3.2-46)$$

$$\lim_{n \rightarrow \infty} T_{p2} = (n - \sqrt{n}) \tau \quad (3.2-47)$$

Substituting these values in equation 3.2-44 and taking the limit of infinite  $n$ , one obtains for the noise energy for the differentiated Gaussian

$$\begin{aligned} \lim_{n \rightarrow \infty} \overline{E_{N,2}^2} &= \frac{e(C_s + C_f) \sqrt{e_N^2 i_N^2}}{Q^2} \left[ \frac{\gamma}{2} + \sqrt{\frac{3\pi}{8}} \right] \\ &= \frac{(C_s + C_f) \sqrt{e_N^2 i_N^2}}{Q^2} \left[ 1.36\gamma + 2.95 \right] \quad (3.2-48) \end{aligned}$$

For no correlation the rms noise becomes

$$\sqrt{\overline{E_{N,2}^2}} = \frac{1.72}{Q} \sqrt{(C_s + C_f) \sqrt{e_N^2 i_N^2}} \quad (3.2-49)$$

The values of noise and optimum time constant for single and double differentiation are given in Table I for several values of  $n$ . Notice that the use of double differentiation increases the rms noise by a factor of 1.2 compared to single differentiation, if the optimum number of integrating networks are used for both cases.

Before leaving this subject, it should be pointed out that the restriction to the simple form for  $F(j\omega)$  given in equation 3.2-9 is neither unique nor necessary. Although the Gaussian pulse shape ( $m=1$ ,  $n=\infty$ ) appears optimum for this type of pulse shaping, other forms involving delay lines can give better noise performance<sup>(2)</sup>. Furthermore, the Gaussian pulse shape can be approximated simply with high accuracy if terms of the form  $1 + p\tau$  are allowed in the numerator of the transfer function<sup>(2,10)</sup>. If a pulse shape averaging to zero in a short time, such as the double-differentiated waveform, is required, then the above analysis indicates that the differentiated Gaussian is not the optimum even for the simple pulse shaping assumed. Double differentiation, double integration, for example, gives significantly less noise. The optimum pulse shape satisfying the zero-mean requirement may thus differ from the symmetrical waveform used in many advanced amplifiers. The calculation of this optimum is beyond the scope of this effort.

---

(2) Fairstein and Hahn, Loc. Cit.

(10) Blankenship and Nowlin, "New Concepts in Nuclear Pulse Amplifier Design," IEEE Transactions on Nuclear Science, NS-13, p 495, June 1966.

n Number of Integrators	A		B		$\tau_{opt}$ Optimum time constant in units of		$T_p$ Peak time in units of		$h_M$ Peak value of transient for unit input	
	Uncorrelated square- average noise in units of		Correlated square- average noise in units of		$(C_s+C_f)\sqrt{e_N^2 i_N^2}$		$(C_s+C_f)\sqrt{e_N^2 i_N^2}$			
	$Q^2$		$Q^2$		$(C_s+C_f)\sqrt{\frac{e_N^2}{i_N^2}}$		$(C_s+C_f)\sqrt{\frac{e_N^2}{i_N^2}}$			
	m=1	m=2	m=1	m=2	m=1	m=2	m=1	m=2	m=1	m=2
1	1.87	2.04	0.60	0.75	1.00	1.73	1.00	1.02	0.368	0.231
2	1.46	1.82	0.54	0.78	0.58	1.00	1.16	1.27	0.272	0.131
3	1.38	1.88	0.53	0.81	0.44	0.77	1.32	1.54	0.225	0.0903
4	1.36	2.04	0.52	0.90	0.38	0.65	1.52	1.80	0.196	0.0593
$\infty$	1.25	2.95	0.50	1.36	0	0	$\infty$	$\infty$	0	0

$$E_{N,opt}^2 = \frac{(C_s+C_f)\sqrt{e_N^2 i_N^2}}{Q^2} (A + \gamma B)$$

$$Q = 4.57 \times 10^{-17} \text{ C/KeV Silicon detector}$$

$$Q = 5.51 \times 10^{-17} \text{ C/KeV Germanium detector}$$

TABLE 1: Noise and Peak Values  
for Optimized Shaping Using Simple Poles

### 3.2.1 Field-Effect Transistor Input Stage

Commonly field-effect transistors are used for the input stage because of their low noise. A typical such amplifier is shown in Figure 3.2.1-1, where the FET noise sources are shown explicitly. The formulas developed in Section 3.2 cannot be used directly because of the frequency dependence of the FET noise. However, the following manipulation of the noise sources allows the final result to be represented in the form of equations 3.2-1 and 3.2-4.

Assume that the total complex admittance from the gate to ground is  $Y_s$  and that the FET has a transconductance  $g_m$ . Then the total equivalent squared-average noise current per unit bandwidth referred to the input becomes

$$\overline{i_{gT}^2} = \left[ i_{Ng} + i_{NR} + \frac{Y_s}{g_m} i_{Nc} + \sqrt{2qI_{LD}} \right]^2 \quad (3.2.1-1)$$

where

$$\overline{i_{NR}^2} = \frac{4kT}{R_f} = \text{squared-average feedback resistor noise current per unit bandwidth}$$

$$\overline{i_{Nc}^2} = 4kTg_m$$

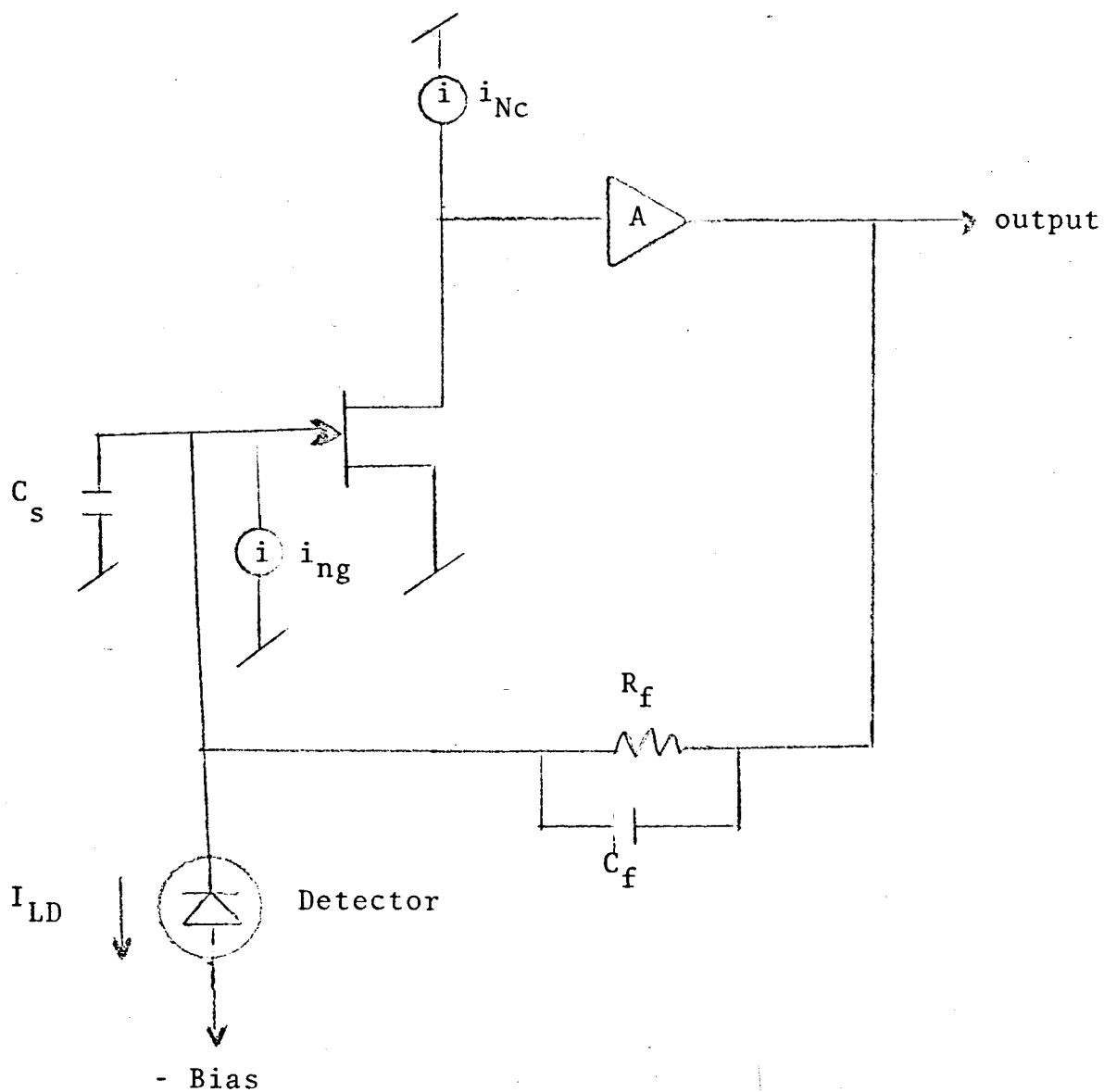
From equation 3.1.4-1 the gate noise current consists of two components

$$\overline{i_{g1}^2} = 2qI_g \quad (3.2.1-2)$$

$$\overline{i_{g2}^2} = \frac{4kTab}{g_m} (\omega C_{gs})^2 \quad (3.2.1-3)$$

where  $i_{g1}$  is uncorrelated with  $i_{Nc}$  and  $i_{g2}$  has the correlation





$I_{LD}$  = detector leakage current

$C_s$  = total source capacitance including the FET input capacitance and the detector capacitance

$A$  = subsequent gain stages producing negligible noise

Figure 3.2.1-1: Typical FET Amplifier Configuration

given in equation 3.1.4-3. The total noise current can then be written

$$\overline{i_{gT}^2} = 2q(I_g + I_{LD}) + \frac{4kT}{R_f} + \left| i_{g2} + \frac{Y_s}{g_m} i_{Nc} \right|^2 \quad (3.2.1-4)$$

The final term can be expanded to give

$$\begin{aligned} \overline{i_{g2}^2} \left\{ 1 - \left| \frac{i_{g2}^* i_{Nc}}{\sqrt{\overline{i_{g2}^2} \overline{i_{Nc}^2}}} \right|^2 \right\} + \frac{\overline{i_{Nc}^2}}{g_m^2} \left| Y_s + g_m \sqrt{\frac{\overline{i_{g2}^2}}{\overline{i_{Nc}^2}}} \frac{i_{g2}^* i_{Nc}}{\sqrt{\overline{i_{g2}^2} \overline{i_{Nc}^2}}} \right|^2 \\ = \overline{i_{g2}^2} (1 - |c|^2) + \frac{\overline{i_{Nc}^2} |Y_s|^2}{g_m^2} \left| 1 + \frac{g_m c}{Y_s} \sqrt{\frac{\overline{i_{g2}^2}}{\overline{i_{Nc}^2}}} \right|^2 \end{aligned} \quad (3.2.1-5)$$

where  $c$  is the complex correlation coefficient.

If the real component of  $Y_s$  is neglected as being small compared to the capacitive component at frequencies contributing most of the noise, then

$$Y_s \approx j(C_s + C_f) \quad (3.2.1-6)$$

and

$$\begin{aligned} \overline{i_{gT}^2} = 2q(I_g + I_{LD}) + \frac{4kT}{R_f} \\ + \frac{4kT a \omega^2 (C_s + C_f)^2}{g_m} \left\{ 1 + \frac{2|c|\sqrt{b} C_{gs}}{C_s + C_f} + \frac{b C_{gs}^2}{(C_s + C_f)^2} \right\} \end{aligned} \quad (3.2.1-7)$$

For

$$\begin{aligned} a &= 0.7 \\ b &= 0.4 \\ c &= j0.4 \end{aligned} \quad (3.2.1-8)$$

Then

$$\begin{aligned} \overline{i_{gT}^2} &= 2q(I_g + I_{LD}) + \frac{4kT}{R_f} \\ &+ \frac{2.8 kT \omega^2 (C_s + C_f)^2}{g_m} \left[ 1 + \frac{0.51 C_{gs}}{C_s + C_f} + \frac{0.4 C_{gs}^2}{(C_s + C_f)^2} \right] \end{aligned} \quad (3.2.1-9)$$

The amplifier output noise becomes

$$\overline{V_{2N}^2} = \int_0^\infty \frac{\overline{i_{gT}^2} R_f^2 |B(j\omega)|^2 d\omega}{(1 + \omega^2 \tau_1)^2} \quad (3.2.1-10)$$

$$\text{where } \tau_1 = R_f C_f$$

This equation becomes formally identical to equation 3.2-7 with

$$\overline{e_N^2} = \frac{2.8kT}{g_m} \left\{ 1 + \frac{0.51 C_{gs}}{C_s + C_f} + \frac{0.4 C_{gs}^2}{(C_s + C_f)^2} \right\} \quad (3.2.1-11)$$

$$\overline{i_N^2} = 2q(I_g + I_{LD}) + \frac{4kT}{R_f} \quad (3.2.1-12)$$

$$\gamma = 0 \quad (3.2.1-13)$$

For most spacecraft applications where cooling is impractical, the detector leakage current noise is the dominating factor in  $\overline{i_N^2}$ . The magnitude of  $R_f$  is limited to values of the order of 1 M in order to maintain adequate amplifier and detector bias stability. Furthermore, the feedback capacitor ( $C_f$ ) cannot be less than about 1 pF because unstable stray capacitance would otherwise dominate the amplifier gain. For such an application, typical values of the quantities of equations 3.2.1-11 and 3.2.1-12 are given in Table 2 for two cases of detector leakage current at room temperature and for double integration with double differentiation. Notice that the presence of detector leakage current severely limits resolution even with the rather large detector capacity (100 pF) assumed.

The calculated resolution is in good agreement with values actually obtained in practical amplifiers (10,11,12). Stringent selection of the FET, however, appears necessary to obtain theoretical noise performance using the 2N3823. The data of Blalock<sup>(12)</sup> appear to indicate that a 1/f noise component can be significant at frequencies above 10 KHz in some units. Improvements in device manufacturing techniques will probably reduce selection problems in the near future.

Improved resolution can also be obtained by cooling (11,12) the FET and critical resistors to about -110°C. This technique is particularly applicable to  $\gamma$  - spectroscopy experiments using cooled germanium detectors. Also, Smith and Cline<sup>(11)</sup> have shown that using several FETs in parallel for the input stage can reduce noise for high detector capacities.

---

(10) Blankenship and Nowlin, Loc. Cit.

(11) Smith and Cline, "A Low-Noise Charge Sensitive Preamplifier for Semiconductor Detectors Using Paralleled Field-Effect Transistors," IEEE Transactions on Nuclear Science, NS-13 p 468, June 1966.

(12) Blalock, "Wide-Band Low-Noise Charge Sensitive Preamplifier," IEEE Transactions on Nuclear Science, NS-13, p 457, June 1966.

Quantity	High Detector Leakage	Low Detector Leakage
Detector Leakage Current ( $I_{DL}$ )	$3 \times 10^{-7} \text{ A}$	$< 10^{-10} \text{ A}$
FET Leakage Current ( $I_g$ ) (2N3823)	$10^{-10} \text{ A}$	$10^{-10} \text{ A}$
Transconductance ( $g_m$ ) (2N3823)	4000 $\mu\text{mho}$	4000 $\mu\text{mho}$
Feedback Resistor ( $R_f$ )	$5 \times 10^5 \Omega$	$10^9 \Omega$
Feedback Capacitor ( $C_f$ )	1 pF	1 pF
Input Capacitance plus Detector Capacitance for $C_D = 100 \text{ pF}$ ( $C_s$ )	107 pF	107 pF
$2qI_g$	$3.2 \times 10^{-29} \text{ A}^2/\text{Hz}$	$3.2 \times 10^{-29} \text{ A}^2/\text{Hz}$
$2qI_{DL}$	$9.6 \times 10^{-26} \text{ A}^2/\text{Hz}$	0
$\frac{4kT}{R_f}$	$3.2 \times 10^{-26} \text{ A}^2/\text{Hz}$	$1.6 \times 10^{-29} \text{ A}^2/\text{Hz}$
$\sqrt{i_N^2}$	$3.58 \times 10^{-13} \text{ A}/\sqrt{\text{Hz}}$	$6.92 \times 10^{-14} \text{ A}/\sqrt{\text{Hz}}$
$\sqrt{e_N^2}$	$1.68 \times 10^{-9} \text{ V}/\sqrt{\text{Hz}}$	$1.68 \times 10^{-9} \text{ V}/\sqrt{\text{Hz}}$
$\tau_{opt}$	0.51 $\mu\text{s}$	2.62 $\mu\text{s}$
Q (Silicon Detector)	$4.57 \times 10^{-17} \text{ C/KeV}$	$4.57 \times 10^{-17} \text{ C/KeV}$
$\sqrt{E_{opt}^2} \text{ (RMS)}$	7.51 KeV	3.32 KeV
$\sqrt{E_{opt}^2} \text{ (FWHM)}$	17.7 KeV	7.70 KeV

TABLE 2: Typical Solid-State Detector  
System Noise Levels

### 3.3 Noise Counting Rates

In some applications the amplifier may be connected to a discriminator with a threshold sufficiently low so that the probability of its being exceeded by noise pulses is significant. This noise counting rate can severely limit some low-energy experiments. In this section, the noise counting rate will be derived based on statistical relations developed by Rice <sup>(4)</sup>.

Assume that the discriminator is an ideal device in that it has zero dead time and hysteresis. Then if a noise signal from an amplifier as shown in the upper curve of Figure 3.3-1 is applied to the discriminator input, the discriminator output is given by the lower curve. We wish to calculate the average number of discriminator transitions per second.

The noise counting rate is the number of times per second that the amplifier output voltage exceeds the threshold ( $D$ ) with a positive slope. Consider the probability distribution function  $p(s, n; t_1) ds dn$ , which represents the probability that the amplifier output voltage  $V_2(t)$  has a value  $s$  within  $ds$  and a slope  $n$  within  $dn$  at the time  $t_1$ . If  $V_2(t)$  is equal to  $s$  at  $t = t_1$  with a slope  $n$ , then a first order expansion about  $t_1$  gives

$$V_2(t) \approx s + n (t - t_1) \quad (3.3-1)$$

so that if  $V_2(t) = D$  within  $dt$  of  $t_1$  then  $s$  and  $n$  must satisfy the inequality

$$t_1 - dt < t_1 - \frac{s - D}{n} < t_1 + dt \quad (3.3-2)$$

---

(4) Rice, Loc. Cit.

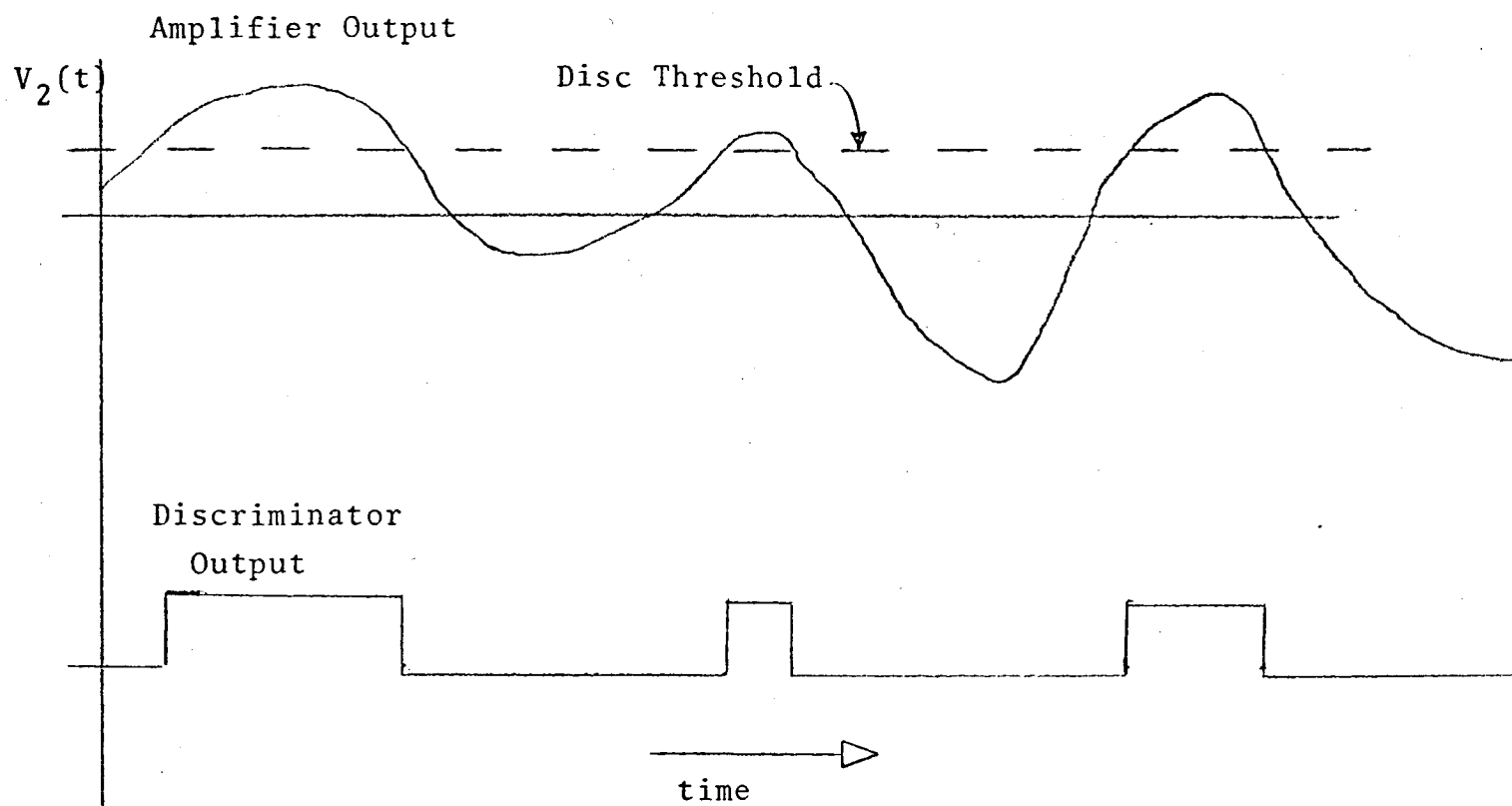


Figure 3.3-1: Discriminator Response

The condition that the slope be positive reduces this inequality to

$$-\eta dt < \xi < -D < 0 \quad (3.3-3)$$

If we integrate over all allowed values of  $\xi$  and  $\eta$ , then

$$P_+(D)dt = \int_0^\infty \int_{D-\eta dt}^D p(\xi, \eta; t_1) d\xi d\eta \\ = \int_0^\infty \eta p(D, \eta; t_1) d\eta dt \quad (3.3-4)$$

where  $P_+(D)dt$  = probability that  $V_2(t)$  crosses  $\xi = D$  with positive slope at  $t_1$  in  $dt$ , and the limit of small  $dt$  has been taken so that  $p(\xi, \eta; t_1) \approx p(D, \eta; t_1)$  throughout the interval ( $\xi = D - \eta dt$ ,  $\xi = D$ ).

If  $p(D, \eta; t_1)$  does not depend on time, then  $P_+(D)$  can be trivially integrated over one second so that the rate  $R$  becomes

$$R = \int_0^\infty \eta p(D, \eta) d\eta \quad (3.3-5)$$

By the central limit theorem, the distribution of amplitude and derivative are known to be normal, and it can also be shown that they are independent. Thus,  $p(D, \eta)$  becomes

$$p(D, \eta) = \frac{1}{2\pi\sigma_0\sigma_1} e^{-\frac{D^2}{2\sigma_0^2}} e^{-\frac{\eta^2}{2\sigma_1^2}} \quad (3.3-6)$$



where  $\sigma_0^2$  = square-average of  $V_2(t)$

$\sigma_1^2$  = square-average of  $\frac{dV_2(t)}{dt}$

From the previous section

$$\sigma_0^2 = \frac{1}{2\pi} \int_0^\infty |i_T(j\omega)|^2 |F(j\omega)|^2 d\omega \quad (3.3-7)$$

where  $i_T(j\omega)$  = total noise expressed as a complex input current

$F(j\omega)$  = Fourier transform of the amplifier transfer impedance

Similarly because the Fourier transform of  $\frac{dV_2}{dt}$  is  $j\omega F(j\omega)$ , then

$$\sigma_1^2 = \frac{1}{2\pi} \int_0^\infty \omega^2 |i_T(j\omega)|^2 |F(j\omega)|^2 d\omega \quad (3.3-8)$$

Substituting equations 3.3-6 into equation 3.3-5, one obtains for the rate

$$R = \frac{\sigma_1}{2\pi\sigma_0} e^{-\frac{D^2}{2\sigma_0^2}} \quad (3.3-9)$$

If  $F(j\omega)$  has the simple form given in equation 3.2-9 and if the equivalent input noise current can be represented by equations 3.2-1, 3.2-4 and 3.2-6, then the quantities  $\sigma_0$  and  $\sigma_1$  referred to the input become for equal time constants

$$\sigma_0^2 = \overline{E_N^2} = \frac{1}{2\pi Q^2 h_M^2} \left\{ \overline{i_N^2} \tau \int_0^\infty \frac{X^{2m-2} dX}{(1+X^2)^{n+m}} \right. \\ \left. + \gamma \sqrt{\overline{e_N^2} \overline{i_N^2}} (C_f + C_s) \int_0^\infty \frac{X^{2m-1} dX}{(1+X^2)^{n+m}} \right. \\ \left. + \frac{\overline{e_N^2} (C_f + C_s)^2}{\tau} \int_0^\infty \frac{X^{2m} dX}{(1+X^2)^{n+m}} \right\} \quad (3.3-10)$$

$$\sigma_1^2 = \frac{1}{2\pi \tau^2 Q^2 h_M^2} \left\{ \overline{i_N^2} \tau \int_0^\infty \frac{X^{2m} dX}{(1+X^2)^{n+m}} \right. \\ \left. + \gamma \sqrt{\overline{e_N^2} \overline{i_N^2}} (C_f + C_s) \int_0^\infty \frac{X^{2m+1} dX}{(1+X^2)^{n+m}} \right. \\ \left. + \frac{\overline{e_N^2} (C_f + C_s)^2}{\tau} \int_0^\infty \frac{X^{2m+2} dX}{(1+X^2)^{n+m}} \right\} \quad (3.3-11)$$

The integrals can be evaluated using equations 3.2-21 to 3.2-23 and

$$\int_0^{\infty} \frac{X^{2m+1} dX}{(1+X^2)^{n+m}} = \frac{m!(n-2)!}{2(n+m-1)!} \quad (3.3-12)$$

$$\int_0^{\infty} \frac{X^{2m+2} dX}{(1+X^2)^{n+m}} = \frac{1}{2} B(m + 3/2, n - 3/2) \quad (3.3-13)$$

where the integrals for  $\overline{e_N^2}$  and for  $\gamma$  diverge for  $n < 2$ . In actual practice these integrals do not diverge even for  $n = 1$  because of amplifier bandwidth limitations neglected in the approximation that A was very large for all frequencies of interest. However, a significant excess counting rate can occur when only single integration is used if voltage or correlation noise is important.

Equation 3.3-9 can be written

$$R = \frac{K_3}{2\pi\tau} \exp \left[ \frac{-D^2}{2\overline{E_N^2}} \right] \quad (3.3-14)$$

where

D = discrimination level in units of equivalent input energy

$\overline{E_N^2}$  = square-average equivalent input noise energy

$K_3$  = constant of the order of one dependent on the details of the pulse shaping

Because  $\overline{E_N^2}$  has been considered in the previous section, the only remaining problem is the determination of  $K_3$ . This constant is given by

$$2 = \frac{\overline{i_N^2} \tau B(m+1/2, n-1/2) + \frac{\gamma \sqrt{\overline{e_N^2} \overline{i_N^2}} (C_f + C_s) m! (n-2)! \overline{e_N^2} (C_f + C_s)^2 B(m+3/2, n-3/2)}{(n+m-1)!} + \frac{\overline{e_N^2} (C_f + C_s)^2 B(m+3/2, n-3/2)}{\tau}}{\overline{i_N^2} \tau B(m-1/2, n+1/2) + \frac{\gamma \sqrt{\overline{e_N^2} \overline{i_N^2}} (C_f + C_s) (m-1)! (n-1)! \overline{e_N^2} (C_f + C_s)^2 B(m+1/2, n-1/2)}{(n+m-1)!} + \frac{\overline{e_N^2} (C_f + C_s)^2 B(m+1/2, n-1/2)}{\tau}}$$

(3.3-15)

Evaluating the B-functions according to equation 3.2-23, one obtains

$$B(m+1/2, n-1/2) = \frac{\pi [1 \cdot 3 \cdot 5 \cdots (2m-1)] [1 \cdot 3 \cdot 5 \cdots (2n-1)]}{(m+n-1)! (n-1/2) 2^{m+n}}$$

(3.3-16)

$$B(m+3/2, n-3/2) = \frac{\pi [1 \cdot 3 \cdot 5 \cdots (2m-1)] [1 \cdot 3 \cdot 5 \cdots (2n-1)] [m+1/2]}{(m+n-1)! (n-1/2) (n-3/2) 2^{m+n}}$$

(3.3-17)

$$B(m-1/2, n+1/2) = \frac{\pi [1 \cdot 3 \cdot 5 \cdots (2m-1)] [1 \cdot 3 \cdot 5 \cdots (2n-1)]}{(m+n-1)! (m-1/2) 2^{m+n}}$$

(3.3-18)

and  $K_3^2$  becomes

$$K_3^2 = \frac{\frac{\overline{i_N^2} \tau}{n-1/2} + \frac{\gamma \sqrt{e_N^2 \overline{i_N^2}} (C_f + C_s) m! (n-2)! 2^{m+n}}{\pi [1 \cdot 3 \cdots (2m-1)] [1 \cdot 3 \cdots (2n-1)]} + \frac{e_N^2 (C_f + C_s)^2 (m+1/2)}{(n-1/2)(n-3/2) \tau}}{\frac{\overline{i_N^2} \tau}{m-1/2} + \frac{\gamma \sqrt{e_N^2 \overline{i_N^2}} (C_f + C_s) (m-1)! (n-1)! 2^{m+n}}{\pi [1 \cdot 3 \cdots (2m-1)] [1 \cdot 3 \cdots (2n-1)]} + \frac{e_N^2 (C_f + C_s)^2}{(n-1/2) \tau}} \quad (3.3-19)$$

Several special cases for  $K_3$  are of interest. For example, for a photomultiplier tube amplifier, current noise resulting from photomultiplier dark current may completely dominate. Then  $K_3$  becomes approximately

$$K_{3i} \approx \sqrt{\frac{m-1/2}{n-1/2}} = \sqrt{\frac{2m-1}{2n-1}} \quad (3.3-20)$$

When an equal number of integrators and differentiators are used,  $K_{3i}$  equals unity.

Another interesting case occurs when the shaping time constant has been chosen to give minimum equivalent input noise energy. Then

$$\tau_{opt} = (C_s + C_f) \sqrt{\frac{e_N^2}{\overline{i_N^2}}} \sqrt{\frac{2m-1}{2n-1}} \quad (3.3-21)$$

and the rate becomes

$$R_{\text{opt}} = \frac{K_4}{(C_s + C_f)} \sqrt{\frac{i_N^2}{e_N^2}} \exp \left[ \frac{-D^2}{2E_N^2} \right] \quad (3.3-22)$$

$$\text{where } K_4 = \frac{K_3}{2\pi} \sqrt{\frac{2n-1}{2m-1}}$$

The constant  $K_4$  can be written as

$$K_4^2 = a_1 \frac{1 + a_3 \gamma}{1 + a_2 \gamma} \quad (3.3-23)$$

where

$$a_1 = \frac{4mn - 4m + 1}{4\pi^2 (2n-3)(2m-1)} \quad (3.3-24)$$

$$a_2 = \frac{(m-1)!(n-1)!2^{m+n-2}}{\pi \sqrt{(2m-1)(2n-1)} [1 \cdot 3 \cdots (2n-3)] [1 \cdot 3 \cdots (2m-3)]} \quad (3.3-25)$$

$$a_3 = \frac{m(2n-1)a_2}{4\pi^2 (n-1)(2m-1)a_1} \quad (3.3-26)$$

for  $n \geq 2$ .

529

For  $\gamma = 0$ , the noise rate becomes

$$R_{\text{opt}} = \frac{1}{2\pi(C_s + C_f)} \sqrt{\frac{\bar{i}_N^2}{e_N^2} \left[ \frac{4mn - 4m + 1}{(2m-1)(2n-3)} \right]} \exp \left[ \frac{-D^2}{2\bar{E}_N^2} \right] \quad (3.3-27)$$

For single differentiation,  $m = 1$  and the constants in  $K_4^2$  are given by

$$a_1 = 0.0253 \left( \frac{4n-3}{2n-3} \right) \quad (3.3-28)$$

$$a_2 = \frac{0.159(n-1)! 2^n}{\sqrt{2n-1} [1 \cdot 3 \cdots (2n-3)]} \quad (3.3-29)$$

$$a_3 = \left( \frac{2n-3}{4n-3} \right) \left( \frac{2n-1}{n-1} \right) a_2 \quad (3.3-30)$$

and the noise rate for  $\gamma = 0$  becomes

$$R_{1,\text{opt}} = \frac{0.159}{(C_s + C_f)} \sqrt{\frac{\bar{i}_N^2}{e_N^2} \left[ \frac{4n-3}{2n-3} \right]} \exp \left[ \frac{-D^2}{2\bar{E}_N^2} \right] \quad (3.3-31)$$

If  $n \rightarrow \infty$  so that Gaussian pulse shaping results, then

$$R_{1,\text{opt}} \rightarrow \frac{0.225}{(C_s + C_f)} \sqrt{\frac{\bar{i}_N^2}{e_N^2}} \exp \left[ \frac{-D^2}{2\bar{E}_N^2} \right] \quad (3.3-32)$$

For double differentiation,  $m = 2$  and the constants in  $K_4^2$  are given by

$$a_1 = 0.00844 \left( \frac{8n-7}{2n-3} \right) \quad (3.3-33)$$

$$a_2 = \frac{0.183(n-1)!2^n}{\sqrt{2n-1} [1 \cdot 3 \cdots (2n-3)]} \quad (3.3-34)$$

$$a_3 = 2 \left( \frac{2n-3}{8n-7} \right) \left( \frac{2n-1}{n-1} \right) a_2 \quad (3.3-35)$$

so that the rate for no correlation becomes

$$R_{2,opt} = \frac{0.0918}{(C_s + C_f)} \sqrt{\frac{\bar{i}_N^2}{e_N^2} \left[ \frac{8n-7}{(2n-3)} \right]} \exp \left[ \frac{-D^2}{2\bar{E}_N^2} \right] \quad (3.3-36)$$

For the case where two integrators are also used, then

$$R_{22,opt} = \frac{0.275}{(C_s + C_f)} \sqrt{\frac{\bar{i}_N^2}{e_N^2}} \exp \left[ \frac{-D^2}{2\bar{E}_N^2} \right] \quad (3.3-37)$$

Various values of the above quantities are given in Table 3.



Number of integrators (n)	$a_1$		$a_2$		$a_3$		$\sqrt{a_1}$	
	m=1	m=2	m=1	m=2	m=1	m=2	m=1	m=2
2	0.127	0.0760	0.368	0.422	0.221	0.280	0.356	0.276
3	0.0759	0.0478	0.380	0.437	0.316	0.385	0.275	0.218
4	0.0658	0.0422	0.385	0.443	0.346	0.412	0.256	0.205
$\infty$	0.0506	0.0338	0.400	0.461	0.400	0.461	0.225	0.184

TABLE 3: Noise Counting Rate Parameters

For the amplifier discussed in Section 3.2.1 the rms noise level, including detector leakage current, was 7.51 KeV. The noise counting rate then becomes

$$R = 5.43 \times 10^5 \exp \left[ \frac{-D^2}{113} \right] \quad (3.3-38)$$

where D = discrimination level in KeV, and the rate is in counts per second. Several values of R are given in Table 4.

Discrimination Level (KeV)	Noise Counting Rate (Counts per second)
10	$1.76 \times 10^5$
20	$1.57 \times 10^4$
40	$3.92 \times 10^{-1}$
80	$2.83 \times 10^{-7}$

(Amplifier parameters given in Table 2 for high detector leakage. Pulse shaping was double-integration, double-differentiation.)

TABLE 4: Typical Noise Counting Rates

### 3.3.1 Photomultiplier Tube System

A common form of x-ray detector is shown in Figure 3.3.1-1. The lower-energy limit of the discriminator threshold (D) is often determined by the noise counting rate, which mostly results from the photomultiplier dark current.

Dark-current noise is caused by statistical variations of thermally generated currents within the photomultiplier. Most of this current results from single-electron events generated by thermionic emission at the photocathode. For this case the dark-current noise at the amplifier input becomes from the discussion of shot noise in section 3.1.2.

$$\overline{i_{Nd}^2} = 2qi_d G^2 \quad (3.3.1-1)$$

where  $i_d$  = dark current referred to the photocathode

$G$  = photomultiplier tube current gain

In actual practice this dark-current noise is increased over the above because of events generated by thermionic emission from the dynodes. A more correct expression then is <sup>(13)</sup>

$$\overline{i_{nd}^2} = 2qi_d G^2 \left[ 1 + \frac{B}{k-1} \right] \quad (3.3.1-2)$$

where  $k$  = secondary emission ratio per stage,  
usually of the order of four.

$B$  = statistical factor of the order of 1.5.

<sup>(13)</sup> Technical Manual PT-60, Radio Corporation of America

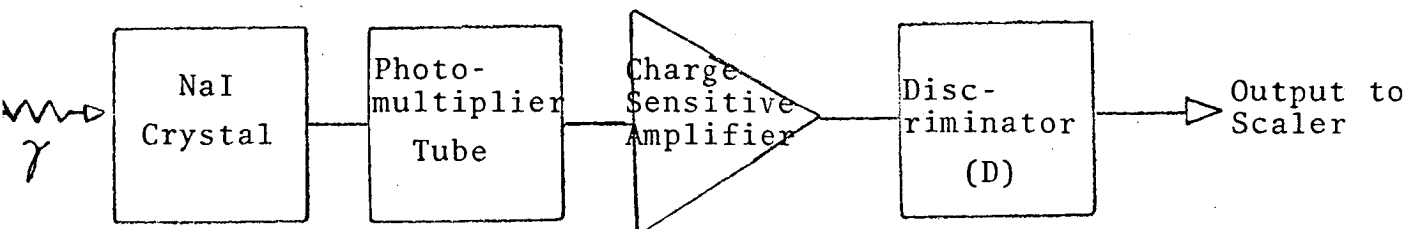


Figure 3.3.1-1: X-Ray Detector System

This current noise adds to the amplifier noise in a similar manner that detector leakage current noise adds to the total noise of a solid-state detector amplifier system. However, because of the large value of current noise and small input capacity compared to solid-state detector systems, the optimum shaping time constant often becomes smaller than the 0.25  $\mu$ s time constant of the NaI scintillation decay. Thus, the optimum time constant case developed in section 3.2 cannot be used, and the noise for equal time constants must be determined directly from equation 3.2-17. Evaluating the integrals using equations 3.2-21, 22, and 23, one obtains for the equivalent squared-input noise energy

$$\begin{aligned} \overline{E_N^2} = \frac{1}{4\pi Q^2 h_M^2} & \left\{ \overline{i_N^2} \tau B(m-1/2, n+1/2) \right. \\ & + \frac{\gamma \sqrt{\overline{e_N^2} \overline{i_N^2}} (C_f + C_s) (m-1)! (n-1)!}{(m+n-1)!} \\ & \left. + \frac{\overline{e_N^2} (C_f + C_s)^2 B(m+1/2, n-1/2)}{\tau} \right\} \end{aligned} \quad (3.3.1-3)$$

where

$$\begin{aligned} B(m-1/2, n+1/2) &= \frac{\pi [1 \cdot 3 \cdot 5 \cdots (2m-1)] [1 \cdot 3 \cdot 5 \cdots (2n-1)]}{(m+n-1)! (m-1/2) 2^{m+n}} \\ B(m+1/2, n-1/2) &= \frac{\pi [1 \cdot 3 \cdot 5 \cdots (2m-1)] [1 \cdot 3 \cdot 5 \cdots (2n-1)]}{(m+n-1)! (n-1/2) 2^{m+n}} \end{aligned}$$

Thus,

$$\begin{aligned}
\overline{E_N^2} = & \frac{[1 \cdot 3 \cdots (2m-1)][1 \cdot 3 \cdots (2n-1)]}{Q^2 h_M^2 (m+n-1)! 2^{m+n+1}} \left\{ \frac{\overline{i_N^2} \tau}{2m-1} \right. \\
& + \frac{\overline{e_N^2} (C_f + C_s)^2}{\tau (2n-1)} \\
& \left. + \frac{\gamma \sqrt{\overline{e_N^2} \overline{i_N^2}} (C_s + C_f) (m-1)! (n-1)! 2^{m+n-1}}{\pi [1 \cdot 3 \cdots (2m-1)][1 \cdot 3 \cdots (2n-1)]} \right\} \\
& (3.3.1-4)
\end{aligned}$$

If an amplifier of the type described in section 3.2.1 is used, then typically

$$\gamma = 0 \quad (3.3.1-5)$$

$$\sqrt{\overline{e_N^2}} = 1.68 \times 10^{-9} \text{ V}/\sqrt{\text{Hz}}$$

$$\sqrt{\overline{i_{Na}^2}} = 6.92 \times 10^{-14} \text{ A}/\sqrt{\text{Hz}}$$

$$C_s + C_f = 20 \text{ pF}$$

where  $\overline{i_{Na}^2}$  = amplifier contribution to  $\overline{i_N^2}$

The photomultiplier dark current depends strongly on the tube used. For example, the RCA 4461 has a typical dark current referred to the anode of  $5 \times 10^{-9}$  A at a gain of  $1.7 \times 10^5$ , yielding

$$i_d = \frac{5 \times 10^{-9}}{1.7 \times 10^5} = 2.94 \times 10^{-14} \text{ A} \quad (3.3.1-6)$$

and from equation 3.3.1-2

$$\overline{i_{Nd}^2} = 4.07 \times 10^{-22} \text{ A}^2/\text{Hz} \quad (3.3.1-7)$$

The EMI 9524BR has a reduced dark current of typically

$$i_d = 7.0 \times 10^{-16} \text{ A} \quad (3.3.1-8)$$

with

$$\overline{i_{Nd}^2} = 9.7 \times 10^{-24} \text{ A}^2/\text{Hz} \quad (3.3.1-9)$$

The total current noise given by

$$\overline{i_N^2} = \overline{i_{Na}^2} + \overline{i_{Nd}^2} \quad (3.3.1-10)$$

becomes indistinguishable from the dark-current noise in both cases.

If the time constant could be optimized for noise, then its value would be of the order of 10 ns. Therefore, as small a value as possible is chosen for  $\tau$  consistent with the 0.25  $\mu\text{s}$  NaI decay time constant. If double integration with double differentiation is used, then  $\tau$  can be 1  $\mu\text{s}$  with about a 5% dependence of the gain on the NaI decay time constant. For this case the voltage noise becomes completely negligible, and



$$\overline{E_N^2} \cong \frac{\tau q i_d G^2 \left(1 + \frac{B}{k-1}\right) \left[1 \cdot 3 \cdots (2m-1)\right] \left[1 \cdot 3 \cdots (2n-1)\right]}{Q^2 h_M^2 (m+n-1)! 2^{m+n} (2m-1)} \quad (3.3.1-11)$$

The charge per unit incident energy (Q) is related to the photomultiplier tube parameters by

$$Q = \frac{Gq}{E_0} \quad (3.3.1-12)$$

where  $E_0$  is the energy per photoelectron and is given by

$$E_0 = \frac{\hbar\omega}{C_P C_L C_S} \quad (3.3.1-13)$$

$\hbar\omega$  = photon energy at the peak of the combined spectral response of the detector and photomultiplier tube. For NaI and  $S_{11}$  response,  $\hbar\omega$  is typically 3.1 eV.

$C_P$  = photocathode efficiency = average number of photoelectrons per collected photon. For the RCA 4461,  $C_P$  is typically 0.14 and for the EMI 9524BR typically 0.16.

$C_L$  = light collection efficiency = probability that a photon produced in the crystal reaches the photocathode. Typically  $C_L$  is 0.20.

$C_S$  = scintillation efficiency = fraction of the incident energy converted to useful photons. For NaI,  $C_S$  is 0.08.

For the above typical values and for the RCA 4461 tube, then

$$E_0 = 1.38 \text{ KeV} \quad (3.3.1-14)$$

and for the EMI 9524BR

$$E_0 = 1.21 \text{ KeV} \quad (3.3.1-15)$$

The total equivalent input noise energy then becomes

$$\overline{E_N^2} \cong \frac{\tau i_d E_0^2 \left(1 + \frac{B}{k-1}\right) \left[1 \cdot 3 \cdots (2m-1)\right] \left[1 \cdot 3 \cdots (2n-1)\right]}{q h_M^2 (m+n-1)! 2^{m+n} (2m-1)} \quad (3.3.1-16)$$

and the noise counting rate becomes using equations 3.3-14 and 3.3-20

$$R = \frac{1}{2\pi\tau} \sqrt{\frac{2m-1}{2n-1}} \exp\left[\frac{-D^2}{2 \overline{E_N^2}}\right] \quad (3.3.1-17)$$

For double differentiation with double integration

$$\overline{E_N^2} \cong \frac{\tau i_d E_0^2 \left(1 + \frac{B}{k-1}\right)}{32 q h_M^2} \quad (3.3.1-18)$$

and

$$R = \frac{0.159}{\tau} \exp\left[\frac{-D^2}{2 \overline{E_N^2}}\right] \quad (3.3.1-19)$$

Several typical values of these quantities are given in Table 5.

291

These estimates should be treated with some care, particularly when very low rates result. First, the normal distribution used in equation 3.3-6 is only approximately correct and fails to be accurate for large values of  $D/\sigma_0$ . Second, noise from other sources such as electrical pick-up, cosmic rays, or residual radioactivity in the phototube, crystal or mounting can certainly dominate rates of the order of  $10^{-5}$  counts<sub>2</sub> per second. Third, the very strong dependence of  $R$  on  $E_N^2$  implies that only small errors in estimating the equivalent input noise energy can produce order-of-magnitude changes in the noise counting rate.

Parameter	RCA 4461	EMI 9524BR
$i_d$ (Typical)	$2.94 \times 10^{-14}$ A	$7.0 \times 10^{-16}$ A
$\tau$	1 $\mu$ s	1 $\mu$ s
$E_0$	1.38 KeV	1.21 KeV
$\overline{E_N^2}$ (RMS)	0.954 KeV <sup>2</sup>	$1.74 \times 10^{-2}$ KeV <sup>2</sup>
R at D = 5.0 KeV	$3.26 \times 10^{-1}$ cts/s	$< 10^{-16}$ cts/s
R at D = 7.07 KeV	$6.69 \times 10^{-5}$ cts/s	$< 10^{-16}$ cts/s
R at D = 10.0 KeV	$2.81 \times 10^{-16}$ cts/s	$< 10^{-16}$ cts/s

TABLE 5: Typical Noise Counting Rates

## References

1. Harold Cramer, Mathematical Methods of Statistics, (Princeton University Press, 1958).
2. Fairstein and Hahn, Nucleonics 23, (July, September, November 1965 and January, March 1966).
3. Y. W. Lee, Statistical Theory of Communication, (John Wiley and Sons, Inc. New York).
4. S. O. Rice, "Mathematical Analysis of Random Noise" from Selected Papers on Noise and Stochastic Processes, edited by N. Wax (Dover Publications, Inc., New York, 1954).
5. W. H. Fonger, "A Determination of  $1/f$  Noise Sources in Semiconductor Diodes and Triodes," Transistors I, RCA Laboratories, Princeton, N.J., 1956.
6. A. G. Di Loreto, Noise Optimization Techniques for Linear Transistor Amplifiers U.S. Naval Ordnance Test Station, China Lake, Calif., Oct. 1963 NAVWEPS Report 8381.
7. A. Van der Ziel, "Thermal Noise in Field-Effect Transistors," Proc. IRE, 50, p 1808, August 1962.
8. A. Van der Ziel, "Gate Noise in Field-Effect Transistors at Higher Frequencies," Proc. IRE, 51, p 461, March 1963.
9. Dwight, "Tables of Integrals and Other Mathematical Data," (The Macmillan Co., New York, N.Y.).
10. Blankenship and Nowlin, "New Concepts in Nuclear Pulse Amplifier Design," IEEE Transactions on Nuclear Science, NS-13, p 495, June 1966.
11. Smith and Cline, "A Low-Noise Charge Sensitive Preamplifier for Semiconductor Detectors Using Paralleled Field-Effect Transistors," IEEE Transactions on Nuclear Science, NS-13 p 468, June 1966.
12. Blalock, "Wide-Band Low-Noise Charge Sensitive Preamplifier," IEEE Transactions on Nuclear Science, NS-13, p 457, June 1966.
13. Technical Manual PT-60, Radio Corporation of America.

## Appendix C

### Magnetic Element Design and Fabrication Instruction

MAGNETIC ELEMENT  
DESIGN AND FABRICATION  
INSTRUCTION

ELEMENT DESCRIPTION
INDUCTOR,
PULSE SHAPING,
2.0 MH
VENDOR NAME
VENDOR PART NO.
ATC SKETCH NO.
A-101703
PROJECT
PHA / U.C.

ATC SPECIFICATION \_\_\_\_\_  
(FOR COMPONENT ENGINEERING USE ONLY)

ELECTRICAL CHARACTERISTICS  
INDUCTOR

INDUCTANCE 2.0 MH @ 0.1 V RMS \_\_\_\_\_ ADC 1000 CPS

RESISTANCE 1.8  $\Omega$   $\pm$  15 %

INDUCTANCE LINEARITY \_\_\_\_\_: SIGNAL LEVEL RANGE \_\_\_\_\_ TO \_\_\_\_\_

CURRENT RANGE \_\_\_\_\_ TO \_\_\_\_\_ @ \_\_\_\_\_ V \_\_\_\_\_ CPS.

TEMPERATURE RANGE -55 TO +85 °C

MAXIMUM LEVEL \_\_\_\_\_ V, \_\_\_\_\_ CPS, \_\_\_\_\_ ADC

SELF RESONANT FREQUENCY > 2.0 MH  $\pm$  @ 0.1 V

STRAY (EXTERNAL) MAGNETIC FIELD:

DC. \_\_\_\_\_ GAUSS MAX @ \_\_\_\_\_ INCHES WITH \_\_\_\_\_ ADC APPLIED.

AC. \_\_\_\_\_ GAUSS MAX @ \_\_\_\_\_ INCHES WITH \_\_\_\_\_ VRMS CPS APPLIED.

VOLTAGE COIL TO CORE \_\_\_\_\_ TO GROUND \_\_\_\_\_

VENDOR NAME
VENDOR PART #
ATC SKETCH # <u>A-101703</u>



TERMINAL NUMBERS	1-2
TURNS	138
TAPS	X
WINDOW FILL	X
WIRE SIZE	#34
INSULATION TYPE	HIS/HPT
SECTOR LENGTH	X
WINDING TYPE	X
LEAD TYPE	#28E TFE
LEAD LENGTH	4"
INSULATION, <del>WRAP</del> WRAP	1/2 MIL, TFE
MEAN LENGTH OF TURN	0.05'
NO LOAD VOLTS	X
FULL LOAD VOLTS	X
AMPERES	X
RESISTANCE	1.8 Ω
TEST VOLTS	X
EXCITING CURRENT	X
NO LOAD WATTS	X
CORE	55037-W4
MFG.	GAUGE MFG. MAGNETICS INC.
GRADE	μ = 200
CORE BOX MATERIAL	X
IMPREGNATION MAT.	X
IMPREGNATION PROC.	X
CAN OR CUP NO.	X
MATERIAL	X

FINISHED: OD X ID X

FARADAY SHIELD BETWEEN X , X

VENDOR NAME \_\_\_\_\_

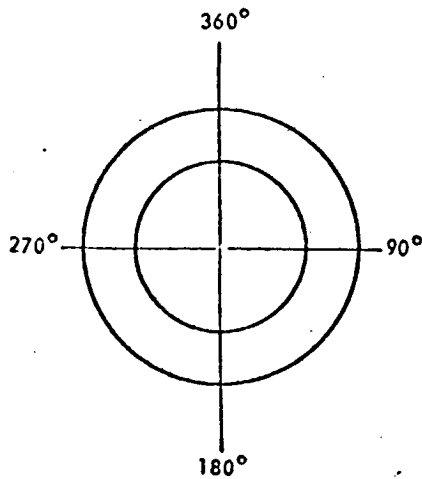
VENDOR PART # \_\_\_\_\_

ATC SKETCH # A-101703

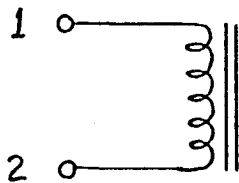
PAGE 2

TOROID TYPE  
MECHANICAL CONFIGURATION

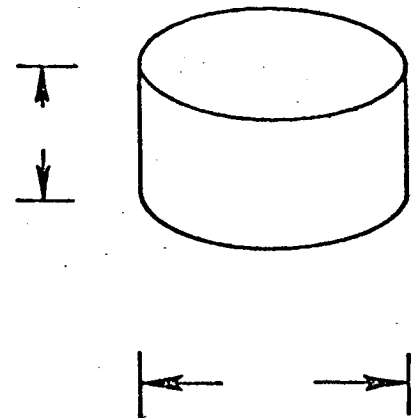
WINDING INFORMATION



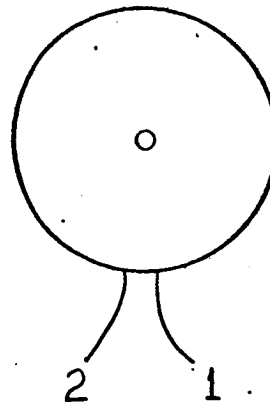
SCHEMATIC



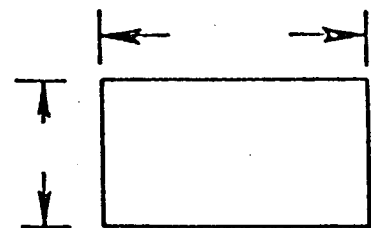
OUTLINE



LEAD BREAKOUT



STUD: \_\_\_\_\_  
TUBE: \_\_\_\_\_  
HOLE: \_\_\_\_\_



MINIMUM IDENTIFICATION:

1. ~~SCHEMATIC DESIGNATION~~
2. ATC # 101703
3. ~~VENDOR #~~
4. ~~SERIAL #~~

VENDOR NAME
VENDOR PART #
ATC SKETCH # A-101703

247